A STUDY ON THE RELIABILITY ANALYSIS DURING PRELIMINARY DESIGN – A ROCKET MOTOR EXAMPLE

A THESIS SUBMITTED TO
THE GRADUATE SCHOOL OF NATURAL AND APPLIED SCIENCES
OF
MIDDLE EAST TECHNICAL UNIVERSITY

BY

KENAN BOZKAYA

IN PARTIAL FULFILLMENT OF THE REQUIREMENTS
FOR
THE DEGREE OF MASTER OF SCIENCE
IN
MECHANICAL ENGINEERING

SEPTEMBER 2006

Approval of the Graduate School of Natural and Applied Sciences

Prof. Dr. Canan ÖZGEN
Director

I certify that this thesis satisfies all the requirements as a thesis for the degree of Master of Science.

Prof. Dr. Kemal İDER
Head of Department

This is to certify that we have read this thesis and that in our opinion it is fully adequate, in scope and quality, as a thesis for the degree of Master of Science.

Prof. Dr. Alp ESİN
Co-Supervisor

Prof. Dr. Metin AKKÖK
Supervisor

Examining Committee Members

Prof. Dr. R. Orhan YILDIRIM (METU, ME) _____

Prof. Dr. Metin AKKÖK (METU, ME) _____

Prof. Dr. Alp ESİN (METU, ME) _____

Assoc. Prof Dr. Suat KADIOĞLU (METU, ME) _____

Bayındır KURAN (M.S.) (TÜBİTAK-SAGE) _____

I hereby declare that all information in this document has been obtained and presented in accordance with academic rules and ethical conduct. I also declare that, as required by these rules and conduct, I have fully cited and referenced all material and results that are not original to this work.

Name, Last Name : Kenan Bozkaya

Signature :

ABSTRACT

A STUDY ON THE RELIABILITY ANALYSIS DURING PRELIMINARY DESIGN – A ROCKET MOTOR EXAMPLE

Bozkaya, Kenan

M.S. in Mechanical Engineering

Supervisor : Prof. Dr. Metin Akkök

Co-Supervisor : Prof. Dr. Alp Esin

September 2006, 145 pages

To be competitive in the market, it is very important to design cost effective and reliable products. For this purpose, it is necessary to consider reliability as an integral part of the design procedure. Therefore, reliability which is a design parameter that affects cost and safety of a system should be taken into consideration in early phases since it is very difficult to change design at the later phases.

Reliability of a rocket motor can be evaluated by reliability testing but these tests are very expensive and difficult since the tests are destructive and test sample size is determined by the binomial law. Because of the difficulties in reliability testing, in early design phases reliability can be evaluated by using reliability prediction results.

This thesis report includes application of probabilistic approach for a solid rocket motor design to evaluate its reliability in preliminary design phase. In this study, it is aimed to assess the solid rocket motor ballistic performance reliability and casing structural reliability, determine important parameters affective on the solid rocket motor reliability and find a new design point to improve the reliability. Variations in dimensions and material properties are considered as the sources of failures and the limit states for acceleration, total impulse and maximum stress in the casing are approximated with response surface method by considering these variations. With the response surface functions, Monte Carlo simulation is used to assess failure probability and distributions of the rocket motor performance. Besides the assessment of the reliability, capability of the response surface functions to estimate the rocket motor performance and effects of the input parameters on the rocket motor performance and performance variation are also examined. By considering the effect of the input parameters, a new design point is proposed to decrease the total probability of failure.

Keywords: Reliability, Rocket Motor, Probabilistic Design, Monte Carlo simulation, response surface method

ÖZ

ÖN TASARIM AŞAMASINDA GÜVENİLİRLİK ANALİZİ ÜZERİNE BİR ÇALIŞMA – ROKET MOTORU ÖRNEĞİ

Bozkaya, Kenan

Yüksek Lisans Tezi, Makine Mühendisliği Bölümü

Danışman : Prof. Dr. Metin Akkök

Eş Danışman : Prof. Dr. Alp Esin

Eylül 2006, 145 sayfa

Piyasada rekabetçi olabilmek için maliyet etkin ve güvenilir ürünler tasarlamak çok önemlidir. Bu amaçla güvenilirliğin tasarım sürecinin bir parçası olarak ele alınması gerekmektedir. Bu nedenle, ilerleyen aşamalarda tasarımda değişiklik yapmak zor olduğundan maliyet ve güvenliği etkileyen güvenilirlik erken tasarım aşamalarında dikkate alınmalıdır.

Roket motorlarının güvenilirliği güvenilirlik testleri ile değerlendirilebilir fakat bu testler tahribatlı olması ve test sayısının binomial kuralı ile belirlenmesi nedeni ile maliyetli ve zordur. Güvenilirlik testlerindeki zorluklar nedeni ile erken tasarım aşamalarında güvenilirlik, güvenilirlik kestirimi sonuçları ile değerlendirilebilir.

Bu raporda, katı yakıtlı bir roket motorunun güvenilirliğinin ön tasarım aşamasında değerlendirilmesi için olasılığa dayalı yaklaşımın uygulanması

sunulmaktadır. Bu çalışmada katı roket motorunun balistik performans güvenilirliğinin ve motor borusunun yapısal güvenilirliğinin tahmini, güvenilirliğe etki eden önemli parametrelerin belirlenmesi ve güvenilirliğinin artırılması için yeni bir tasarım noktasının bulunması amaçlanmıştır. Ölçülerdeki ve malzeme özelliklerindeki değişkenlikler yetmezliklerin kaynağı olarak ele alınmış ve ivme, toplam darbe ve motor gövdesinde oluşan en yüksek stres için sınır koşullar bu değişkenlikler dikkate alınarak Cevap Yüzeyi Yöntemi ile belirlenmiştir. Cevap yüzeyi fonksiyonları ile Monte Carlo Simülasyonu kullanılarak yetmezlik olasılığı ve roket motorunun performans dağılımı hesaplanmıştır. Güvenilirlik tahmininin yanı sıra cevap yüzeyi fonksiyonlarının roket motoru performansını tahmin etme yeteneği ve girdi parametrelerinin roket motorunun performansına ve değişkenliğe olan etkileri de incelenmiştir. Bu parametrelerin etkileri dikkate alınarak toplam yetmezlik olasılığının düşürülmesi için yeni bir tasarım noktası önerilmiştir.

Anahtar Kelimeler: Güvenilirlik, Roket Motoru, Olasılığa dayalı tasarım, Monte Carlo Simülasyonu, Cevap Yüzeyi Yöntemi

ACKNOWLEDGMENTS

I would like to express my deepest gratitude to my supervisor Prof. Dr. Metin Akkök and co-supervisor Prof. Dr. Alp Esin for their guidance, advice, criticism, encouragements and insight throughout the research.

I would also like to thank Bayındır Kuran and Dr. Mehmet Ali Ak for their suggestions and comments.

I would like to extend my special thanks to my colleagues at TÜBİTAK SAGE Sinan Hasanoğlu, Cengizhan Yıldırım, Bülent Sümer and Aysun Çelebi for their discussions on the subject and cooperation.

Finally greatest thanks to Özlem Akçınar and my family for their endless support and trusts throughout this study.

TABLE OF CONTENTS

LIST OF TABLES

LIST OF FIGURES

LIST OF SYMBOLS

a_a	Arming acceleration
a_L	Acceleration at launch
a_{max}	Maximum acceleration of the rocket
a_r	Burn rate constant of the propellant
b	Main effect coefficient in response surface model
CL	Confidence level
D	Grain diameter
d	Port diameter
f	Order of the fraction
g	Gravitational acceleration
g(x)	Limit state function
g_i	i^{th} limit state
H	Enthalpy of propellant combustion
I_t	Total impulse
k	Factor to set factorial points in response surface method
L	Grain length
n	Number of random variables
N, S_n	Sample size
N_f	Number of failed items
N_s	Number of survived items
P	Probability.
P_c	Chamber pressure.
P_f	Probability of failure,
Pf^T_i	Probability of failure for i^{th} limit state at a temperature T
r	Burn rate of the propellant

R(t), R	Reliability
S	Strength of the material
SF	Safety factor
SM	Safety margin,
$S_{T,Casing}$	Ultimate tensile strength of the casing material
S_{Temp}	Temperature sensitivity of the burn rate
T	Temperature
t	Time
t_1	Casing thickness
t_2	Minimum case thickness at case-nozzle interface
t_3	Lockwire thickness
t_L	Life
X_i	i^{th} random variable
x^c	Coded value of variable x
Zi	i^{th} random variable transformed into standardized normal distribution
α	Factor to set axial points in response surface method
ζ	Tapered angle of the grain
$\lambda(t)$, λ	Failure rate
λ_b	Base failure rate of the component
μ_i^T	Mean value for i^{th} response at a temperature T
μ_x	Mean of random variable x
π_E	Environment factor
π_Q	Quality factor
π_T	Temperature factor
ρ	Density of Propellant
σ_{max}	Maximum stress in the material
σ_i^T	Standard deviation for ith response at a temperature T
σ_x	Standard deviation of random variable x
χ_i	i^{th} limit value
Φ_{Exit}	Nozzle exit diameter
Φ_{Throat}	Nozzle throat diameter
ϕ	Standard normal distribution function

CHAPTER 1

INTRODUCTION

1.1 GENERAL

Reliability analysis became an important issue during the World War II when many failures occurred especially in electronic components and weapon systems. Then, it has been an important design parameter not only for military system but also for commercial products including aeronautical industry, nuclear industry and chemical industry.

Reliability can be briefly defined as the probability of designed part, component or system will perform it's the designed-for functions without failure for a specified period of time under specified set of conditions and reliability is a basic parameter which affects availability, cost, readiness and mission success and safety [1]. Therefore, this basic parameter should be considered in all system development phases to obtain a competitive product.

System development can be divided into three main phases which are:

- Design phase (Conceptual design, preliminary design and detailed design)
- Process development phase
- Manufacturing phase

The sources of unreliability in these phases are:

- Uncertainties in design
- Variations in manufacturing processes
- Variations in the operating environment
- Product deterioration

Variations in manufacturing processes can be treated in all three phases but other variations can only be reduced in the design phase. Moreover, if reliability is not considered in early design stages, radical changes must be done in further stages to increase reliability [2]. As a result, when a complex system design is considered, reliability studies of any product must be started at early design phases since it is very costly to improve reliability in later phases.

Special attention should also be paid for military system's reliability since reliability studies are generally more difficult for these systems as these systems are designed for severe environmental conditions and for long dormant periods. Additionally, military equipments generally include one-shot devices where reliability is determined by large amount of destructive tests. Moreover, it is impossible to check one-shot devices for failure prior to the usage since testing usually results in their destruction. Although, it is difficult to test a one-shot device during the design and impossible to test before the usage, reliability required for one-shot devices is generally high since they are generally safety critical components. [3]. Because of the cost and difficulties in testing, reliability studies must be carefully planned for military systems especially for one-shot systems or systems including one-shot devices. Therefore, as a part of the reliability engineering studies of such components, all failure modes and causes should be evaluated systematically.

The main purpose of the reliability engineering studies should be eliminating possible failures. In cases where the failure cannot be eliminated, the severity of the effect of the failure should be decreased. However, after any design change performed to increase reliability, system reliability must be reevaluated. The

traditional way of reliability determination is real time testing and number of test samples is determined by binomial law for one-shot devices. Therefore, sample size required in the tests increases rapidly with the increasing reliability. When the reliability test of an expensive and safety critical system is considered e.g. a rocket motor, it is seen that such tests are difficult because of cost and safety requirements during testing. Also, it is difficult to perform failure analysis for individual components as they are all destructed during the test. Because of the difficulties in demonstrating reliability by testing, other approaches to assess the reliability of the components/system should be used during the early stages of the design.

As a result, reliability is one of the most important measures of the system performance but it is difficult and costly to obtain a reliable product.

1.2 SCOPE OF THE STUDY

Because of the difficulties in the monitoring reliability while designing a new system, especially a one shot device, it is needed to apply a method which can be used to assess reliability in preliminary design phase and which can throw light on the detailed reliability studies in later design phases.

This thesis work is an analytical investigation of the ballistic performance reliability and the casing structural reliability at the preliminary design stage of a solid rocket motor. It is also aimed to evaluate the applicability of the probabilistic methods to a one shot systems which will facilitate to monitor reliability during early design phases where enough number of test prototypes are not yet available.

To assess the applicability of the method employed, an example study was performed with a solid rocket motor developed by TÜBİTAK SAGE. In this example, failure modes of a solid rocket motor casing and propellant, as regards decrease in performance as well, were determined and the variates that are used to construct a response surface were selected by considering the design parameters and environmental conditions that are related with possible critical failure modes. With the failure modes determined, based on the data collected from initial testing

and variation analysis, reliability of the one shot system is predicted and a new design point is proposed to improve the rocket motor reliability.

This thesis report comprises of the following 7 chapters which are outlined below: An introduction on the solid propellant rocket motors and their possible failure modes are outlined in Chapter 2. Basic concepts of reliability, which will shed light on the theoretical aspects of this thesis, are discussed in Chapter 3 and Chapter 4. Chapter 4 also includes a design of experiments (DOE) approach, the response surface method (RSM), which is used to obtain a simple formulation of the system performance. Chapter 5 which includes main method and calculation procedures used in this study follows the chapter for reliability methods. All calculations and results obtained from this study are given in Chapter 6. This chapter includes the formation of the response surfaces for the system performance, reliability approximation with Monte Carlo simulation (MCS), sensitivity analysis based on the approximated formulas and improvements in the system reliability by determining a new design point. Finally, discussions, conclusions and suggested further extensions are given in Chapter 7.

1.3 LITERATURE SURVEY ON ROCKET MOTOR RELIABILITY

The area of reliability has grown at a tremendous rate in the past decades, after the first reliability studies which were started after the World War II. One of the first to delve into reliability research was Wernher Von Braun who assumed that a system would be as reliable as the least reliable part. Then Pieruschka and Braun showed that reliability of a system is equal to the product of the reliability of its components and the first documented modern predictive reliability model was created.

However, main problem of the reliability studies during the design phase was predicting the reliability of the components. Such studies are mainly focused on the structures and structural reliability methods are developed.

Hasofer et. al. [4] suggested an iterative algorithm which was later used by Rackwitz et. al. [5] in conjunction with probability transformation techniques. This family consists of such techniques which can be grouped into two types, namely, First- and Second-order reliability methods (FORM and SORM) For FORM, the random variables are characterized by their first and second moments of the distribution. Truncation of the Taylor's series expansion of the function forms the basis of this method. Higher moments, which might describe the skewness and kurtosis of the distribution, are ignored. For SORM, a higher order approximation for the failure probability computation is used because of the high nonlinearity of some limit state functions. This algorithm has been widely used due to its simplicity. However it may not converge in some cases, if the nonlinearity is high. Liu et. al. [6] have shown that this method diverges when a principal curvature of the limit state surface at the design point is greater than 1.

Although, using FORM and SORM simplifies the estimation procedure, it is difficult to apply these methods to the problems with large number of variables and nonlinear limit states. Therefore, Monte Carlo simulation (MCS) of finite element codes has been also widely used in structural reliability calculations to evaluate the probability integral at failure region. However, for structures with a low failure probability a large number of finite element analyses are required in MCS which is not a practical application. Therefore, more efficient and accurate procedures are needed for estimating failure probabilities.

Bucher et al. [7] represented the system behavior by a response surface method (RSM) which was developed by Box et al [8]. In this method, RSM was utilized in conjunction with advanced Monte Carlo simulation techniques to obtain the desired reliability estimates. Response surface method (RSM) has been also proposed by a number of researchers, e.g., Faravelli [9], Rajashekhar et. al. [10]. Liu et al. [11] used a sequential response surface method together with Monte Carlo Importance Sampling to calculate the reliability. Recently, higher order approximation methods in which the limit state surface is approximated by higher order polynomials have been proposed by Grandhi et. al [12].

Although, reliability analysis took interest in the past and many studies were performed on different types of components, solid rocket motor reliability studies are limited to structural reliability of casing and thermal reliability of insulation.

Rajagopalan et. al. [13] had illustrated the implementation of stress strength interference approach to a rocket motor casing. Statistical distributions of the environmental stress acting on the casing and the component's ability to withstand that stress were taken into account to evaluate the affect of safety factor on the reliability of the casing. In this study, shell thickness, weld efficiency, uniaxial ultimate strength, radius of motor case, longitudinal weld mismatch and ultimate design pressure were taken as random variables.

Ekstrom et. al. [14] had presented Thiokol Corporation's probabilistic approach to solid rocket motor composite casing. Reliability of the casing was evaluated by considering the case hoop burst which was defined as the event of hoop stress exceeding hoop strength. Then, it was proposed to utilize first order second moment approach to assess the rocket motor casing reliability. In this study, hoop stress was calculated by using laminate plate theory and variation of the hoop stress was calculated by using Monte Carlo simulation of a hyper plane equation. Uniform distribution and normal distribution was used to define input parameters.

Zheng [15] was designed a solid rocket motor case according to the stress-strength interference theory, which involves the reliability design based on the strength and fracture toughness of material. In this study, structural reliability design of case based on strength and based on fracture toughness was evaluated separately. For the design of case based on strength, stress at the casing was calculated by using basic pressure vessel hoop stress formula and the design based on the fracture toughness was performed by assuming an unthrough crack of semiellipse in the meridian of cylinder case.

In addition to these studies on the structural reliability of solid rocket motor casing, Smith et. al. [16] predicted thermal reliability of a rocket motor by using a characterized insulator. In this study, by using test results statistical variability of

the insulator properties were determined and a Monte Carlo technique was used to provide an analytical prediction of the thermal reliability of a case insulation design. The approach was based upon using a statistically significant number of analyses for a given point in which the parameters that affect the insulation's thermal performance are varied randomly about their statistical distribution. The predicted distribution of motor case temperatures and heat-affected depths were used to ascertain the thermal reliability of the insulation design.

CHAPTER 2

SOLID PROPELLANT ROCKET MOTORS AND THEIR FAILURE MODES

2.1 GENERAL INFORMATION ON ROCKET MOTORS

Basically, a rocket motor is a simple form of energy conversion device. In a rocket motor source of the motion is the propellant which can be solid or liquid. There are two main categories of rocket engines; liquid propellant rockets and solid propellant rockets. In a liquid propellant rocket, the fuel and the source of oxygen (oxidizer) necessary for combustion are stored separately and pumped into the combustion chamber of the nozzle where burning occurs. In a solid rocket motor (SRM), the fuel and oxidizer are mixed together and packed into a solid cylinder and burning is initiated by the igniter. When it is burned, movement of gases through the nozzle results in the conversion of heat energy into kinetic energy. Once the burning starts, it will proceed until all the propellant is burned. However, a solid rocket motor is much simple than a liquid rocket motor [17].

Although solid rocket motors are known as simpler type of rocket motors they have many different failure modes, which make it difficult to predict their reliability. To illustrate the failure modes of a rocket motor it is important to understand the expected properties and functions of the components.

A simple solid rocket motor consists of four main components: Propellant grain, casing, igniter and nozzle (Figure 2.1). In addition to these components, some

parts and materials to match these components may be used, such as insulation, liner or fasteners.

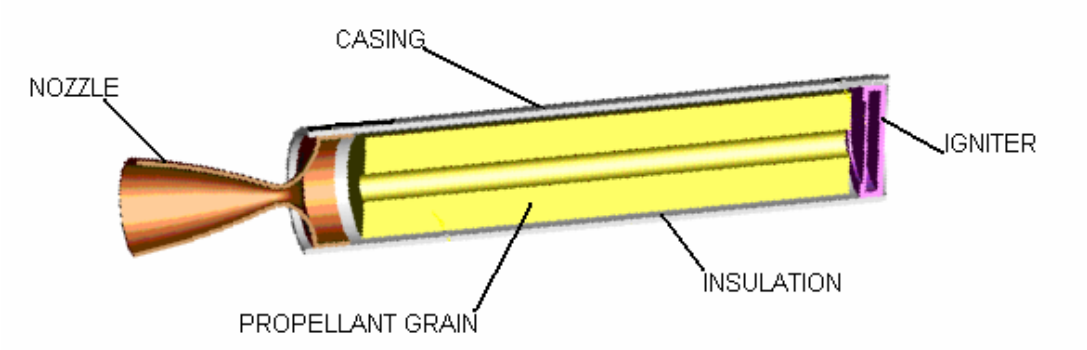

Figure 2.1. Solid rocket motor

Information about some of these components is given in the following sections.

2.1.1 Casing

Main function of a solid rocket motor casing is to provide structural integrity of the rocket motor. The case is a thin walled cylindrical pressure vessel with a head closure at one end and a nozzle at the other. Case must be strong enough to withstand the maximum expected operation pressures at the maximum expected temperature.

Since weight is a critical factor in motor design, steel is mainly used in construction due to its high strength/weight ratio. Aluminum can also be used as the casing material for small diameter rocket motors. Due to the differences in strength the wall thickness for an aluminum case is about three times that of a steel wall. In addition to strength properties, manufacturing capabilities also affect the casing material selection since it is difficult to manufacture very thin walls with ordinary techniques. For this reason, for large motors steel is often used as the casing material and small diameter motors utilize aluminum since it is easier to maintain closer tolerances with thicker case walls. The main disadvantage of using aluminum is that the strength rapidly decreases with increasing temperature.

Therefore, if an aluminum casing is used, the wall should not be directly exposed to the propellant flames and insulation should be used to limit the heating of rocket chamber walls [18].

Failure of the case may occur either as a brittle or ductile failure depending on the material selected. The use of material that is subjected to ductile failure is generally based on the determination of the actual material strength as fabricated as a pressure vessel. This determination is usually performed by testing flat uniaxial test specimens.

Environmental conditions are other major cause of the motor case failures. Motor case is subjected to heating from several sources, these sources are aerodynamic heating, radiant and conductive heating during handling and the most severe one; internal heating from the propellant. The most encountered influence of the thermal environment on a case is the change in mechanical properties of the material with a change in temperature [19].

Besides the loading conditions, variation in material properties may also be a reason of the failure. Materials strength properties are generally affected from the environmental conditions, fabrication method and the properties of the raw material. Work hardening associated with forming process may degrade materials while increasing the material strength level. Also changes in thermal processes affect the case material properties.

2.1.2 Propellant

Thrust is formed by the production of hot gases during the combustion of the propellant and acceleration of those gases to high velocities through the nozzle. Therefore, propellant is the most important component of rocket motor since it produces the energy required to cause a rocket to move from the launch site to its target.

The simplicity of a solid rocket motor compared with that for a liquid motor makes solid rocket motors more attractive but the difficulty in making good solid

rockets lies mostly in the design and manufacture of the propellant and solid propellant is not a homogeneous material and it is obvious that its properties will have variations from batch to batch. To obtain a reliable rocket motor design, an efficient and stable propellant should be manufactured. A good propellant should have constant burn rate, should be durable in storage and should have proper mechanical properties to prevent cracking during storage and firing. [20]

Using a weak propellant generally may cause catastrophic failures. For example a crack in the grain causes a sudden increase in the burn area and therefore an increase in chamber pressure which may cause the rocket motor to explode. It is very important that the solid propellants be sufficiently flexible in order to prevent cracking under handling and transportation loads. Besides the handling loads, the propellant should be capable of withstanding acceleration loads during the flight to prevent crumbling. In addition, to prevent erosion the propellant should have good erosion resistance since gases at high temperatures and velocities peel off the top layers of the propellant.

Because of these requirements and their important effects on the rocket motor performance, it is very important to control the properties of the solid propellant. In reference 21, properties of an ideal solid propellant were summarized as below:

1. High level chemical energy release to develop maximum thrust from each unit of propellant (specific impulse) for high performance.
2. Low molecular weight of combustion products.
3. Stability (resistance to chemical and physical change) over a long period of time.
4. High density
5. Resistance to the effects of atmospheric conditions, such as humidity, heat, cold, etc.
6. Resistance to accidental ignition from high temperature or impact.
7. Maximum possible physical strength to withstand the effects of forces imposed by heat and pressure during motor operation.

8. Very small change in volume with each degree of change in temperature, preferably matching that of the case material, to minimize stresses and strains in the two structures.
9. Ease of production.
10. Relative insensitivity of performance characteristics and fabrication techniques to impurities or small processing variations.
11. Durable in storage and operating temperatures.
12. Smokeless exhaust gas to avoid deposition of smoke particles at operational locations and detection in military usage.
13. Noncorrosive and nontoxic exhaust.
14. Burn at steady, predictable rate at motor operating conditions.

2.1.3 Insulation

One of the most serious problems in a rocket motor design is the high temperatures developed in the combustion chamber. The problem of protecting metal parts from temperatures that exceed the melting point of the material is solved by using a protective material which is designated as insulation which often completely coats the surface of the component being protected. An ideal insulation material should have lightweight to occupy a minimum volume, resist chemical degradation and resist thermal stresses [5, 22].

2.1.4 Liner

Liners are used to bond the propellant to the case or to the insulation. It ensures bonding between the propellant and the insulation layer. In addition, it inhibits burning so that propellant burning only occurs on free surfaces. It is desirable that the propellant to liner bond be strong enough to be sure that the bond failure under excessive thermal and mechanical stresses will not occur, so that, a new burning surface which cause a sudden increase in the pressure is not created [21].

2.1.5 Igniter

The igniters used to initiate the burning of the rocket motor. A pyrotechnic igniter usually contains an electrically heated wire which is surrounded by a small

amount of primer. The primer propellant is substance which is sensitive to temperature and will ignite readily and burn when heated. The main igniter charge is immediately adjacent to the primer it produces a hot flame which ignites the rocket grain [20].

Generally, the igniter is put into the forward end of the chamber with the exhaust products flowing down the center port. This arrangement provides efficient utilization of energy from the igniter and from the ignited portions of the grain since the hot gases flow over the unignited portion of the propellant. Where there is no center port in the propellant grain, the igniter must be mounted to the aft end. In this case, when propellant ignition is achieved the igniter case must be safely melted or must remain intact without affecting ballistic performance.

Igniter is also important because of the safety reasons. Sensitivity of an igniter to electrical energy flowing through the firing circuit must be such that it will operate within restrictive upper and lower limits. Also, the wires to the igniter or any attached vehicular structure can act as a receiving antenna and if there is a transmitter close enough, current may be generated. Igniters are protected from these types of hazards by enclosing the complete device including all circuitry and switching in a conductive shield or inserting a radio frequency interference filter between the transmission line and the igniter device. Besides the electromagnetic energy, electrostatic potentials may cause arcing and heat sensitive primer charges may be ignited by this spark. These electrostatic hazards are minimized or eliminated through the combined use of insulation techniques and non conductive ignition materials [20, 23, 24].

2.2 ROCKET MOTOR PERFORMANCE

A rocket motor which is used for military applications should satisfy some requirements depending on the mission that it is going to be used.

First of all it is necessary to carry the warhead to the target point, so that; a rocket motor should give a certain amount of impulse to obtain a definite range. Besides, limiting values for the instantaneous thrust and acceleration are introduced for the

rocket motor to be sure that the rocket will function properly. For example, since some fuses are activated when they are subjected to a certain amount of acceleration for a specific duration, rocket motor should supply this acceleration for a predetermined time to be sure that the warhead will be activated. However, high acceleration values may cause damage on the other components of the rocket, therefore the thrust given by the rocket motor should be high enough to supply the range requirements but not exceed the critical value.

Performance of a solid rocket motor depends on the propellant properties such as burn rate, density and the geometry of the components such as propellant grain geometry, nozzle geometry etc. Some of these properties are explained in following sections.

2.2.1 Burn Rate

The rate at which a propellant burns is usually described by a reference value at a specific pressure and it depends on ambient temperature and local pressure. Burn rate can be represented by Saint Robert's burn rate law which defines burn rate as a function of pressure at a specific ambient temperature [25]:

$$r = a_r . P_c^n \qquad \text{Eq (2.1)}$$

where r is the burn rate of the propellant, a_r and n are constant numbers depending on the propellant, P_c is the chamber pressure.

Burn rate also depends on the ambient temperature. The relation between the initial grain temperature and the burn rate is [25]:

$$r = r_{ref} . e^{S_{Temp} . (T - T_{ref})} \qquad \text{Eq (2.2)}$$

where r is the burn rate of the propellant, r_{ref} is the burn rate at a reference temperature T_{ref} and S_{Temp} is a constant defining temperature sensitivity of the burn rate. [17, 18, 25, 26]

2.2.2 Grain Geometry

Ballistic performance of rocket motor highly depends on the grain geometry. Depending on the performance requirements, for example pressure vs. time curve or thrust vs. time curve, the grain geometry can be in different configurations since the desired thrust curve determines the desired burning area.

Propellant grains may be divided into two main groups, these are free-standing grains and case bonded grains. Free standing grains are introduced into rocket motor cases after manufacture. Grains of the second type are bonded to the motor case during the casting and curing. Case bonded grains generally have a central port where the combustion process occurs and the outer surface of the propellant grain is bonded by a liner to the motor case. During the firing combustion of the propellant is initiated on the internal surface of the central port and proceeds radially toward the case. Grain geometries are not limited to the exact geometric shapes but examples for some common grain geometries are explained below [27]:

a. End Burning Grain: The end burning grain burns totally in the longitudinal direction as shown in Figure 2.2. Its burning surface is defined by the end area with other surfaces are inhibited. In its simplest form the end burning grain is defined by two variables the length and diameter of the grain.

If end burning grain is used, chamber wall continuously exposed to hot gases therefore the motor case requires significantly more insulation than that required for internal burning grains. This creates an additional weight on the motor. However, highest total propellant volume achieved with this grain shape. End burning grains are applicable to missions which require relatively long durations and low thrust levels [25].

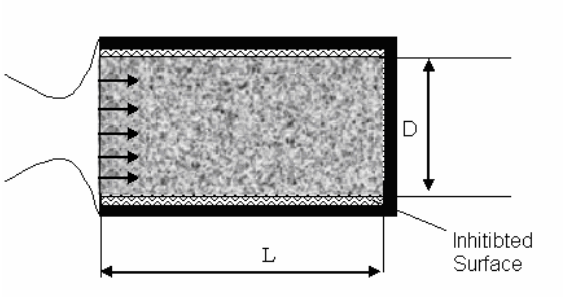

Figure 2.2. Schematic representation of end burning grain

b. Internal Burning Tube: The internal burning tube is a radially burning grain and typically it is case bonded which inhibits the outer surface (Figure 2.3). The internal burning grain is defined by length L and two diameters D and d.

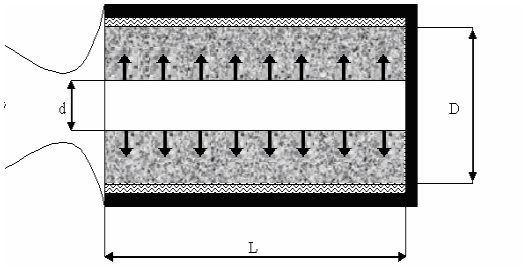

Figure 2.3. Schematic representation of internal burning tube

c. Star Grain Geometry: Star geometry is a radially burning grain which can be defined by seven independent parameters which are shown in Figure 2.4 with a half arm of the star.

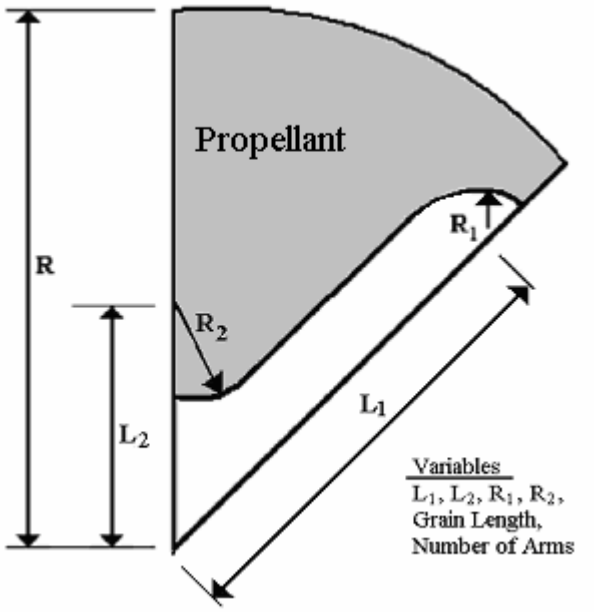

Figure 2.4. Parameters describing the star grain geometry

2.3 FAILURE MODES OF THE SOLID ROCKET MOTORS

Based on the literature survey conducted [17 18 19 27 28, 29], common failure types of a solid rocket motor and their causes are listed in Table 2.2. These failures are grouped according to the life phases given in Table 2.1.

Table 2.1. Life phases of a rocket

Phase Number	Description
1	Storage (Rockets are stored in specific storage areas until they are used)
2	Transportation (Rockets may be transported to different areas in their container for maintenance or for a mission.)
3	Handling (During maintenance operations)
4	Loading to the platform (Start of a mission)
5	Captive carry (Rockets are carried by the platform to the launch location)
6	Launch (Ignition of the rocket motor)
7	Flight to the target

Table 2.2. Solid rocket motors' failures

#	**Failure**	**Phase**	**Cause**
1	Ignition of the rocket motor out of a mission	3,4	Static voltage → Electrostatic potentials may cause arcing and heat sensitive igniters may be ignited
2	Over-pressurization beyond the motor casing's ultimate limits	5	Vibration, bullet impact → Friction may cause the ignition of the propellant or the pyrotechnic material in the igniter.
3		6	Chocked nozzle → Due to the high temperature, pressure and acceleration igniter may experience fracture and fractured parts may chock the throat which causes a rapid increase in the chamber pressure and motor explosion
4		1,2	Rocket motor exposed to fire → When the motor internal temperature reaches to the auto ignition temperature of the propellant, the motor is over pressurized
5		7	High burn rate → High burn rate of the propellant causes the overpressure in the rocket motor which may lead to the explosion of the casing,

Table 2-2. Solid rocket motors' failures (Continued)

#	Failure	Phase	Cause
6	Over-pressurization beyond the motor casing's ultimate limits	7	Cracks in propellant → Cracks increase the burn area which affects the internal pressure of the rocket motor. Cracks may be formed because of the manufacturing, mishandling, storage conditions (humidity, temperature cycling)
7			Voids in the propellant → Voids are formed during mixing/casting and they increase the burn area which affects the internal pressure of the rocket motor.
8			Liner or seal failures → Liner or seal failure creates additional burn area on the propellant grain which increases the internal pressure and changes the thrust vs. time curves. These failures are generally because of using insufficient liner thickness, insufficient curing time during the production, aging of the material and material migration during the storage
9			Detonation of the propellant
10			Improper grain geometry
11			Nozzle clogged by debris or chunk of propellant
12			Combustion instability → Shock waves within chamber which is a function of the grain geometry cause instable burning of the propellant

Table 2-2. Solid rocket motors' failures (Continued)

#	**Failure**	**Phase**	**Cause**
13	Casing failure	7	Under-designed casing → Thin, wrong material
14			Improperly manufactured casing → Scratches leading to stress fractures, Improper heat treatment, Improper assembling
15			Loss of temper → During the flight, casing may be over heated because of the insulation failure because of weak insulation material or insufficient insulation thickness
16			Weak casing material
17			Deformed casing → Transportation loads or shock during handling creates deformed parts on the casing.
18	Nozzle Joint failure	7	Weak material or high internal pressure
19	Nozzle failure	7	Weak material
20			Loss of temper in nozzle case material → Heat transfer through graphite to case material
21	Missing the target	7	Low specific impulse, thrust vector misalignment
22	Fuse cannot be activated	7	Improper acceleration profile → Some fuses are activated when they are exposed to a specific acceleration for a specific period of time.

Table 2-2. Solid rocket motors' failures (Continued)

#	Failure	Phase	Cause
23	Specific impulse is below the desired level	7	Eroded nozzle throat
24			Seal leaks between nozzle insert (i.e. graphite) and nozzle casing.
25			Improper burning → Improperly prepared propellant (wrong oxidizer vs. fuel ratio, incomplete mixing, etc.)
26	Rocket cannot be launched	6	Igniter failure → Igniter materials cannot be activated in high humuditive environments also aged igniters may fail to start the ignition.

To obtain a reliable design, these failure modes and their causes should be well investigated and necessary precautions should be taken. While investigating the possible failure modes the most important thing is to determine the failure mode's risk priority. This priority is generally determined by considering the failure mode's effects on the system by the judgment of its severity of its consequences, probability of occurrence. By considering failures in Table 2.2, nine basic failure modes of a rocket motor have been evaluated for risk priority according to values in Table 2.3. Predicted risk priorities are given in Table 2.4.

Table 2.3. Risk grades [30]

Frequency of Occurrence	Hazard Severity			
	1 Catastrophic	**2 Critical**	**3 Marginal**	**4 Negligible**
A Frequent ($x>10^{-1}$)	Unacceptable (1A)	Unacceptable (2A)	Unacceptable (3A)	Undesirable (4A)
B Probable ($10^{-1}>x>10^{-2}$)	Unacceptable (1B)	Unacceptable (2B)	Undesirable (3B)	Acceptable with Review (4B)
C Occasional ($10^{-2}>x>10^{-3}$)	Unacceptable (1C)	Unacceptable (2C)	Acceptable with Review (3C)	Acceptable with Review (4C)
D Remote ($10^{-3}>x>10^{-6}$)	Unacceptable (1D)	Undesirable (2D)	Acceptable with Review (3D)	Acceptable without Review (3E)
E Improbable ($10^{-6}>x$)	Undesirable (1E)	Undesirable (2E)	Acceptable without Review (3E)	Acceptable without Review (3E)

Table 2.4. Failures risk priorities

#	Failure	Severity	Occurrence	Risk Priority
1	Over-pressurization beyond the motor casing's ultimate limits	1	C	1C
2	Fuse cannot be activated	2	C	2C
3	Specific impulse is below the desired level	2	C	2C
4	Casing Failure	1	D	1D
5	Nozzle Joint failure	1	D	1D
6	Nozzle Failure	2	D	2D
7	Missing the target	3	C	3C
8	Rocket cannot be launched	2	D	2D
9	Ignition of the rocket motor out of a mission	1	E	1E

CHAPTER 3

RELIABILITY CONCEPT

3.1 INTRODUCTION

Common expected output of any system is performing its intended functions. System effectiveness is a term which is generally used to describe the over all capability of a system to accomplish its function. If a weapon system is called effective, the system is capable of completing its mission and one of the major attributes determining system effectiveness is reliability [31].

"Reliability is the probability that an item will perform a required function under stated conditions for a stated period of time" [2]. The stated conditions are the total physical environment, including mechanical, thermal, and electrical conditions. The stated period of time is the time during which satisfactory operation is desired. "A more general definition of the reliability is the probability that a system will operate successfully when called upon to do so under specified conditions" [31]. Main difference between these two definitions of the reliability is time which is not consideration in second definition. Since the second definition is a general one, it also includes one shot devices which are the systems or components that are expected to operate once in their life and time to failure is not important for these devices' reliability value.

3.2 TIME AND RELIABILITY

If the life of an item or a system is defined by a random variable then the reliability function R(t) of that item or system at time t > 0 is defined with a probability function:

$$R(t) = P(t_L > t) \qquad \text{Eq (3.1)}$$

Which means that R(t) is the probability of an items life t_L is greater than a given time period of t, so the item does not fail in the time interval (0, t]. In terms of the failure rate function λ, reliability is defined as:

$$R(t) = \exp\left[-\int_0^t \lambda(\tau).d\tau \right] \qquad \text{Eq (3.2)}$$

If the failure rate is constant, i.e. failure rate is defined by an exponential distribution then reliability is:

$$R(t) = e^{-\lambda.t} \qquad \text{Eq (3.3)}$$

The exponential distribution is the only failure law having a failure rate function that does not change over time. Given that an object has already survived until time t, the probability of its surviving for an additional t time units is just the same as the probability that a new object of the same type survives for t time units. Thus the Exponential Life Model can be used to model objects that fail only because of random incidents.

If the failure rate of an item is a function of time, then; unit failure numbers over time are observed and failure rate λ(t) by time can be estimated. By collecting failure data and fitting failure rate versus time curve, a graph such as Figure 3.1 can be obtained. Because of the shape of this failure rate curve, it is known as the "Bathtub" curve.

The initial region that begins at time zero when a customer first begins to use the product is characterized by a high but rapidly decreasing failure rate. This region is known as the Early Failure Period (Infant Mortality Period). This decreasing failure rate typically lasts several weeks to a few months depending on the product, the use conditions and the screening test that are applied to the product before usage.

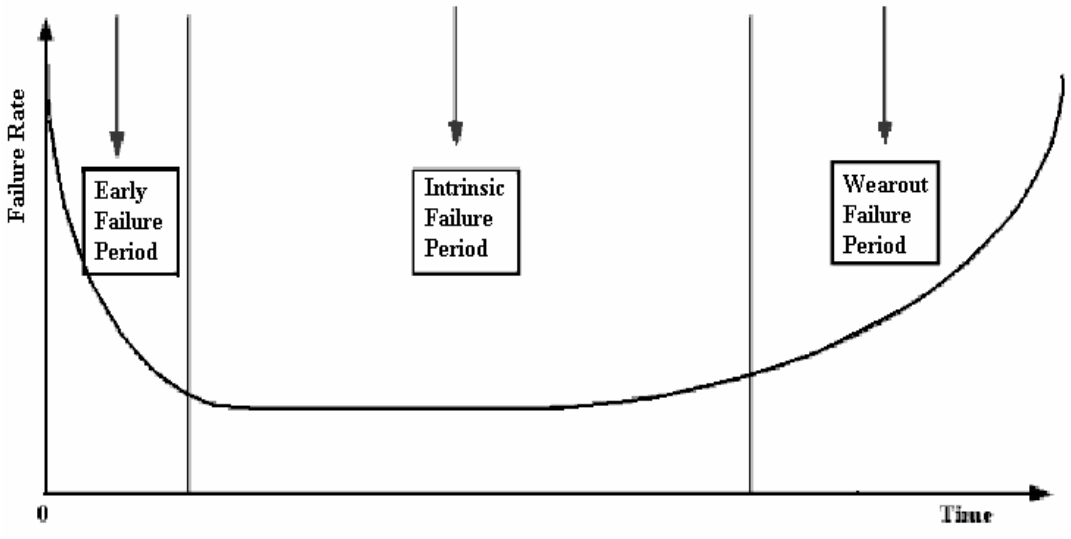

Figure 3.1. Illustration of the Bathtub Curve

Next, the failure rate remains almost constant for the majority of the useful life of the product. This long period of a level failure rate is known as the Intrinsic Failure Period (also called the Constant Failure Rate Period or Useful Life Period) and in this part of the bathtub curve only chance failures occur. This constant failure rate part of the bathtub curve is generally longer than the other parts of this curve.

Finally, if units from the population remain in use, the failure rate begins to increase as materials wear out and degradation failures occur at an ever increasing rate. This is the Wearout Failure Period [1,32].

Bathtub curve shows dependence of the failure rate to time and defined with three regions. However, not all the components have a curve with these three regions depending on the component type, manufacturing quality and screening tests. Systems may have different failure rate vs. time curves, depending on the type, as shown in Figure 3.2.

However, bathtub curve and failure rate are not applicable to one shot devices since their success is not measured with time. Generally, failure rate is considered as the basic metric for reliability calculations. Metrics such as Mean Time Between Failure (MTBF) and Mean Time To Failure (MTTF) are derived from failure rates. These do not appropriately characterize the reliability of a one-shot system that does not have a significant period of operation. Rather, one would like to know the probability of successful function when needed to operate. This may be referred to as a demand probability, one that does not have an associated operating time. Thus failure probability, rather than failure rate, is the important underlying metric for one-shot systems. [33]

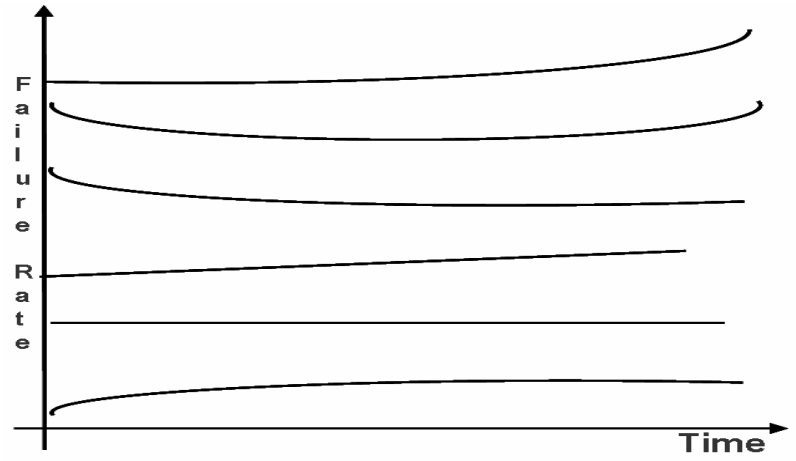

Figure 3.2. Different types of failure rate vs. time curves

3.3 SAFETY FACTOR AND RELIABILITY

Safety Factor is a multiplier applied to the calculated maximum load (force, torque, bending moment or a combination) to which a component or assembly will be subjected. Thus, a safer design is obtained by using materials with higher strength or including redundant systems.

In real life stress is not uniform; materials do not have homogeneous properties, manufacturing processes often create stresses within the component. Therefore safety factor is used and it accounts for imperfections in material, flaws in assembly, material degradation and uncertainty in load estimates. An appropriate factor of safety is chosen based on several considerations. Prime considerations are the uncertainty in load, manufacturing defects, the consequences of failure and the cost of over engineering.

The conventional design methodology is deterministic design which uses single values for the maximum stress in the component and single value for the nominal strength of the material. The design load is determined by using a multiplier to the calculated stress value. By this way a safe stress value that can be used in the design is obtained. The safety factor is:

$$SF = \frac{S}{\sigma} \qquad \text{Eq (3.4)}$$

In addition to safety factor, the term “margin of safety” is also used to describe the similar concept. The relation between safety factor and safety margin is:

$$SM = \frac{S - \sigma}{\sigma} = SF - 1 \qquad \text{Eq (3.5)}$$

where SM is the safety margin, SF is the safety factor, S and σ are strength and stress. [34, 35]

For a constant safety factor, reliability may be varied in three ways; first the mean of the stress and the mean of the strength may be changed with the same proportion while their standard deviation is kept constant. By this way the safety factor does not change as illustrated in Figure 3.3 and Figure 3.4 where the shaded areas show the failure regions. In this case, with the same safety factor, probabilities of failure are not same for these two sample cases.

Second, standard deviation of the stress and the standard deviation of the strength may be varied but the mean of the stress and the mean of the strength is kept constant. In this case again safety factor does not changes as given in Figure 3.3 and Figure 3.5. However, a lower standard deviation means low variability in the strength or stress, then reliability increases if the standard deviation decreases. If the standard deviation increases for any variable than the distribution of the variable become spread and the variability increases which means a decrease in reliability while the safety factor is same for both cases.

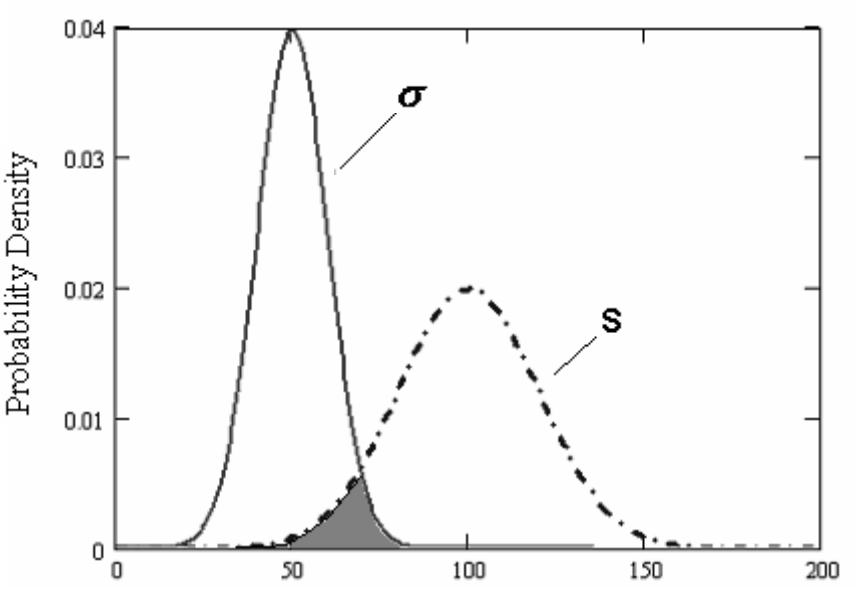

Figure 3.3. Unreliability region for normal distributed stress and strength (σ=N(50,10), S=N(100,20)

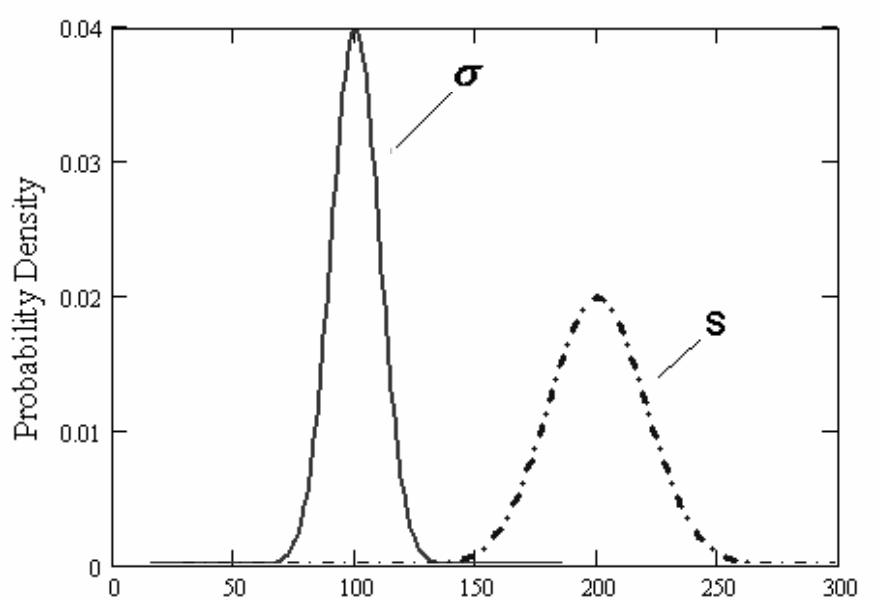

Figure 3.4. Unreliability region for normal distributed stress and strength (σ=N(100,10), S=N(200,20)

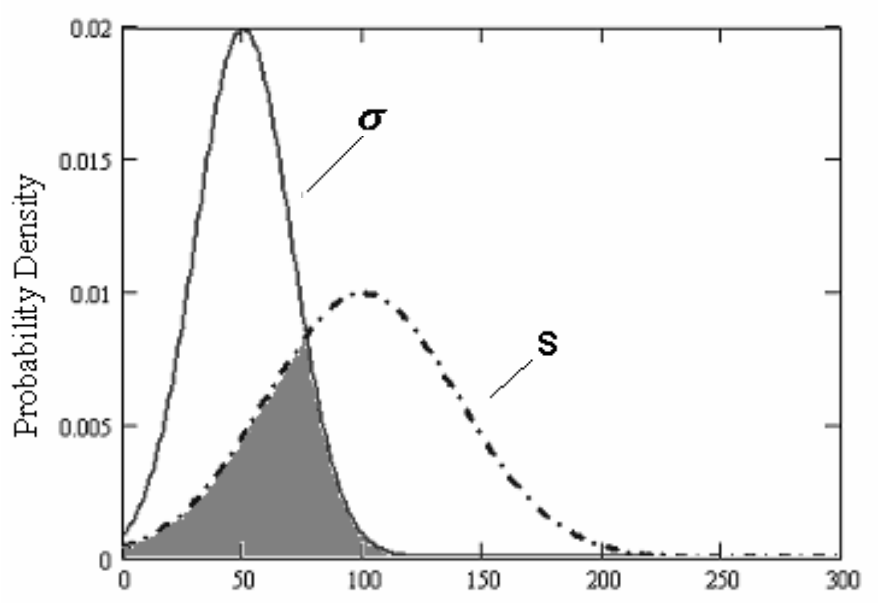

Figure 3.5. Unreliability region for normal distributed stress and strength (σ=N(50,20), S=N(100,40)

Finally, safety factor can be kept constant while changing mean values with the same proportion and changing standard deviation at the same time. Then one can

vary reliability from relatively low values to hundred percent with the same safety factor. “It is obvious that the central safety factor is a fallacious indicator of failure incidence and hence of reliability and design integrity or safety” [36]. Then, it can be said that same safety factor value does not mean the same reliability as shown in Table 3.1.

In structural design safety factor is used to compensate uncertainties and variations in design load and material properties such as stress and strength. Similar to variation in stress and strength, all engineering parameters are also variable such as electrical parameters, physical properties of materials, dimensions etc., also all environmental and other conditions such as temperature, humidity and vibration. These variations affecting reliability is usually complex and difficult to deal with since they generally do not follow a known distribution. For instance, because of the usage of the gauges or other measurements there is a lower and upper limit set. That’s why variations and probability distribution of the dimensions will be a truncated.

Table 3.1. Reliability for different strength, stress and safety factor values

Strength		**Stress**					
Mean	**Standard Deviation**	**Mean**	**Standard Deviation**	**Safety Factor**	**Safety Margin**	**Reliability Index**	**Reliability**
100	20	50	20	2	50	2.8284	0.997661
200	20	100	20	2	100	6.3640	0.999999
100	40	50	20	2	50	1.3416	0.910144
200	40	100	40	2	100	2.8284	0.997661
200	40	200	20	1	0	3.5777	0.999827
400	80	200	40	2	200	3.5777	0.999827
400	100	160	20	2.5	240	2.9417	0.998368
600	100	150	50	4	450	4.4721	0.999996
600	200	150	50	4	450	1.9403	0.973827

3.4 RELIABILITY PREDICTION

Predicting the reliability of a complex system is an important part of the reliability studies. Reliability prediction facilitates design reviews and trade-offs and provides a basis for logistics and life-cycle cost planning.

As far as electronic systems are considered, MIL-HDBK-217 [37] proposes two prediction methods; parts count method and part stress method. With these methods reliabilities of electronic components are predicted in terms of failure rate by assuming exponential model which is valid for the chance failure region shown in the bathtub curve in Figure 3.1. Hence, reliability is defined by an exponential model:

$$R(t) = e^{-\lambda t} \qquad \text{Eq (3.6)}$$

According to this model, failure rate does not vary with time as long as environmental and operating conditions do not change.

In MIL-HDBK-217, general form of the formula which gives an electronic part's failure rate is

$$\lambda = \lambda_b \times \pi_T \times \pi_E \times \pi_Q \times \prod_{i=1}^{n} \pi_i \qquad \text{Eq (3.7)}$$

λ_b: Base failure rate of the component,
π_T: Temperature factor,
π_E: Environment factor,
π_Q: Quality factor.

The value of λ_b is obtained from component test data where the data is generally presented in the form of failure rate versus normalized stress and temperature factors.

For mechanical components and structural members failure rate vary with time and a single exact failure rate value cannot be found for these components but

alternatively an average failure rate over the mission duration is used. Unfortunately, very few sources provide such failure rate values for mechanical components. For mechanical and electromechanical components (such as bearings, electric motors, solenoids), failure rate is determined by NSCW-98 [38] but the range of the components is very narrow. For the complex mechanical and structural components probabilistic analysis of the design is used to predict the components reliability. [39]

3.5 ONE SHOT DEVICES AND RELIABILITY

"One shot device is an item which is required to perform its function only once during normal use. Such items are usually destroyed during their normal operation and cannot therefore be fully tested and reliability required from one-shot devices is normally high" [3]. For example a rocket is a one shot device since once it is ignited it is not possible to shut it off and it is not possible to restart the mission with the same rocket.

For an item whose success is measured by operating time, reliability is determined by using test results which includes life time distributions. In these tests, environmental conditions which are expected to be experienced by the system are applied in combination and failure time is collected from the test data. Generally, these tests can be accelerated to reduce the testing cost by decreasing the failure times by the application of higher stresses. Detailed information about life testing and accelerated life testing can be found in the references 40, 41 and 42.

When a one shot device is taken into consideration, tests are not accelerated and the time of the test is not an output of the test which has to be collected. Reliability calculation of one shot devices are performed according to the binomial law:

$$CL = 1 - P(r \leq k) \qquad \text{Eq (3.8)}$$

where CL is the confidence level and P(r ≤ k) is the probability of having k or less failure which is given by the binomial law:

$$P(r \le k) = \sum_{r=0}^{k} \frac{n!}{r!.(n-r)!}.p^{r}.(1-p)^{(n-r)} \qquad \text{Eq (3.9)}$$

where p is the probability of failure, n is the sample size, r is the number of failure observed during the test. For a reliability goal of 0.99, one must perform minimum 230 tests without failure to demonstrate the reliability with a 90% confidence. A sample table which shows necessary number of test to verify a reliability value of 0.99 for a one shot device is given in Table 3.2.

Table 3.2. Number of tests to demonstrate %99 reliability

	Confidence Levels				
Number of Failures	**60%**	**80%**	**90%**	**95%**	**99%**
0	92	160	230	299	459
1	202	299	388	467	662
2	310	424	526	625	838
3	417	551	664	773	1002
4	522	671	789	913	1157
5	625	785	926	1049	1307

Testing reliability is a costly and time consuming method but it gives true reliability of the system with a confidence interval determined by the sample size in the test.

CHAPTER 4

RELIABILITY ESTIMATION METHODS

4.1 INTRODUCTION

Deterministic design employs the idea of either performing analysis with input variables at their worst case values or performing analysis with input variables at their nominal values and applying a safety factor to the final result of the output variable. In general, the result of using either of these methods is unknown. Also, assuming that the input distributions are correct, applying worst case scenarios may give reliable but too conservative designs. Reliability analysis based on probabilistic methods recently became popular since it gives fast and reasonable estimates of probability of failure and can be used as the basis of the design optimization. It relies on statistical distributions applied to the input variables to assess reliability, or probability of failure, for the output variable by specifying a design point. Any response value passing beyond this design point is considered in the failure region [43]. Probability of the failure is given by:

$$P_f = P\left[g(x) \leq 0\right] = \int_{g(x)\leq 0} f_x(x).dx \qquad \text{Eq (4.1)}$$

where P_f is the probability of the failure, g(x) is the limit state function and $f_x(x)$ is the joint probability density function. These variables are illustrated in Figure 4.1.

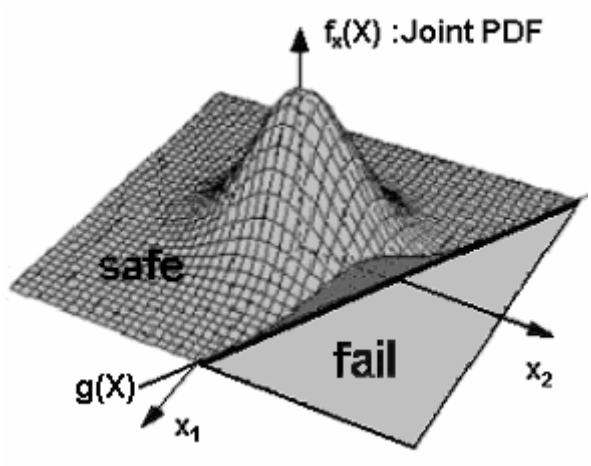

Figure 4.1. An example for Joint Probability Distribution and g(X)

General steps to use probabilistic methods in reliability analysis are given as [44]:

1. Potential failure modes of the determined loading conditions are identified.
2. An acceptable probability of failure (or minimum reliability) is established for each failure mode
3. Design variables affecting the response of the system is determined
4. Variations of the design parameters are defined.
5. Existing models, computer simulations are used to determine the systems response for each failure mode
6. Probabilistic analysis methods are applied to determine the probability of failure
7. System probability of failure is calculated, by using the system reliability block diagram or by joining the probabilities of different failure modes.

Different methods can be used in step 6 which is the determination of the probability of failure. These methods can be divided into two groups as:

- Analytical calculation methods
- Direct methods

Analytical methods include:

- First Order Second Moment Approach (FOSM)
- First and Second Order Reliability Methods (FORM and SORM)

Direct methods include:

- Monte Carlo simulation
- Simulation with response surface approximation

These methods are explained in the following sections.

4.2 FIRST ORDER SECOND MOMENT APPROACH

Second moment approach is the fastest method to estimate the probability of failure. In this method, only first and second moments of the basic design variables are taken into consideration and all the variables are assumed to have normal distribution. In First Order Second Moment (FOSM) approach, required input parameters are mean and a measure of the variability (variance, standard deviation etc.).

To apply FOSM first a limit state function which defines a state beyond which a part will no longer fulfill the conditions for which it is designed is determined. Generally, limit state function is expressed by g(X) and it is defined as g(X)<0 is the failure state and g(X)=0 gives the failure surface.

With the assumption of the linear limit state function, probability of failure P_f can be calculated by using the formula:

$$P_f = \phi(-\beta) \qquad \text{Eq (4.2)}$$

and ß is the reliability index which is defined as:

$$\beta = \frac{\mu_c - \mu_l}{\sqrt{\sigma_c^2 + \sigma_l^2}} = \frac{\mu_M}{\sigma_M} \qquad \text{Eq (4.3)}$$

where μ_c is the mean value of the capacity, μ_l is the mean value of the load, σ_c, σ_l are the standard deviation and ß is the reliability index which was defined by Cornell for a first order limit state function and in general form with n variables

$$\mu_M = f(X_1, X_2, \ldots X_n)$$

$$\sigma_M^2 = \sum_{i=1}^{n} \left(\frac{\partial f}{\partial X_i} \right)^2 \sigma_{Xi}^2 + \sum_{i \neq j} \sum \left(\frac{\partial f}{\partial X_i} \right) \cdot \left(\frac{\partial f}{\partial X_j} \right) \cdot \rho_{ij} \cdot \sigma_{Xi} \cdot \sigma_{Xj} \qquad \text{Eq (4.4)}$$

where ρ_{ij} is the covariance of i^{th} and j^{th} variable.

Derivation of Reliability Index for a linear limit state function is given in Appendix A [43] and relation of reliability index and reliability is shown in Figure 4.2.

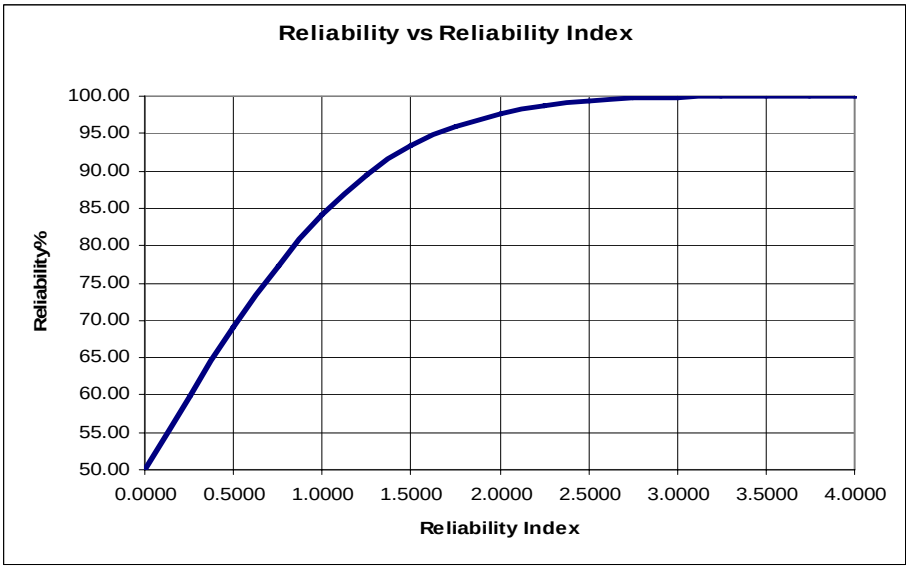

Figure 4.2. Reliability vs. Reliability Index

This method gives exact results when the load and capacity are both normally distributed and the limit state function linear. For other distributions and non linear limit state functions this method can be used as a first estimation for the reliability with normal distribution and linear limit state assumption but depending on the distribution types and limit state function, large amount of error can be introduced. To eliminate this problem First Order Reliability Method (FORM) and Second Order Reliability Method (SORM) can be used.

4.3 FIRST AND SECOND ORDER RELIABILITY METHODS

First and Second Order Reliability Methods gives approximate results for the joint probability integral which cannot be calculated analytically for most cases. In these two methods, first the distributions of the random variables, x_i, are determined and then they are transformed into standardized normal distributions which have a zero mean and unit standard deviation

$$z_i = \frac{x_i - \mu_{X_i}}{\sigma_{X\,i}} \qquad \text{Eq (4.5)}$$

by this way the variable space become rotateable around the origin (Figure 4.3 and Figure 4.4) .

$$g(X_1, X_2, ..., X_n) = 0 \rightarrow g(Z_1, Z_2, ..., Z_n) = 0$$

Then, the Most Probable Failure Point (MPFP) is determined. MPFP is defined as the nearest point of the $g(x_i)$ function to the origin where g(xi) is the limit state function used to define failed condition. After the determination of MPFP, probability of failure can be calculated by using the joint probability integral in the failure region where limit state function g(x) is smaller than zero.

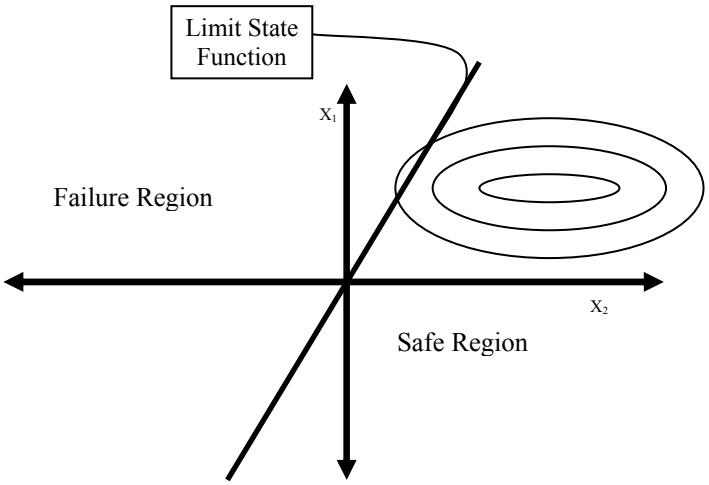

Figure 4.3. Variable space before transformation

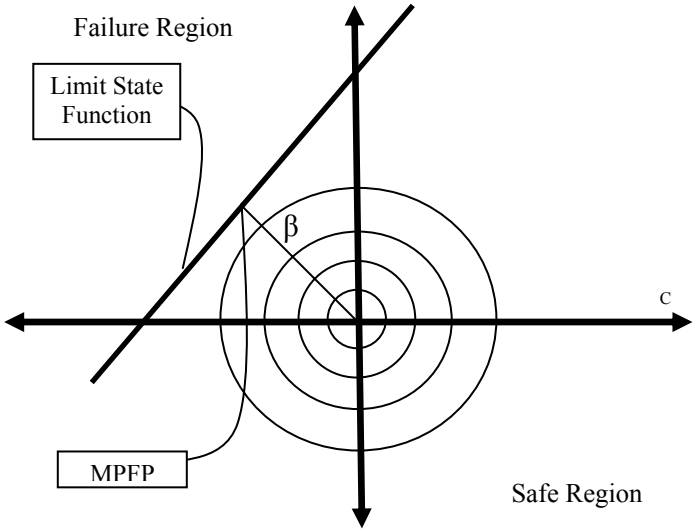

Figure 4.4. Variable space after transformation

Reliability index β can be found by solving the following optimization problem

$$\beta = \min\left[\left(\sum Z_i^2\right)^{1/2}\right] \text{ subject to } g(Z_i)=0$$

The First Order Reliability Method approximated the failure surface as a tangent line, tangent plane or a tangent hyperplane at the Most Probable Failure Point. Since the variables are transformed into the standardized normally distributed variables, coordinate system is rotated about the origin and new axes (x→v, y→z) are produced.

$$P_f = \int_{\beta}^{\infty} \phi(z)dz \qquad \text{Eq (4.6)}$$

where P_f is the probability of failure and Φ is the cumulative normal distribution function. Once the Most Probable Point is determined this method also gives a fast approximation of failure and it gives exact solution for the problems which has a linear limit state function. Besides it is known that this method gives good approximations with non-linear limit states and this method is widely used method for the probability of failure calculations.

Second Order Reliability Method does not assume a linear limit state function but it uses the curvature information at the Most Probable Failure Point. This method gives better estimates for reliability but it is difficult to implement this method to all kind of problems. Information on these methods can be found in references 4, 5, 44, 45, 46.

4.4 MONTE CARLO SIMULATION

The Monte Carlo simulation (MCS) provides approximate solutions to a variety of mathematical problems by performing statistical sampling experiments on a computer. The general idea of this method is to solve mathematical problems by the simulation of random variables. Monte Carlo simulation selects variable values at random to simulate a model.

In reliability calculations, Monte Carlo simulation can be said to be most frequently utilized method. In analytical reliability methods generally the joint probability integral cannot be calculated but approximated using some

assumptions and since these methods use analytical solutions to the failure integral, it is generally difficult to evaluate it for few numbers of random variables. By using Monte Carlo method large number of random variables and limit state functions can be handled. “To understand what kinds of problems are solvable by this method, it is important to note that the method enables simulation of any process whose development is influenced by random factors. Monte Carlo simulation is a widely used technique for probabilistic structural analysis, serving two main purposes: First, validating analytical methods and second, solving large, complex systems when analytical approximations are not feasible.” [44].

Main steps in MCS are as below (Figure 4.5):

1. Define the relation between the inputs and the response
2. Generate a vector of random variables for inputs
3. Evaluate the response
4. Repeat 2^{nd} and 3^{rd} steps until enough number of trials are performed.

The more iteration is done, the lower the standard error of the mean result since the error is inversely proportional to square root of iteration number.

In order to evaluate the failure probability corresponding to a known performance function, g(X), same procedure is followed. In this case, the Monte Carlo simulation method would consist of the following steps:

1. According to the probability density functions of the random variables in the limit state function, generate a random value for each variable.
2. Calculate the value of the limit state function. ($g(X) < 0 \rightarrow$ system failure)
3. Repeat steps 1 and 2 until required sample, Sn, size is obtained.
4. Estimate the probability of failure by $P_f = N_f / Sn$, where N_f is the number of failures.

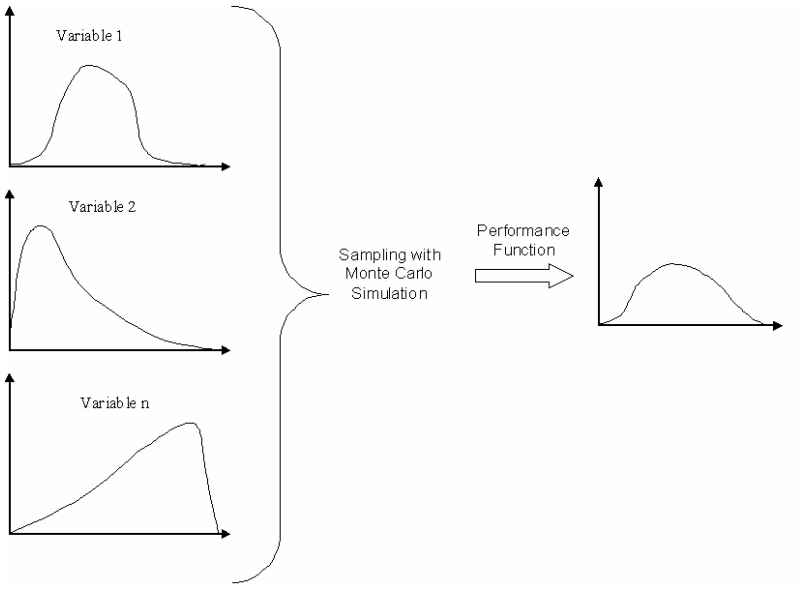

Figure 4.5. Monte Carlo simulation

Most random number generators produce variates that are uniformly distributed. Variates for other distributions are generated using cumulative distribution functions of those distributions. The CDF describes the probability that a variate X takes on a value less than or equal to a number x. The value of the CDF "F(x)" takes values between 0 and 1. First a number between 0 and 1 is generated and then by using the inverse cumulative distribution function random value of x is calculated (Figure 4.6).

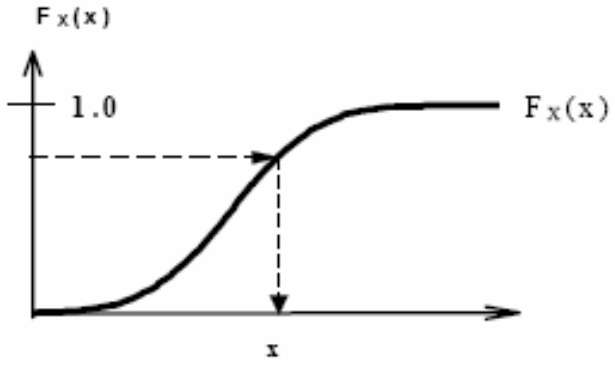

Figure 4.6. Random number generation in MC simulation

Mainly three different Monte Carlo simulation techniques are used in reliability calculations [44]:

- Direct Monte Carlo simulation
- Importance Sampling
- Latin Hypercube Sampling (LHS)

In Direct Monte Carlo simulation, limit state function is calculated in all region of the response. That's why the number of the sampling in simulation is needed to be increased to obtain accurate results.

"Importance Sampling technique concentrates sampling points in the region which mainly contributes to the failure probability, instead of spreading them out evenly across the whole range of possible values of each random variable. Instead of generating a huge amount of successful (in the sense that the performance function $g(X) > 0$) simulations, this technique seeks to generate only a few simulations, most of which lead to failure. This is done by modifying each variable's PDF to generate these important samples." [44].

Latin Hypercube Sampling (LHS) is a sampling technique where the random variable distributions are divided into equal probability intervals. A probability is randomly selected from within each interval for each basic event. Generally, LHS will require fewer samples than simple MCS for similar accuracy. However, it may take longer to generate a random number [44].

Direct Monte Carlo simulation gives almost accurate solutions to the joint probability integral since all region of the probability is searched in the simulation. Monte Carlo simulation method has the advantage of accurate result but calculation time is also increased tremendously as the error range is directly related with the number of simulations. Depending on the expected accuracy of the result, number or the sampling can be defined but for the cases where performance function calculation is performed by using a finite element code or other softwares, calculation time is generally too long.

Detailed information on Monte Carlo simulation can be found in References 36, 44, 47, 48.

4.5 RESPONSE SURFACE APPROACH IN RELIABILITY ANALYSIS

Response surface method (RSM) is a design of experiment methodology which gives estimate functions for the investigated behavior of the system. This method allows the designer to rapidly estimate the local response of a system by a close form formulation which consists of interactions and higher order effects. By using response surface method, optimum design point can be approximated and critical parameters in the design can be determined. To obtain a response surface, the system is simulated/tested several times for different configurations and the response data of the system is collected. These data points are then used to fit a plane or hyper surface to the performance of the examined system, such as in Figure 4.7. For complex system which requires large number of analyses response surface method is used and system behavior is estimated by a polynomial function.

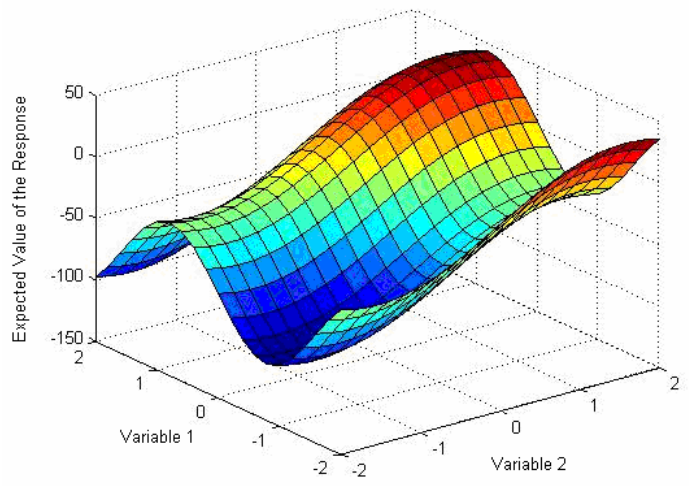

Figure 4.7. Response surface example for two variables

Classical way of performing experiments is based on one factor at a time method which varies only one factor or variable at a time while other variables are kept at their constant values. However, statistically designed experiments that vary several factors simultaneously are more efficient when working with the functions which are expected to be influenced by multiple factors. When the one factor at a time method and design of experiment methods are compared, it is seen that design of experiments requires less resources for the same amount of information obtained. In this study, this resource is the computer calculation time. Also, with the design of experiments the estimates of the effects of each factor are more precise and the interaction between each factor can be evaluated systematically where these interactions are possibly estimated by performing a hit and miss scattershot sequence of experiments if classical one factor at a time method is used. [49]

Design of experiments methods are generally used for process optimization studies but in this study, RS method is used to approximate the performance function of the system which is generally very difficult to express exactly in realistic problems. By this way an efficient way is obtained to handle the reliability problems which require complex analysis. By the utilization of response surface, the procedure in Monte Carlo simulation is simplified and the calculation time is decreased for a fixed number of sampling.

In RSM, if data follows a flat surface, a first order model is usually sufficient. If there is curvature in the data, a first order model would show a significant lack of fit and a higher order model must be used, such as:

$$y = b_0 + \sum_{i=1}^{k} b_i X_i + \sum_{\substack{i=1, j=2 \\ i<j}}^{k} b_{ij} X_i X_j + \sum_{i=1}^{k} b_{ii} X_i^2 \qquad \text{Eq (4.7)}$$

or a cubic response surface

$$y = b_0 + \sum_{i=1}^{k} b_i X_i + \sum_{i=1, j=i+1}^{k} b_{ij} X_i X_j + \sum_{i=1}^{k} b_{ii} X_i^2 + \sum_{i=1}^{k} b_{ii} X_i^3$$

$$+ \sum_{i=1, j=i+1, h=j+1}^{k} b_{ijh} X_i X_j X_h + \sum_{\substack{i=1, j=1 \\ i \neq j}}^{k} b_{ij} X_i^2 X_j \qquad \text{Eq (4.8)}$$

where y is the response of the system, X is the random variable and b are the constants of the close form response formulation.

After forming the response surface, limiting value for the response beyond which the system fails is defined (Figure 4.8). Then, numerical integration is performed to calculate the probability of failure.

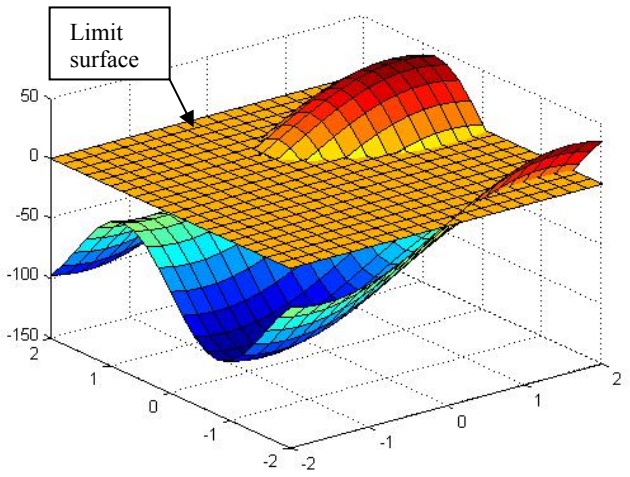

Figure 4.8. A sample response surface with a limit value plane

If it is desired to have a response value higher than the limit value the failure region can be illustrated as Figure 4.9.

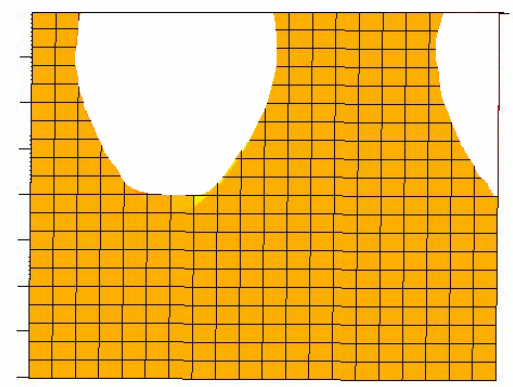

Figure 4.9. Failure region for the response given in Figure 5.5

Two most common designs generally used in response surface modeling are Central Composite (CC) designs and Box-Behnken (BB) designs. In these designs inputs take three or five distinct values (levels), but not all combinations of these values appear in the design to reduce the number of runs [32].

Details of this method can be found in References 32, 50, 51 and from the view of this study, information from these references are summarized in the following five sections.

4.5.1 Central Composite Designs

Central Composite Design method was first introduced by Box&Wilson and it is also known as Box-Wilson Design. To picture a central composite design, factors having low and high values between -1 to +1 are used since all variables are standardized to -1 and 1 in RS design [8].

This experimental design consists of factorial runs and runs at center point which are augmented with a group of `star points' that allow estimation of possible curvatures. The fractional points are at the corners of a unit cube that is the product of the intervals [-1, 1] and star points are along the axes at or outside the cube and center points at the origin. Central composite designs are of three types: Circumscribed (CCC) Inscribed (CCI) and Faced (CCF) designs [32].

CCC designs are the original form of the Central Composite design. Based on the number of factors in the design, star points are at a distance α from the center. And these designs require 5 levels for each factor. In short, augmenting an existing factorial design with star points can produce this design which is shown in Figure 4.10.

If the limits specified for factor settings are strict, experiments cannot be performed at the star points of the circumscribed design. CCI design uses the limit values as the star points and creates a factorial or fractional factorial design within those limits, in other words, a CCI design is a scaled down CCC design with each factor level of the CCC design divided by α to generate the CCI design by this way the star points take the values -1 and +1, and the cube points lie in the interior of the cube. This design also requires 5 levels of each factor (Figure 4.11).

In CCF design the star points are at the center of each face of the factorial space, so α = ± 1 (Figure 4.12). This type of design requires 3 levels of each factor.

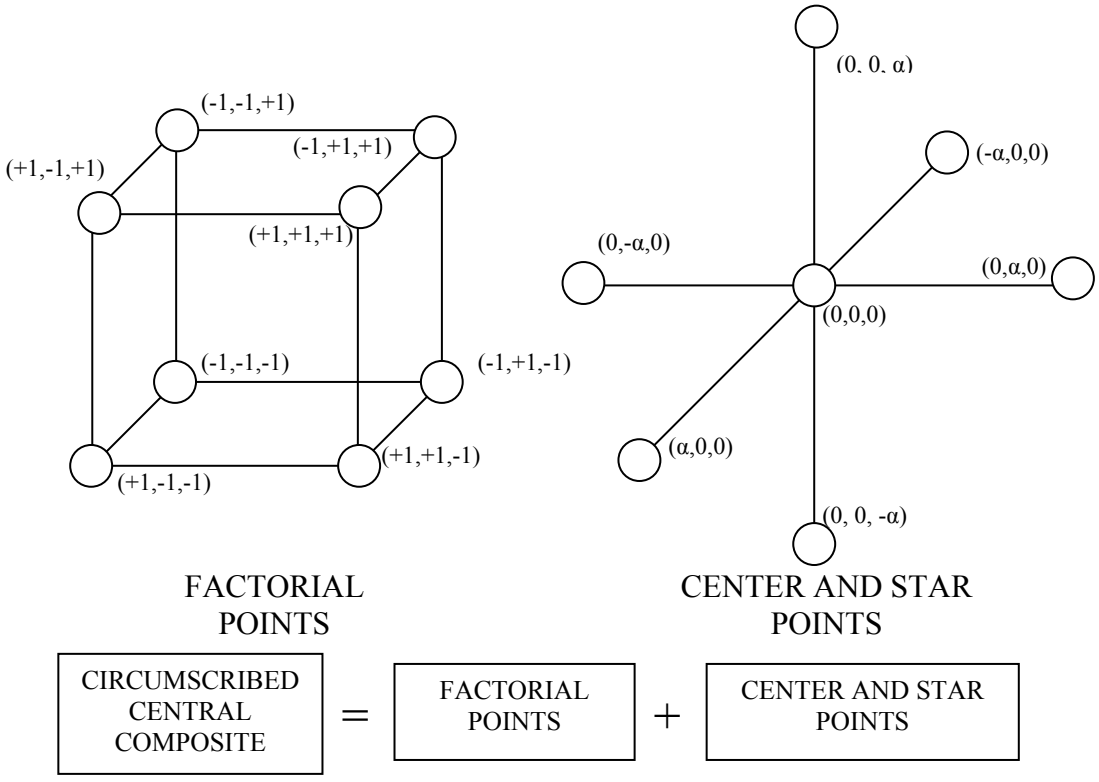

Figure 4.10. Central Composite Circumscribed (CCC) Design

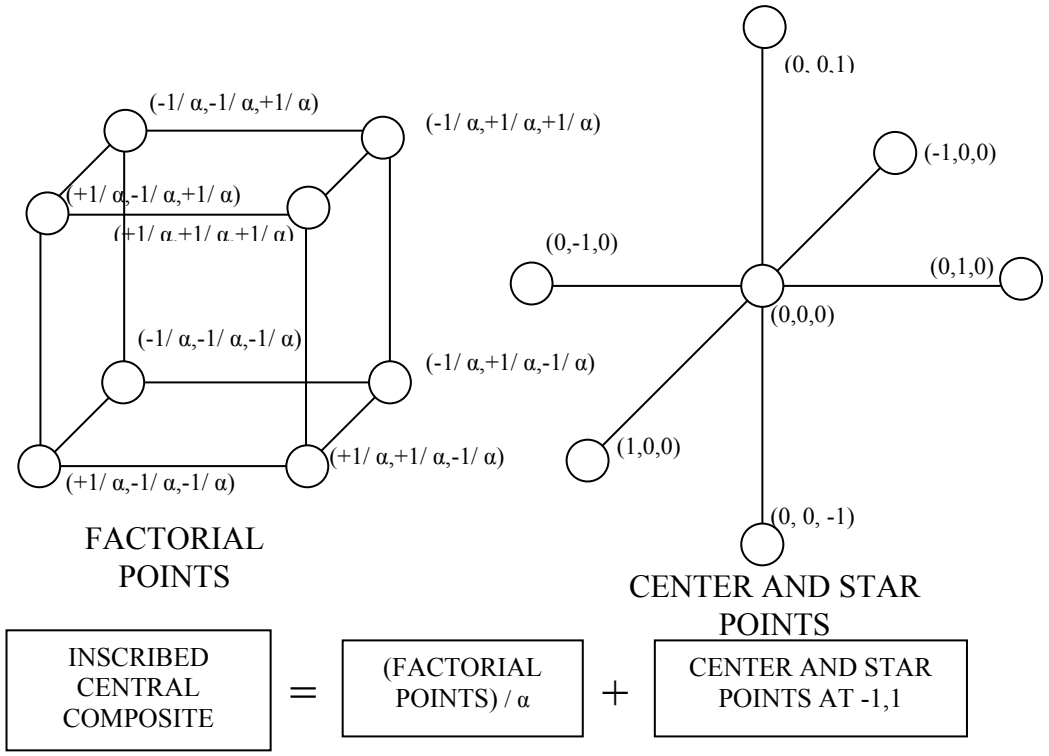

Figure 4.11. Central Composite Inscribe (CCI) Design

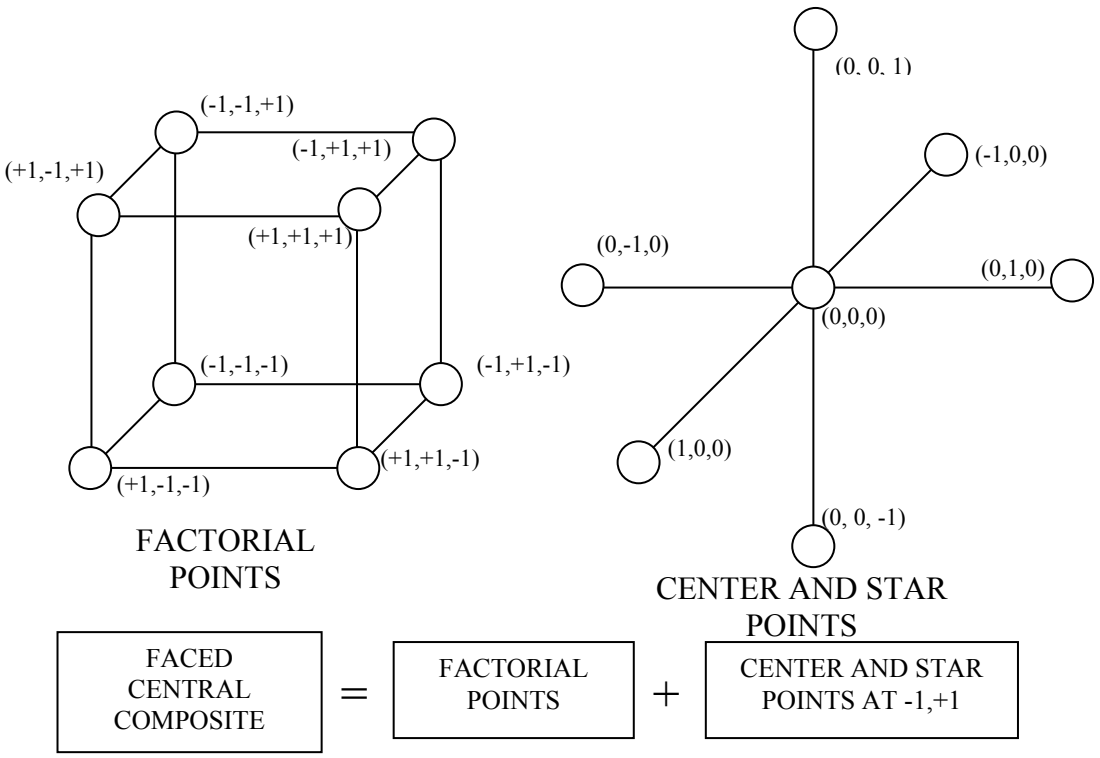

Figure 4.12. Central Composite Faced (CCF) Design

4.5.2 Box-Behnken Designs

Box-Behnken designs are response surface designs that can be used to fit a full quadratic model. Different than central composite designs, Box-Behnken designs use just three levels of each factor. Figure 4.13 shows a Box-Behnken design for three factors, with the circled point appearing at the origin.

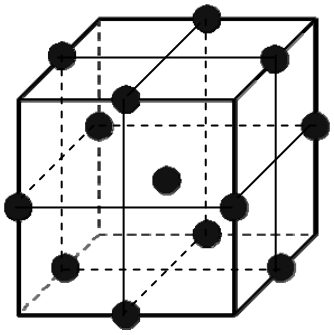

Figure 4.13. Box-Behnken Design

The Box-Behnken design is an independent quadratic design which does not contain an embedded factorial or fractional factorial design. Advantage of the Box-Behnken designs is that they generally provide adequate information with the least number of runs. Other designs generally produce more runs than needed for a quadratic fit. Box-Behnken's biggest pitfall is that it doesn't provide much information on the corners.

Comparison of the different design types are shown in Table 4.1. In this study CCC design is expected to be used more efficiently and to give better results since it recovers a larger are compared to other designs but to make comparisons and to illustrate its efficiency all the design types are examined. [32]

Table 4.1. Comparison of the response surface methods [32]

Design Type	Comment
CCC	CCC designs provide high quality predictions over the entire design space but require factor settings outside the range of the factors in the factorial part. Requires 5 levels for each factor.
CCI	CCI designs use only points within the factor ranges originally specified, but do not provide the same high quality prediction over the entire space compared to the CCC. Requires 5 levels of each factor.
CCF	CCF designs provide relatively high quality predictions over the entire design space and do not require using points outside the original factor range. However, they give poor precision for estimating pure quadratic coefficients. Requires 3 levels for each factor.
Box-Behnken	These designs require fewer treatment combinations than a central composite design in cases involving 3 or 4 factors. Its "missing corners" may be useful when the experimenter should avoid combined factor extremes. This property prevents a potential loss of data in those cases. Requires 3 levels for each factor.

4.5.3 Determination of “k” and “α”

k value sets how far are the data points will be from their mean values, such that:

- -1 in the response surface design is equal to $\mu - k.\sigma$
- 0 in the response surface design is equal to μ
- 1 in the response surface design is equal to $\mu + k.\sigma$

where μ is the mean value of the variables and σ is the expected standard deviation with normal distribution assumption for all the variables included in the response surface design. In reference 52, it was advised to use values between 1 and 3 for k

Similar to k, α is used to form response surface input matrix. α value is used to determine star points in the central composite design. At a star point, a variable get values equal to $\mu \pm \alpha .k.\sigma$ while other variables are at their mean vales i.e. at center point 0.

α depends on the number of experimental runs in the factorial portion of the central composite design:

$$\alpha = \left[2^{n-f}\right]^{\frac{1}{4}} \qquad \text{Eq (4.9)}$$

where n is the variable number and f is the order of the fraction used in the factorial design [32].

4.5.4 Fractional Design

As stated in section 4.5.1, Central Composite Design is a combination of 2-level factorial design points and star points. When the number of variables increases, the number of experimental runs becomes very large. For example, an experiment with 10 variables requires 2^{10} factorial points plus 20 star points and a center point. These large number of experiments cannot be performed and similarly for the method used in this study it is not possible to run a design code, i.e. a finite element code for thousands times.

Number of runs can be decreased by using fractional design with ½ ¼ or more fraction. This experiment reduction technique can simply be explained with a factorial design with three variables. This experiment requires 2^3 data points if full factorial design is used with the experiment points shown in Figure 4.14 and Table 4.2. However in these 8 runs can be reduced to 4 with a ½-fractional design

as shown in Figure 4.15 and Table 4.3. The disadvantage of fractional design is combining the interaction effect of X1 and X2 with the main effect of X3. In this experiment main effect of X3 will also include the interaction effect of other variables. The important thing while eliminating the experiment points for a 3-variable factorial design is not to have three points on a single plane. By this way, all main effect can be seen at the end of the experiments. For three variables; elimination can be done visually by using three axes but it is not possible to visualize the design for four and more variables. For this purpose the design resolution is calculated before deciding the elimination of the experiments.

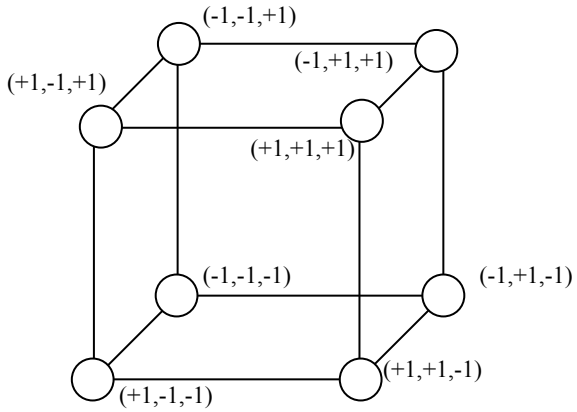

Figure 4.14. 2-level factorial design with 3 variables

Table 4.2. 2-level factorial design with 3 variables

Run Number	X1	X2	X3
1	-1	-1	-1
2	+1	-1	-1
3	-1	+1	-1
4	+1	+1	-1
5	-1	-1	+1
6	+1	-1	+1
7	-1	+1	+1
8	+1	+1	+1

Design resolution is a measure which the quality of the experiment elimination and it is the minimum variable number in an interaction term which has an effect augmented to a main effect of any variable. For example in this case design resolution is two since X3 includes the interaction effects of tow variables X1 and X2. In this study, response surface design is performed with 12 variables and using fractional factorial designs is a necessity but best design resolution is obtained by seeking different combinations before constructing the response surface input matrix.

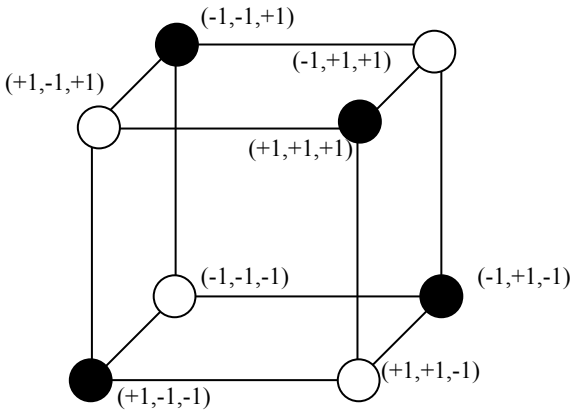

Figure 4.15. 2-level 1/2 fractional factorial design with 3 variables

Table 4.3. 2-level 1/2 fractional factorial design with 3 variables

Run Number	X1	X2	X3=X1.X2
1	-1	-1	+1
2	+1	-1	-1
3	-1	+1	-1
4	+1	+1	+1

4.5.5 Least Squares Regression

Suppose that v depends on the variables x and y, i.e. v=f(x,y) and n number of observation for x,y and v is performed. Then an equation in the following form which provides the least-squares fit of the data can be written:

$$v(x,y) = A + Bx + Cy + Dx^2 + Ey^2 + Fxy \qquad \text{Eq (4.10)}$$

This equation is found by using multiple linear regression. The equation seen above is a full quadratic model with 2 variables. The coefficients A, B, C, D, E, and F can be found by solving the following linear system.

$$\begin{bmatrix} n & \sum x & \sum y & \sum x^2 & \sum y^2 & \sum xy \\ \sum x & \sum x^2 & \sum xy & \sum x^3 & \sum xy^2 & \sum x^2y \\ \sum y & \sum xy & \sum y^2 & \sum x^2y & \sum y^3 & \sum xy^2 \\ \sum x^2 & \sum x^3 & \sum x^2y & \sum x^4 & \sum x^2y^2 & \sum x^3y \\ \sum y^2 & \sum xy^2 & \sum y^3 & \sum x^2y^2 & \sum y^4 & \sum xy^3 \\ \sum xy & \sum x^2y & \sum xy^2 & \sum x^3y & \sum xy^3 & \sum x^2y^2 \end{bmatrix} \cdot \begin{Bmatrix} A \\ B \\ C \\ D \\ E \\ F \end{Bmatrix} = \begin{Bmatrix} \sum v \\ \sum xv \\ \sum yv \\ \sum x^2v \\ \sum y^2v \\ \sum xyv \end{Bmatrix}$$

When there is large number of variables, the size of the matrix seen above increases dramatically. Every new variable brings its first and second order terms and also its interaction terms with other variables. When the number of variable increased, solving such a large linear system of equations becomes computationally hard. Since conventional matrix inversion and Gauss elimination techniques may produce bad fits in case of ill conditions in matrix operations, singular value decomposition (SVD) which is one of the methods to solve such large linear equation systems can be used.

4.6 DISCUSSION ON RELIABILITY CALCULATION METHODS

Analytical methods mentioned in this chapter are expected to give results with large errors since they applied for linear performance functions or they can be used after linearization of the performance function. For non-linear functions linearization may lead to large errors. Also it is not a good way to use these

methods for multiple failure modes where the correlations among these failure modes are unknown. For example; if a rocket motor is considered, a variable which affects the thrust time curve of the rocket may also affect the maximum pressure in the chamber which is the load for the structural reliability of the casing. In this case, if analytical methods are used i.e. FOSM, probability of the casing failure and probability of the thrust failure are calculated separately and without the correlation information total probability of failure is calculated by summing the failure probabilities which results in an over estimated probability of failure. In this study direct Monte Carlo simulation which is a well proven reliable method is going to be used since it can be performed with a simple algorithm and results can be obtained with any desired accuracy by changing the sampling number in the simulation. However, increasing sample size in MCS will increase the simulation time.

A common problem for all these methods is the definition of the performance function. For simple problems, analytical definition of the performance can be written but for real life applications generally it is not possible to write an expression for the system performance, i.e. for a structural analysis, performance of the structure is predicted by a finite element code. In these cases analytical methods are not applicable to predict the reliability but Monte Carlo simulation can still be used by running the finite element code for each sampling. However, the accuracy of the prediction code i.e. finite element code affects the Monte Carlo simulation results and for the cases where complex analyses are needed simulation time increases tremendously. To decrease the calculation time in Monte Carlo simulation, response surface method is used to determine performance functions.

CHAPTER 5

CALCULATION PROCEDURE USED TO ASSESS RELIABILITY

5.1 GENERAL

Assessments in this study are based on the calculation of the probability integral given in Equation 4.1. Since this integral is difficult to calculate analytically, Monte Carlo simulation (MCS) is utilized to calculate the probability integral and response surface method (RSM) is used to determine performance functions since there is not any analytical formulation for the responses under consideration.

Briefly, the calculation procedure is as follows: First, failures which are thought to be effective on the system reliability and then the variables which change the system performance related to these failures are determined. If possible, variations of the input variables measured or the coefficient of variation values in the literature for the same variable is used. With the statistical data on the input variables (i.e. distribution type, distribution parameters), experiments are designed by using response surface method.

Depending on the system these experiments can be real time experiments or the results are obtained by a computer code such as finite element calculations. Knowing the system performance on different points determined by the design of experiment method, a polynomial function with the higher order terms and interaction terms is fitted for each mode of failure. Finally, random data generated

for all variables and each failure function is evaluated for this randomly generated system state. Random generation is repeated many times and at the end of the simulation, ratio of the failure number and simulation number will give an approximation for the probability of the failure.

In this study, a software is developed to perform all of these calculations to decrease the calculation time and to increase reliability and repeatability. The computer code which was written in Delphi programming language is introduced in following sections while explaining the calculation procedure in details.

5.2 SOFTWARE DEVELOPED FOR RELIABILITY ASSESSMENT

The main part of the reliability calculations in this study is the application of a numerical method –Monte Carlo simulation- to calculate the probability integrations. Monte Carlo simulation can only be done with a computer code as it requires millions of runs, calculation time in Monte Carlo simulation may take days if the simulation is performed with a finite element code. Therefore, Monte Carlo simulation is not a time effective way to calculate reliability if the simulated function cannot be defined with simple functions. For the cases where the performance function cannot be analytically defined; response surface method is used to define such a function. For response surface design and fitting some commercial codes can be used but these codes are not able to perform Monte Carlo simulation at the same time.

Results in this study are obtained by combining two different methods which are not suitable for manual calculation. In addition to necessity of using computer codes for Monte Carlo simulation and response surface method, an interface between the code used for simulation and the code used for response surface approximation is needed since it is not practical to transfer functions from one code to an other for a system with multiple failure modes and several input variables since the polynomial functions include many terms. Also when the number of the input variables increases many commercial codes that can be used for response surface design are failed to give results since number of variable in these softwares are generally limited to ten variables. Moreover, they generally

can fit only quadratic functions. A computer code which is expected to be used in this type of calculations should be capable of response surface designing without a variable limitation and can fit cubic functions since the higher the order of the performance function, better is the response surface approximation for non linear system behaviors. Besides these properties, the code should be capable of evaluating multiple functions for each random sampling since each failure mode is represented by a different performance function in these analyses. In this study to perform these operations, a computer code is developed by using Delphi and the user interface of the developed code is given in Figure 5.1.

This software is capable of designing response surface experiments based on Box-Behnken Design, Full Central Composite Design and Fractional Composite Design without limitations on the fraction value and number of variable. Besides the response surface design and fitting, it can perform Monte Carlo simulation with the functions determined by the response surface method or entered manually by the user. With the limit states entered, it gives the integration result which is the estimation of Probability of failure, P_f.

The two flow charts which explain the procedure followed in this study and also in the developed software are given in Figure 5.2 and Figure 5.3. With this software, two methods can be used for failure probability calculations: user can select either direct Monte Carlo simulation with a computer program which can predict the system performance or to use response surface method and Monte Carlo simulation together.

If Monte Carlo simulation is used alone, random numbers are generated for the input variables of the code used to predict the system performance and outputs are collected for each simulation. In this study, to predict the rocket motor's ballistic performance, a software (SimP(x)) which is a FORTRAN based software developed by TÜBİTAK-SAGE Internal Ballistic Division was used. Information on this software is given in 5.3.

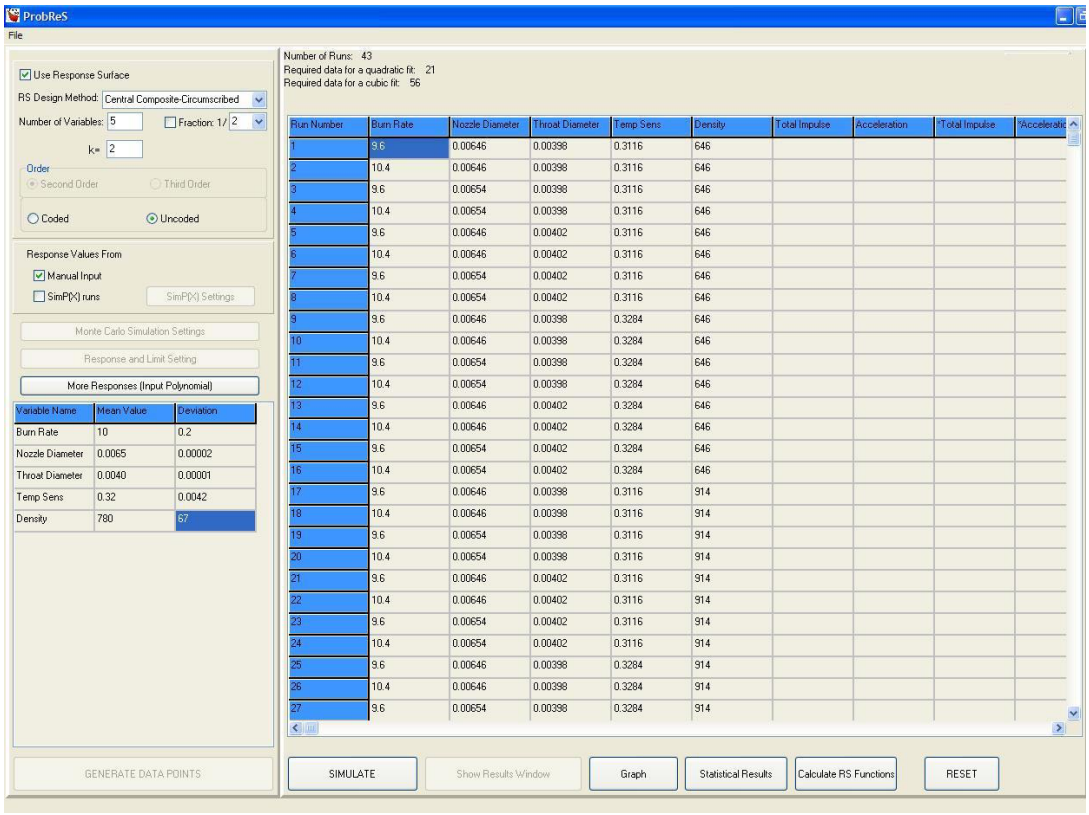

Figure 5.1. User interface of the developed computer code

If response surface method is selected to predict system performance then ballistic performance prediction software is executed with the input files which include the values determined by the response surface method. After collecting the outputs, polynomial functions are fitted to this data with the method mentioned in Subsection 4.5.5. Then, Monte Carlo simulation is performed with the fitted functions by generating random numbers to the input variables.

Besides the rocket motor ballistic performance calculations, response surface method is also used with the finite element analyses where the calculation time is an important measure when they are used in Monte Carlo simulation.

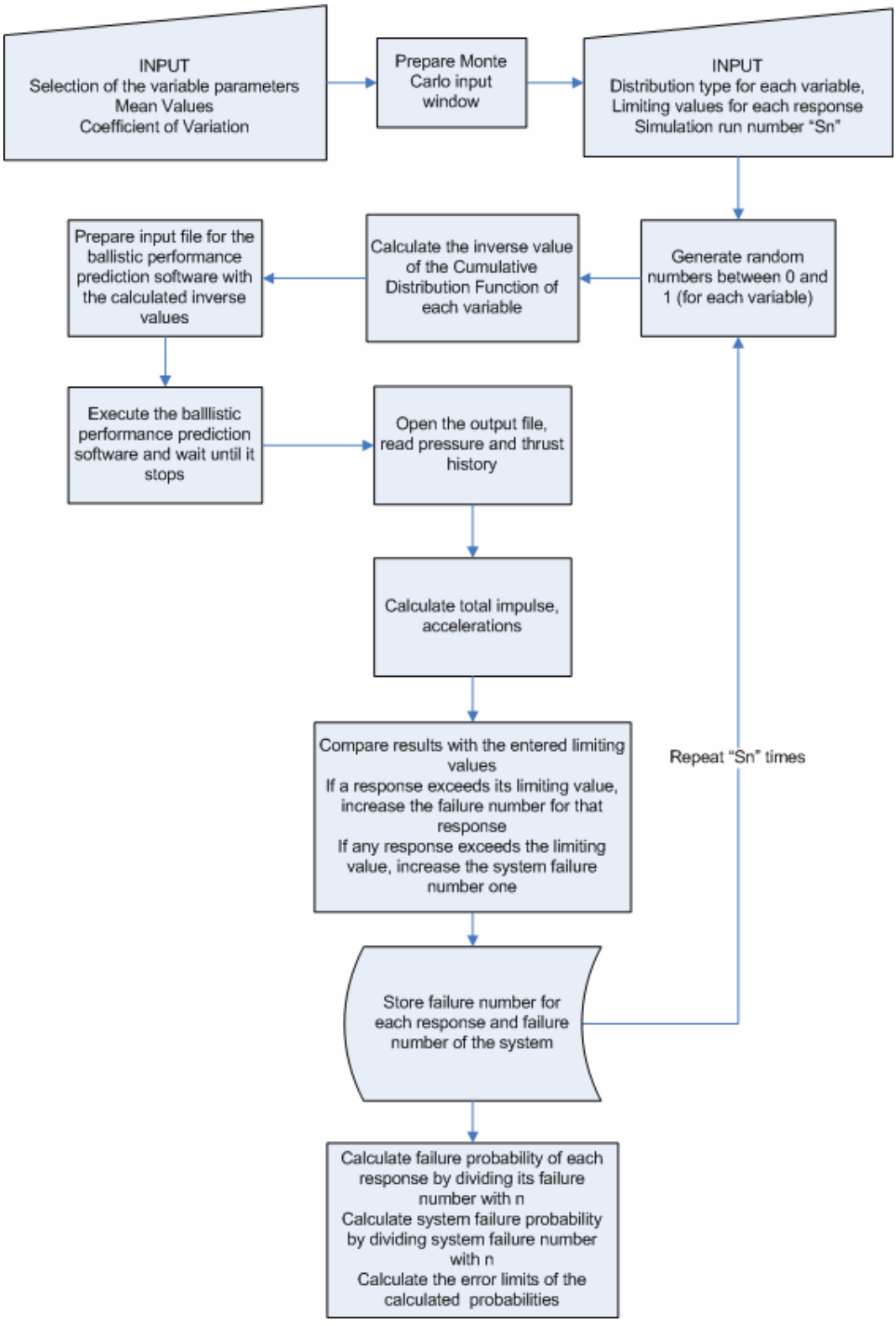

Figure 5.2. Flowchart for Monte Carlo simulation without response surface

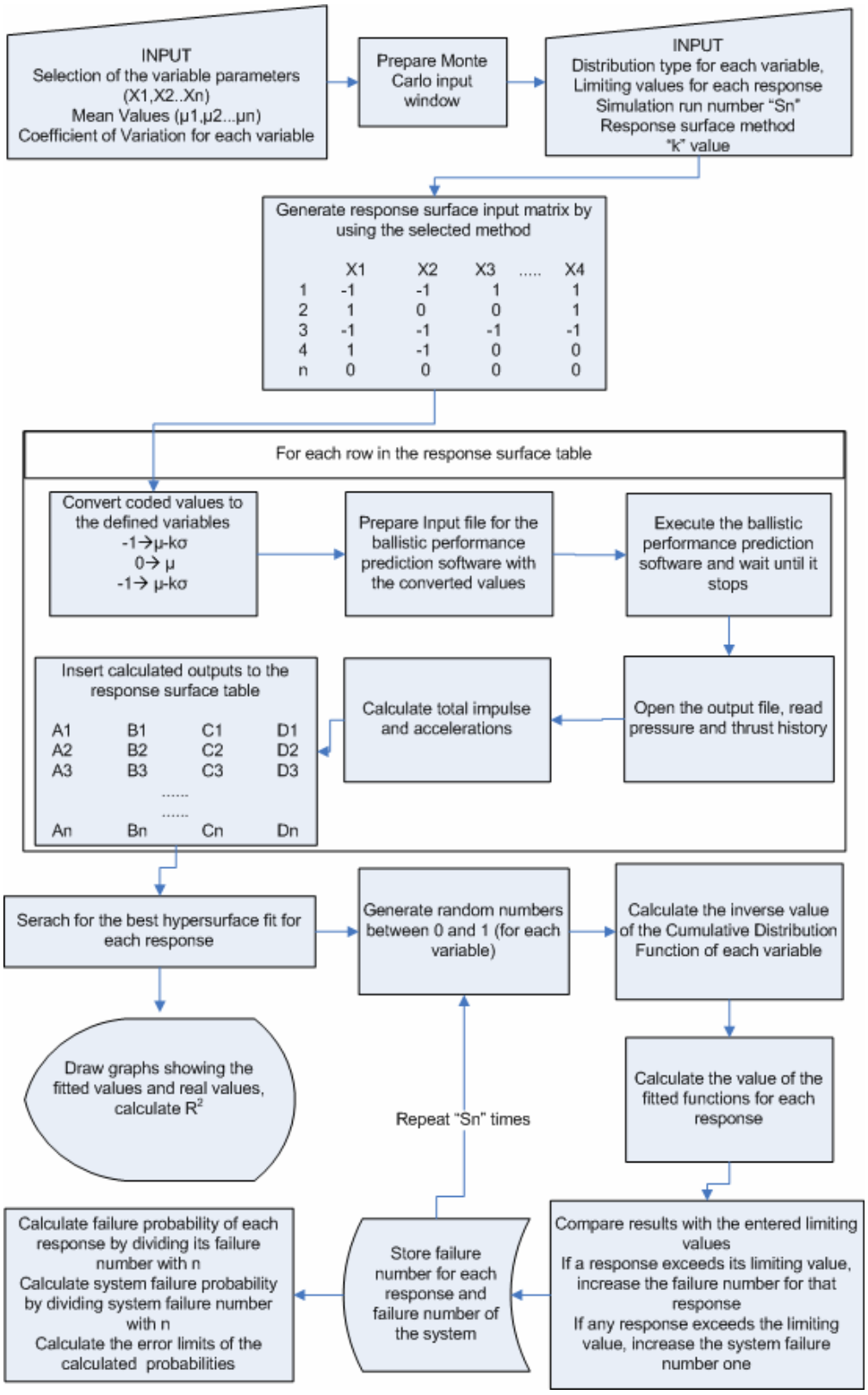

Figure 5.3. Flowchart for Monte Carlo simulation with response surface fitting

5.3 BALLISTIC PERFORMANCE PREDICTION CODE

In this study, rocket motor performance prediction calculations are performed by utilizing software which was developed by Internal Ballistic Division of TUBITAK-SAGE. In this software, pressure, density and velocity distributions along the rocket motor case is found by solving one-dimensional steady conservation equations of mass, momentum and energy numerically. In this software, solid propellant grain is divided into finite number of cells and the regressing solid propellant grain surfaces are modeled as injection surfaces which inject high temperature combustion gases inside the solid motor case. The propellant surfaces regress during the operation of the motor, therefore the geometry is updated during the performance calculation. Solid propellant grain surfaces are obtained for discrete burn back steps.

Accuracy of this simulation tool was tested with static firing test of a solid propellant rocket motor similar to the rocket motor examined in this study.. A graph to compare test results and simulation results is given in Figure 5.4. The difference between the maximum pressure predicted in the simulation and measured in the experiment was found to be 1.7%.

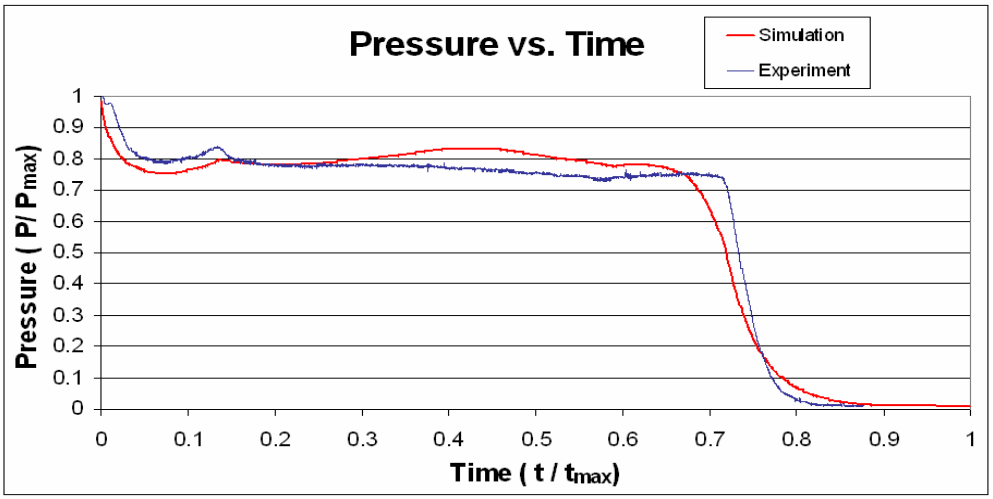

Figure 5.4. Comparison of Pressure vs. Time curve obtained from the experiment and simulation for a solid rocket motor

CHAPTER 6

ROCKET MOTOR RELIABILITY ANALYSIS AND RESULTS

6.1 GENERAL

In this chapter, reliability of a solid propellant rocket motor which was developed by TÜBİTAK-SAGE is investigated. For this purpose, the procedure outlined in chapter 5 was applied by considering its performance requirements which were determined from the specifications. In addition to assessing reliability, sensitivity of the rocket motor performance to these parameters was also determined and a new design point is proposed to increase the reliability of the rocket motor. Applicability of response surface method to a rocket motor and its effects on the results are also discussed.

Since Monte Carlo simulation is a well proven method and the accuracy of the simulation depends on sampling number, with this method, one can estimate the results with the desired accuracy. In this case the error source is the ballistic performance calculations, only. Using a response function creates additional error by the response surface experiment design and surface fitting. This additional error and how it is affected from the experiment design method is also discussed in this chapter. For this purpose, different response surface design techniques such as Circumscribed Composite, Faced Composite and Box-Behnken design with different k values and different fractions were used.

Failure modes of a rocket motor were discussed in section 2.3 and risk priorities were given in Table 2.4. In section 2.3, the most critical failure mode was determined as the over pressurization of the motor beyond its ultimate limits which causes a casing failure, moreover, casing failure due to the production faults and weak material is also graded as unacceptable. Besides the casing failure, other failures are directly related with the ballistic performance of the rocket motor. In this chapter, these failures are analyzed and the progress is explained in the following sections.

6.2 LIMIT STATE FUNCTIONS OF THE ROCKET MOTOR

Performance requirements of the rocket motor studied in this thesis are determined by considering the mission requirements of the rocket. During the conceptual design phase the following ballistic performance requirements are defined and ballistic reliability is examined with these limit values. These performance requirements are required to be fulfilled in a temperature range of -35° C to +60° C.

i. The total impulse of the motor shall be grater than 7500 N.s. to obtain desired range. Then the limit state function for this requirement is:

$$g_1 = I_t - 7500 \qquad \text{Eq (6.1)}$$

where I_t is the total impulse obtained from any rocket motor.

ii. To activate the fuse of the rocket, the rocket motor must supply an acceleration greater then 27g for at least 0.63 second. Arming acceleration for fuse: a_a>27g, for a duration of at least 0.63 s. Limit state function for this performance requirement is:

$$g_2 = \Delta t\left(a_a > 27g\right) - 0.63 \qquad \text{Eq (6.2)}$$

iii. The acceleration of the rocket at launcher exit shall be grater than 35g and the limit state function g_3 is:

$$g_3 = a_L - 35 \qquad \text{Eq (6.3)}$$

where a_l is the launch acceleration.

iv. As a loading limit obtained by considering the structural capacity of all components of the rocket motor, the maximum acceleration of rocket shall be less than 100g. Then limit state function is:

$$g_4 = 100 - a_{\max} \qquad \text{Eq (6.4)}$$

v. Addition to ballistic performance, the structural performance of the casing with 1.84 mm nominal thickness and with the material 2014-T6 aluminum alloy is also estimated. The maximum stress in any part of the motor case shall be less than tensile strength of the case material

$$g_5 = S_{T,case} - \sigma_{\max} \qquad \text{Eq (6.5)}$$

Hence, there are five performance functions to evaluate in the probability integral to obtain ballistic performance reliability and structural reliability of the casing.

6.3 RESPONSE SURFACE DESIGN FOR LIMIT STATE FUNCTIONS

With these performance functions, reliability analysis is divided into two groups: ballistic performance reliability and structural reliability. As stated in chapter 5, first it is needed to fit a response surface model to the performance functions defined above and for this purpose inputs that have effect on the performance functions are determined.

The parameters included for the ballistic performance calculations are:

a) The propellant properties
   i. Burn rate constant (a_r)
   ii. Temperature sensitivity of burn rate(S_{Temp})
   iii. Density (ρ)
   iv. Enthalpy of the combustion gases (H)

b) Motor dimensions
   i. Nozzle throat diameter
   ii. Nozzle exit diameter
   iii. Propellant grain geometry (L_1, L_2, R_1, R_2, Grain Length) (Figure 2.4)
   iv. Tapered angle of the grain (ζ)

The ballistic performance parameters such as internal pressure, total impulse and acceleration profile all depend on the parameters listed above. Ambient temperature has also effect on the results and calculations are performed at different operating temperatures -35ºC, +20 ºC and 60ºC.

In addition to the parameters given above, such parameters must be defined for the structural calculations. The rocket motor casing (Figure 6.17) can be thought as a cylindrical tube with one end is open and the nozzle is mounted to the open end of the casing by using a lockwire.

The parameters included in the response surface models to estimate the maximum stress at the rocket motor casing are:

a) Case dimensions
   i. Case thickness (t_1)
   ii. Case thickness at nozzle interface (t_2)
   iii. Thickness of the lock wire at the nozzle joint (t_3)

b) Internal pressure of the rocket motor

Since the rocket under consideration is an unguided rocket, the aerodynamic forces assumed to be negligible compared to the pressure load in the rocket motor. Taking the internal pressure as an input parameter for the stresses at the casing, the ballistic performance becomes an input parameter for the structural calculations.

Hence, there are five different performance functions and if one of these functions takes a value smaller than zero, rocket motor fails to fulfill its function. Defined limit state functions are:

$$g_1 = I_t(a_r, S_{Temp}, \rho, \xi, H, \phi_{Throat}, \phi_{Exit}, L_{Grain}, L_1, L_2, R_1, R_2) - 7500 \quad \text{Eq (6.6)}$$

$$g_2 = \Delta t_{a>27g}\left(a_r, S_{Temp}, \rho, \xi, H, \phi_{Throat}, \phi_{Exit}, L_{Grain}, L_1, L_2, R_1, R_2\right) - 0.63 \quad \text{Eq (6.7)}$$

$$g_3 = a_L(a_r, S_{Temp}, \rho, \xi, H, \phi_{Throat}, \phi_{Exit}, L_{Grain}, L_1, L_2, R_1, R_2) - 35 \quad \text{Eq (6.8)}$$

$$g_4 = 100 - a_{\max}(a_r, S_{Temp}, \rho, \xi, H, \phi_{Throat}, \phi_{Exit}, L_{Grain}, L_1, L_2, R_1, R_2) \quad \text{Eq (6.9)}$$

$$g_5 = S_{T,case} - \sigma_{\max}(a_r, S_{Temp}, \rho, \xi, H, \phi_{Throat}, \phi_{Exit}, L_{Grain}, L_1, L_2, R_1, R_2, t_1, t_2, t_3) \quad \text{Eq (6.10)}$$

Then, ballistic performance reliability depends on the variation of 12 random variables and structural reliability depends on 16 random variables. Variations of the propellant properties were determined by using data including twenty measurements for each of them. In addition to the propellant properties, the dimensional variables are assumed to be normally distributed in the range of tolerances. Material properties and their distributions are found from the literature. Input variables and their distributions are given in Table 6.1.

Table 6.1. Input variables

#	Variable Name	Coeff. Of Variation	Distribution Type
X1	a_r (Burn Rate Constant of the Propellant)	0.0283	Normal
X2	ρ (Density of Propellant)	0.0033	Normal
X3	H (Enthalpy of Propellant Combustion)	0.0088	Normal
X4	S_{Temp} (Temperature Sensitivity of the burn rate)	0.35	Normal
X5	ζ (Tapered Angle of the Grain)	0.029	Normal
X6	L_{Grain} (Grain Length)	0.0047	Normal
X7	Φ_{Throat} (Nozzle Throat Diameter)	0.008	Truncated Normal
X8	Φ_{Exit} (Nozzle Exit Diameter)	0.021	Truncated Normal
X9	R_1 (Grain Geometry Parameter)	0.005	Normal
X10	R_2 (Grain Geometry Parameter)	0.01	Normal
X11	L_1 (Grain Geometry Parameter)	0.0007	Normal
X12	L_2 (Grain Geometry Parameter)	0.0009	Normal
X13	t_1 (Casing Thickness)	0.023	Truncated Normal
X14	t_2 (Casing Thickness at the Nozzle Interface)	0.015	Truncated Normal
X15	t_3 (Lockwire thickness)	0.004	Truncated Normal
X16	S_{Casing} (Casing Material Ultimate Tensile Strength)	0.058	Truncated Normal

In this study, the performance of the rocket motor is estimated in two ways, at first direct Monte Carlo simulation is used with the ballistic performance prediction code. Secondly, a response surface experiment is designed in order to fit response surface function to the performance values obtained from the ballistic

performance prediction software solutions and then these functions are used in the Monte Carlo simulation.

To evaluate the applicability of the response surface method for the ballistic performance estimation, calculations are done with and without using response surface functions. For comparison purposes, this calculation repeated several times with different response surface experiment designs.

For 12 random variables, different response surface designs require different number of runs. These numbers are given in Table 6.2.

Table 6.2. Required number of runs for different response surface designs (For 12 variables)

Response Surface Design Method	Fraction	Number of Runs
Central Composite (Circumscribed, Inscribed, Faced)	1	4121
	1/2	2073
	1/4	1049
	1/8	537
	1/16	281
	1/32	153
	1/64	89
Box-Behnken	1	193

The reason for using response surface approximation in the reliability estimation is to decrease the calculation time. However, it is seen that, using a response surface design without fraction has almost no advantage on calculation time since it again requires large number of runs. Then it is not a practical way to use response surface designs up to ¼ fraction for the simulations with large number of variables. In this case, for 12 variable, 91 data point is required to fit a quadratic response surface, therefore 1/64 fraction, which gives 89 data points, cannot be used. For this reason fractions between 1/4 and 1/32 are used in RS design and

results are compared with the results obtained from the Monte Carlo simulations without response surface functions.

6.4 COMPARISON OF DIFFERENT RESPONSE SURFACE METHODS

Since functions obtained by using response surface method are used in the simulations as a substitute of the performance prediction software or finite element analysis software, response surface method's accuracy is very important and may have effects on the results. For this reason, to proceed further in calculations, it is important to be sure that response function is accurate enough. To evaluate different types of response surface method, maximum pressure estimation is used as a case study since the pressure characteristics of a rocket motor is directly related with other performance measures.

The pressure profile of a rocket motor is mainly affected by propellant properties, grain geometry and nozzle geometry. Then, maximum pressure is a function of a_r, S_{Temp}, ρ, H, ζ, φ_{Throat}, φ_{Exit}, L_{Grain}, L_1, L_2, R_1, R_2. With these input parameters and constant ambient temperature at +60ºC, maximum pressure distribution is estimated by two different methods. Firstly, it is estimated by using Monte Carlo simulation with ballistic performance prediction software. Secondly, the same calculations are performed with response surface functions which are formed by following the procedure outlined in Section 4.5.

The results obtained from the first method are used as a basis for comparing the different response surface methods. Although all results in this thesis study are obtained by one million sampling, in this part of the study 20000 sampling is used because of the long calculation time of Monte Carlo simulation when it is used without response surfaces. To seek the best combination of k, fraction and RS design method, second method is repeated 21 times with different experiment design methods, different k values and different fractions. In each case, a hypersurface function is obtained for the maximum pressure and Monte Carlo simulation was performed with these functions. To have results comparable with the first method's results again 20000 samples are used. Results obtained by using Monte Carlo simulation with ballistic performance prediction software are given

in Table 6.3. MC simulation result shows that maximum pressure of the rocket motor has a normal distribution characteristic (Figure 6.1).

Table 6.3. Results for maximum pressure obtained by MCS with ballistic performance prediction software

Monte Carlo simulation Number	Mean [bar]	Standard Deviation [bar]	95% Confidence Interval of Mean		95% Confidence Interval of St. Dev		Simulation Time [hours]
			Lower	Upper	Lower	Upper	
20000	121.18	5.34	121.10	121.25	5.29	5.40	39

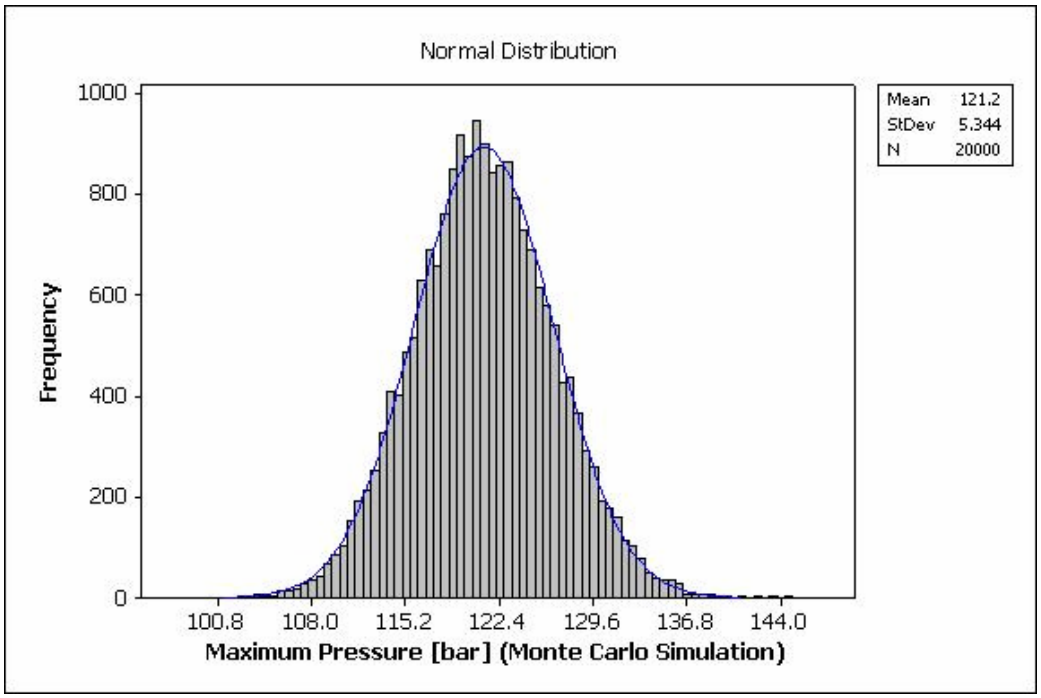

Figure 6.1. Maximum pressure distribution with Normal Distribution Curve

The results obtained by using response functions obtained for 21 different cases are tabulated in Table 6.4. Calculation time and R^2 value which is a commonly used measure of fitting quality is also given in this table for each case. Although R^2 values for all cases are greater than 0.99, the mean and standard deviation

estimations are not consistent with the results obtained by MC Simulation with ballistic performance prediction software. The calculated means and standard deviations by using Central Composite Circumscribed response surface design and Central Composite Faced response surface designs are almost same with the result given in Table 6.3. However, it can be seen that Box-Behnken Design gives large errors. At this point, it is important to note that BB Design uses 193 data points for 12 variables and Central Composite designs with 1/32 fraction use 89 data points for the same number of variable (Table 6.2). R^2 values calculated for the Box-Behnken Designs are also larger than Central Composite designs with 1/32 fraction. Although Box-Behnken design uses 104 extra data points and have larger R^2 value it is unable to estimate mean and standard deviation of maximum pressure. This conflict is illustrated in Figure 6.2 and Figure 6.3. Figure 6.2 shows the real values versus estimated values at the Box-Behnken design points. A function which has an R^2 value close to 1 is expected to give estimations on x=y axis of the expected vs. fitted values graph.

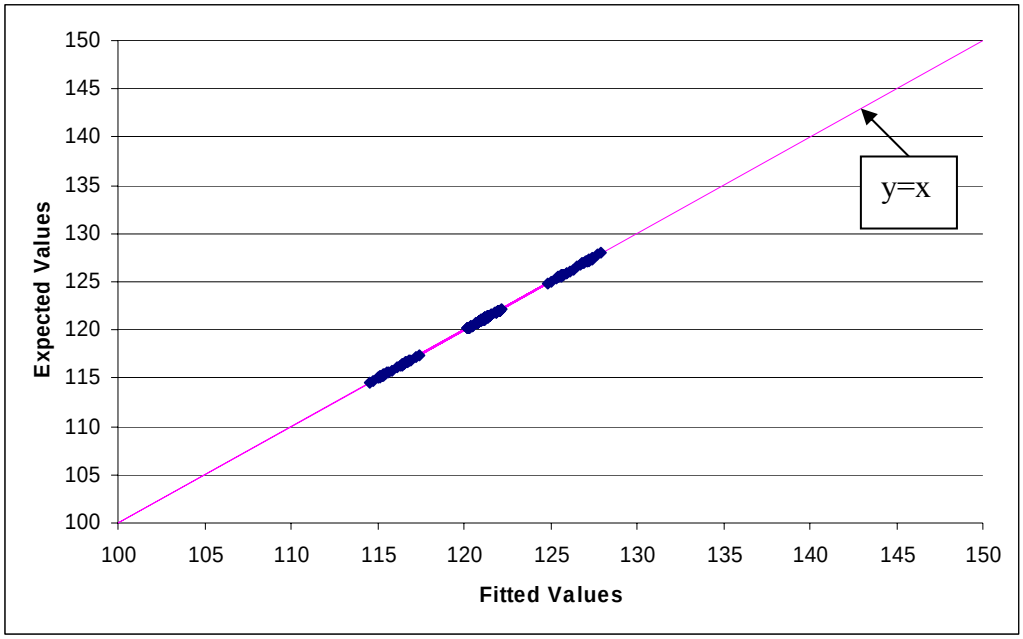

Figure 6.2. Expected vs. Fitted values for Box-Behnken design at response surface design points

Table 6.4. Response surface&Monte Carlo simulation results for maximum pressure estimation

Response Surface Method	Mean	StDev	R^2 for RS Fitting	Calculation Time (Hours)
CCC 1/8 k=1	121.12	5.37	0.999665	1.15
CCC 1/8 k=2	120.46	5.46	0.996940	1.15
CCC 1/8 k=3	121.24	5.56	0.998809	1.15
CCC 1/16 k=1	121.2	5.31	0.999925	0.65
CCC 1/16 k=2	121.11	5.46	0.997262	0.65
CCC 1/16 k=3	121.31	5.57	0.999099	0.65
CCC 1/32 k=1	121.22	5.36	0.999993	0.40
CCC 1/32 k=2	121.71	5.49	0.997856	0.40
CCC 1/32 k=3	121.69	5.69	0.996255	0.40
CCF 1/8 k=1	121.21	5.32	0.999991	1.15
CCF 1/8 k=2	121.21	5.36	0.999691	1.15
CCF 1/8 k=3	121.19	5.53	0.999049	1.15
CCF 1/16 k=1	121.14	5.32	0.999991	0.65
CCF 1/16 k=2	121.24	5.38	0.999863	0.65
CCF 1/16 k=3	121.25	5.59	0.999408	0.65
CCF 1/32 k=1	121.19	5.27	0.999992	0.40
CCF 1/32 k=2	121.21	5.31	0.999849	0.40
CCF 1/32 k=3	121.16	5.45	0.999296	0.40
Box-Behnken k=1	65.9	1265.35	0.999966	0.48
Box-Behnken k=2	55.91	486.53	0.999992	0.48
Box-Behnken k=3	60.2	178.69	0.999299	0.48

Since the calculated points are on the x=y line, it can be said that this function gives correct results on the RS design points. Although Figure 6.2 is generally accepted as an evidence of a good fit, weakness of the Box-Behnken design for this case can be shown by using cross validation of the fitted function with the ballistic performance prediction software. In cross validation, all variables are assumed to have uniform distribution and random numbers are generated for these variables for several cases. For each randomly generated data set, the maximum pressure is estimated by using ballistic performance prediction software and at the same time by using RS function obtained from Box-Behnken Design Method.

Graph which shows the cross validation results is given in Figure 6.3. Figure 6.2 and Figure 6.3 shows that RS function obtained from BB design does not represent maximum pressure characteristic in the range of the variation but only gives good estimations on special points which are the design points of BB Design. Then, it can be concluded that BB design cannot be used to estimate the response of the rocket motor examined in this study and R^2 is not a valid parameter to evaluate the quality of a surface fitting.

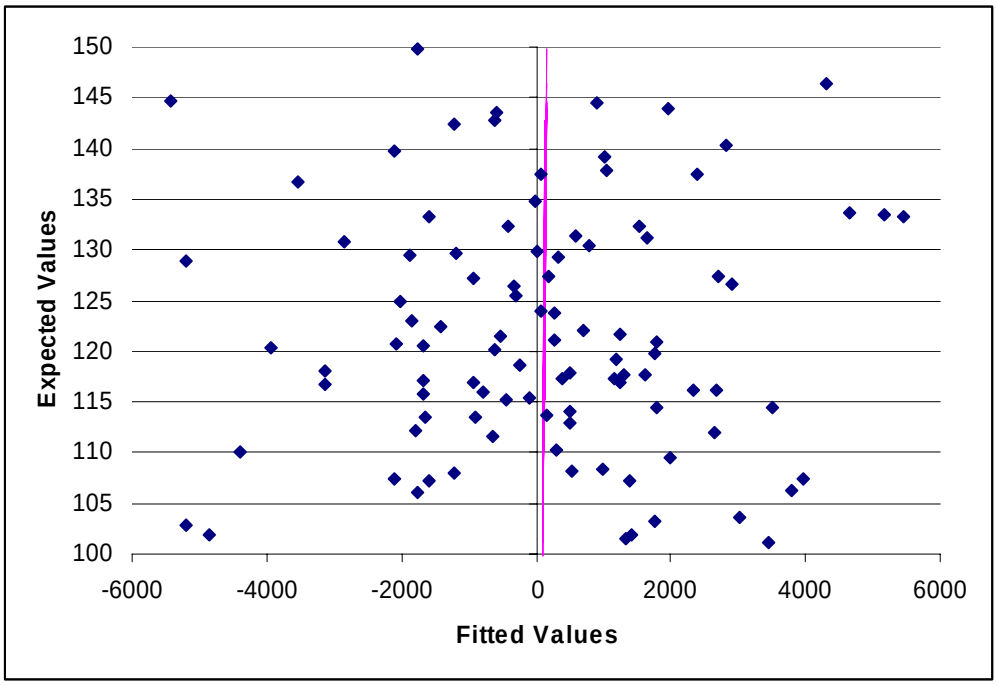

Figure 6.3. Expected vs. Fitted values for Box-Behnken design at random points

Since it is not possible to use infinite number of samples in the simulation an error bound always exist for the estimations. Although, CC designs give results with small deviations, a comparison among these methods can be made by using lower and upper limits of the mean and standard deviations. These values are given in Table 6.5 and presented visually in Figure 6.4 and Figure 6.5. Although errors are very small for all CC designs, it can be seen that results obtained from the CCF design with k value 3 and results obtained from the CCC design with k values 2 and 3 are statistically different than the Monte Carlo simulation solutions. With

20000 samples, such a conclusion cannot be made for the other cases since there is an intersection between the confidence intervals.

To determine the best combination in RS design, sample size should be increased which will also increase the calculation time. Since the errors are small enough, decision is made by using 20000 samples. By considering the results and calculation time, Central Composite Circumscribed design with 1/32 fraction and k=1 is going to be used in the further stages of this study.

Table 6.5. 95% Confidence interval for the mean and standard deviations obtained from different methods

Method	**95% Confidence Interval for Mean**		**95% Confidence Interval for St.Dev**	
	Lower	**Upper**	**Lower**	**Upper**
Monte Carlo simulation	121.10	121.25	5.29	5.40
CCC 1/8 Fraction, k=1	121.05	121.19	5.32	5.43
CCC 1/8 Fraction, k=2	120.39	120.54	5.4	5.51
CCC 1/8 Fraction, k=3	121.16	121.32	5.51	5.61
CCC 1/16 Fraction, k=1	121.12	121.27	5.27	5.37
CCC 1/16 Fraction, k=2	121.03	121.18	5.41	5.51
CCC 1/16 Fraction, k=3	121.23	121.39	5.52	5.63
CCC 1/32 Fraction, k=1	121.15	121.3	5.31	5.42
CCC 1/32 Fraction, k=2	121.64	121.79	5.44	5.55
CCC 1/32 Fraction, k=3	121.62	121.77	5.63	5.74
CCF 1/8 Fraction, k=1	121.14	121.29	5.27	5.37
CCF 1/8 Fraction, k=2	121.14	121.29	5.31	5.42
CCF 1/8 Fraction, k=3	121.12	121.27	5.48	5.59
CCF 1/16 Fraction, k=1	121.07	121.21	5.27	5.37
CCF 1/16 Fraction, k=2	121.16	121.31	5.33	5.43
CCF 1/16 Fraction, k=3	121.17	121.33	5.54	5.65
CCF 1/32 Fraction, k=1	121.12	121.27	5.21	5.32
CCF 1/32 Fraction, k=2	121.14	121.28	5.26	5.37
CCF 1/32 Fraction, k=3	121.11	121.22	5.41	5.49
Box-Behnken k=1	48.36	83.43	1253.07	1277.87
Box-Behnken k=2	49.17	62.65	481.81	491.35
Box-Behnken k=3	57.72	62.68	176.96	180.46

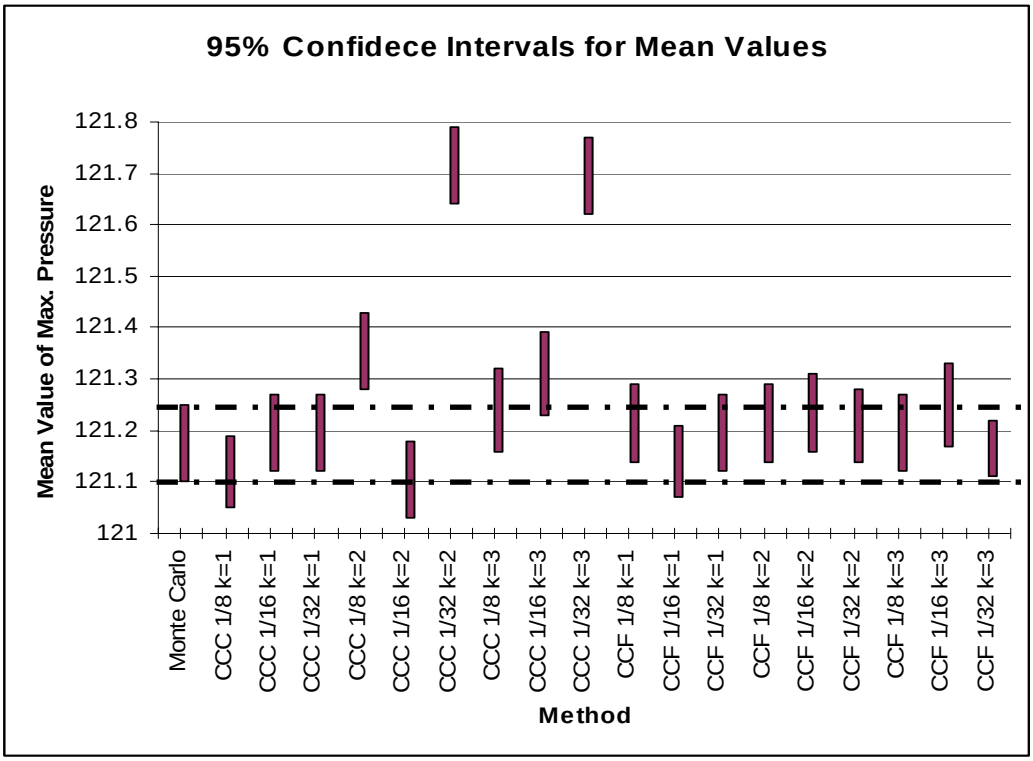

Figure 6.4. 95% Confidence intervals for estimated means with different RS methods

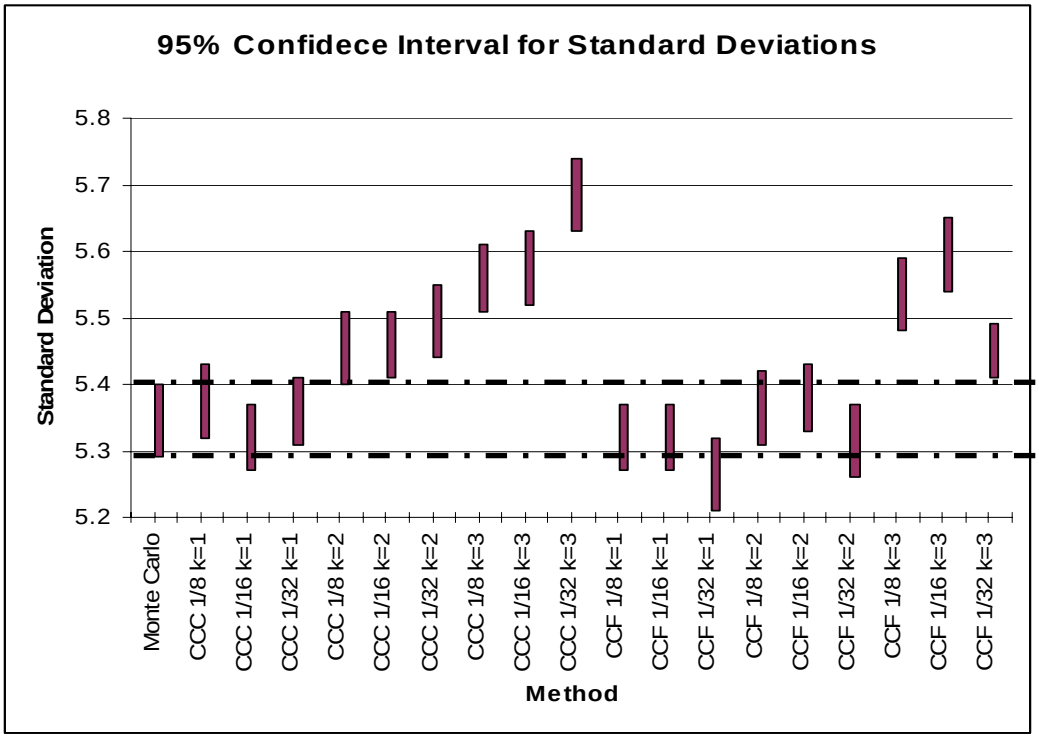

Figure 6.5. 95% Confidence intervals for estimated standard deviations with different RS methods

The accuracy of the selected response surface function is not only examined by considering confidence intervals of estimated mean and standard deviation but also estimated distribution, fitted values versus expected values graphs are also examined for Central Composite Circumscribed Design with 1/32 fraction and k=1.

The histogram plot of the estimated maximum pressure is given in Figure 6.6. From this plot, it is seen that maximum pressure has normal distribution behavior with a coefficient of variation 4.4% and distribution characteristics are also consistent with the results obtained from Monte Carlo simulation.

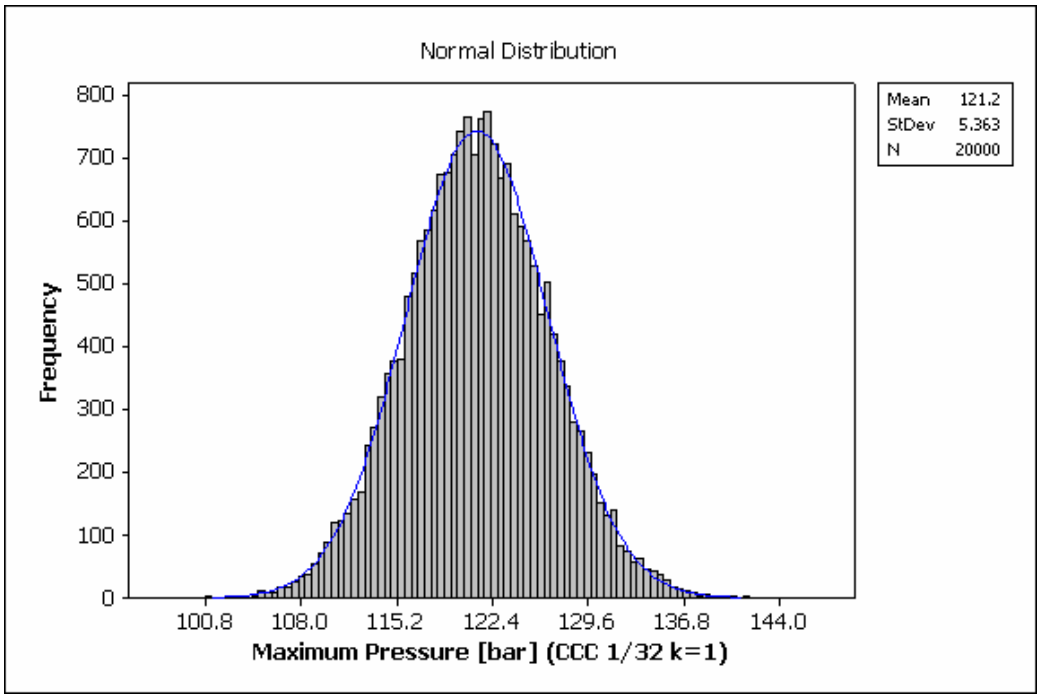

Figure 6.6. Distribution of maximum pressure (simulation with CCC 1/32 Fraction k=1)

The most important measure to determine whether a response function can be use in reliability prediction calculations is the expected values versus fitted values graph. Expected values versus fitted values at the points used to fit the response surface function is shown in Figure 6.7 and to evaluate the accuracy of Central

Composite Circumscribed Design with 1/32 fraction. Cross validation is performed and the results obtained from the cross validation are given in Figure 6.8. From cross validation results, it is seen that selected response function can be used to represent rocket motor response behavior in the variation range.

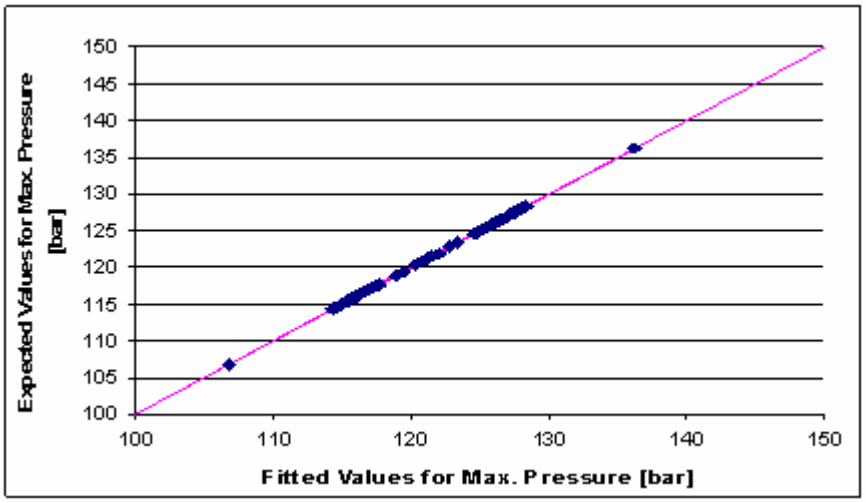

Figure 6.7. Expected vs. Fitted values for CCC Design with 1/32 fraction at response surface Design Points

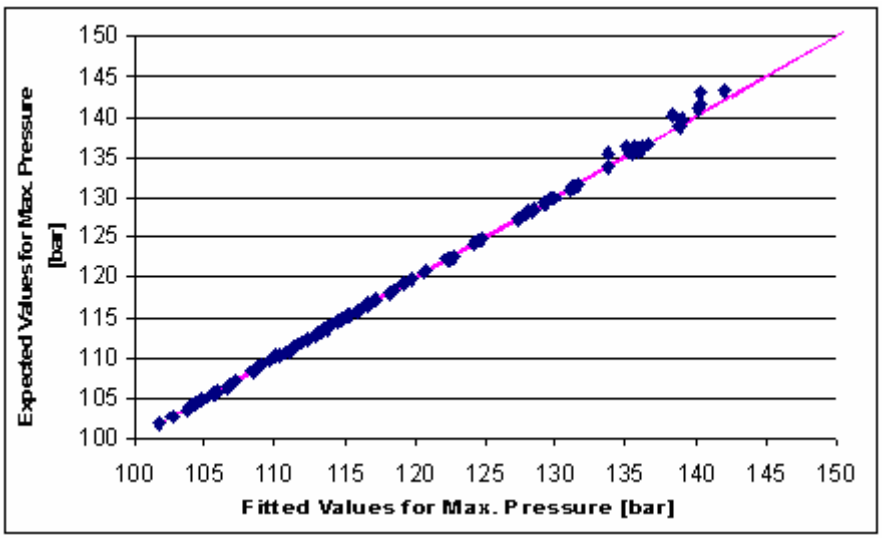

Figure 6.8. Expected vs. Fitted values for CCC Design with 1/32 fraction at random points (Cross Validation)

6.5 VARIATION IN BALLISTIC PERFORMANCE

Since the maximum pressure is correlated with all limit state functions, it is expected to obtain similar results with other ballistic performance measures. After setting k value and fraction of the RS Method, other ballistic performance measures are estimated with CCC design with 1/32 fraction. To evaluate the accuracy of the estimated functions, cross validation is performed. The Cross validation results are shown in Figures 6-9 to 6-12 for the functions valid for +60ºC ambient temperature and cross validation graphs for other ambient temperatures are given in Appendix B. Fitted response functions can be found in Appendix C.

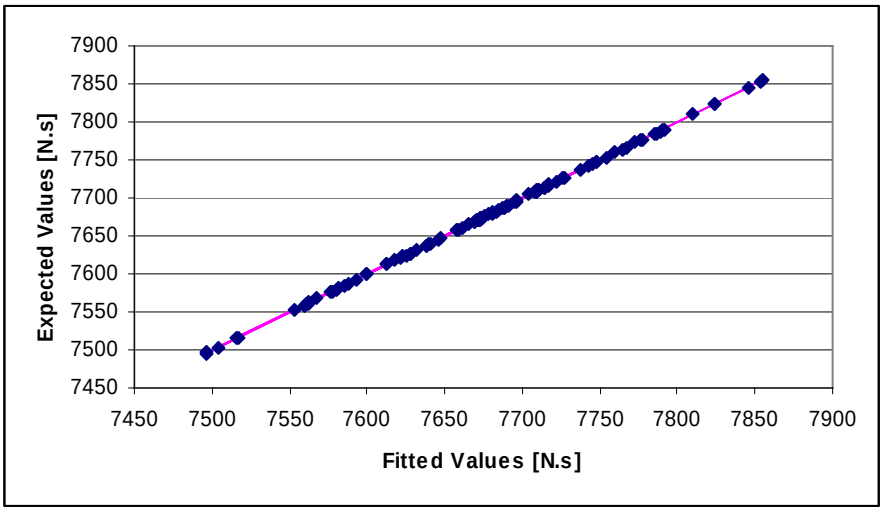

Figure 6.9. Expected vs. Fitted values for total impulse
(Max. absolute error = 1.36)

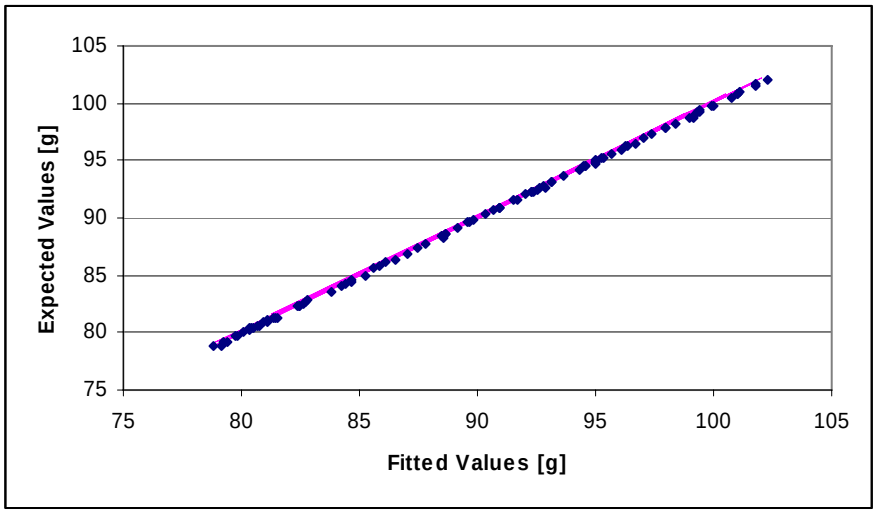

Figure 6.10. Expected vs. Fitted values for maximum acceleration
(Max. absolute error = 0.358)

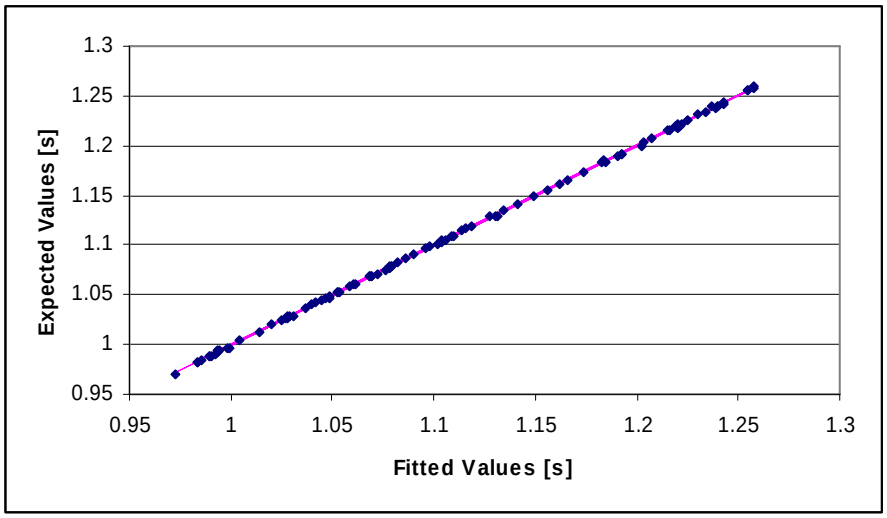

Figure 6.11. Expected vs. Fitted values for arming acceleration duration
(Max. absolute error = 0.0023)

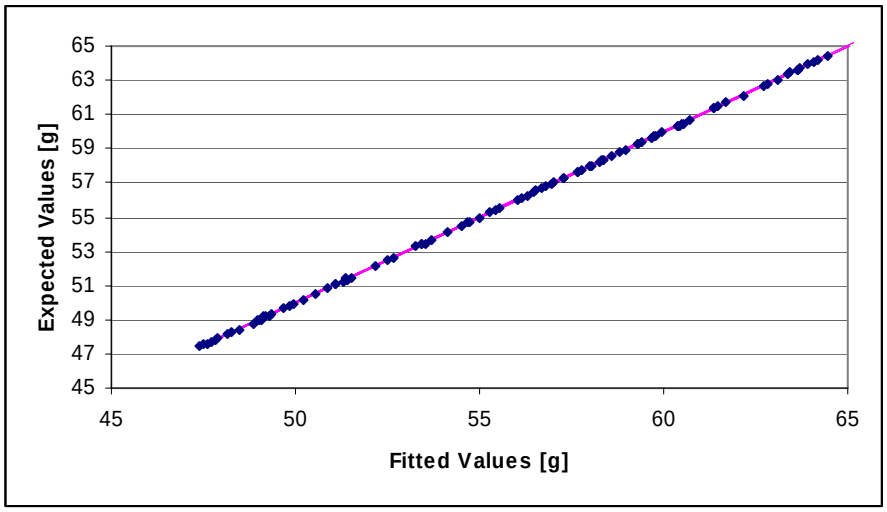

Figure 6.12. Expected vs. Fitted values for launch acceleration
(Max. absolute error = 0.113)

After fitting the response functions, Monte Carlo simulation is performed with 20000 samples to estimate variations in these performance parameters. Distributions for the response variables are given in Figures 6.13 to 6.16 for +60° C and similar figures for 20°C and -35°C are given in Appendix D. All ballistic performance parameters are found to be normally distributed and estimated mean and standard deviations are given in Table 6.6.

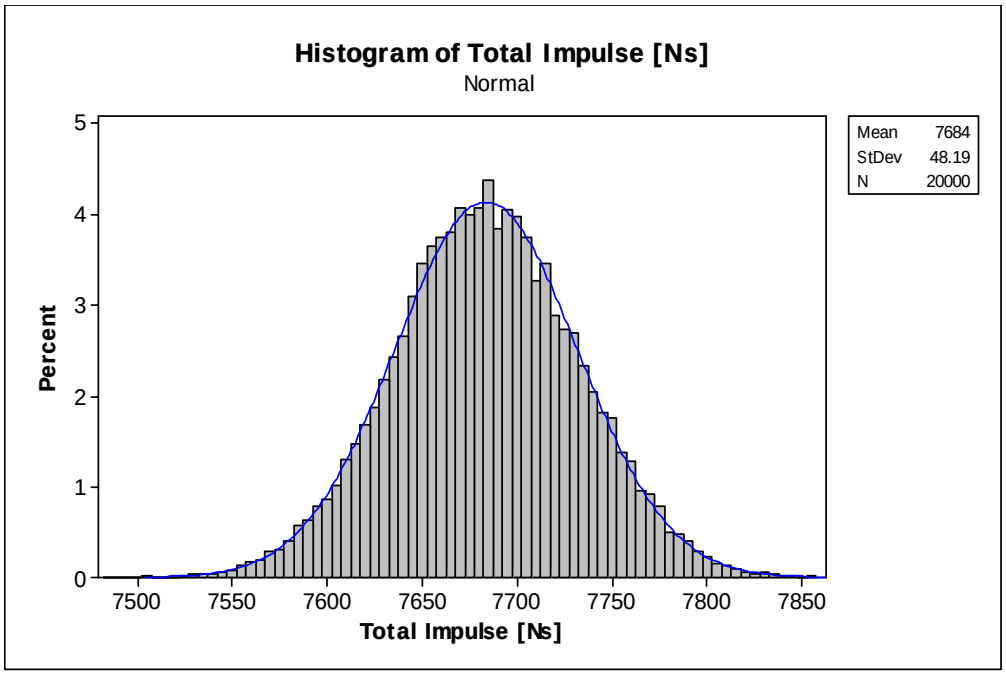

Figure 6.13. Distribution of total impulse at +60°C

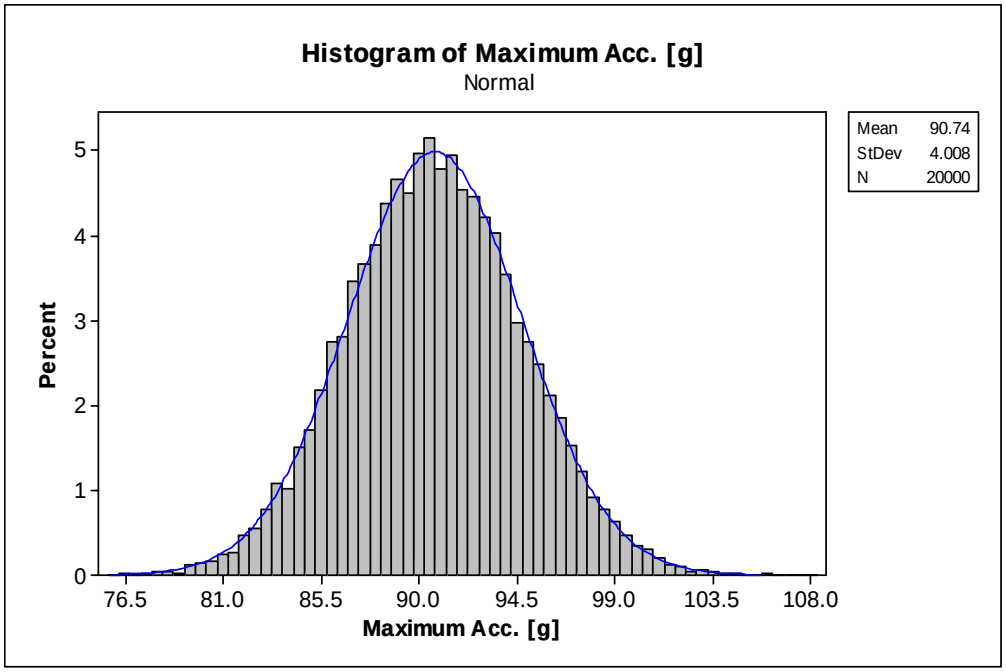

Figure 6.14. Distribution of maximum acceleration at +60°C

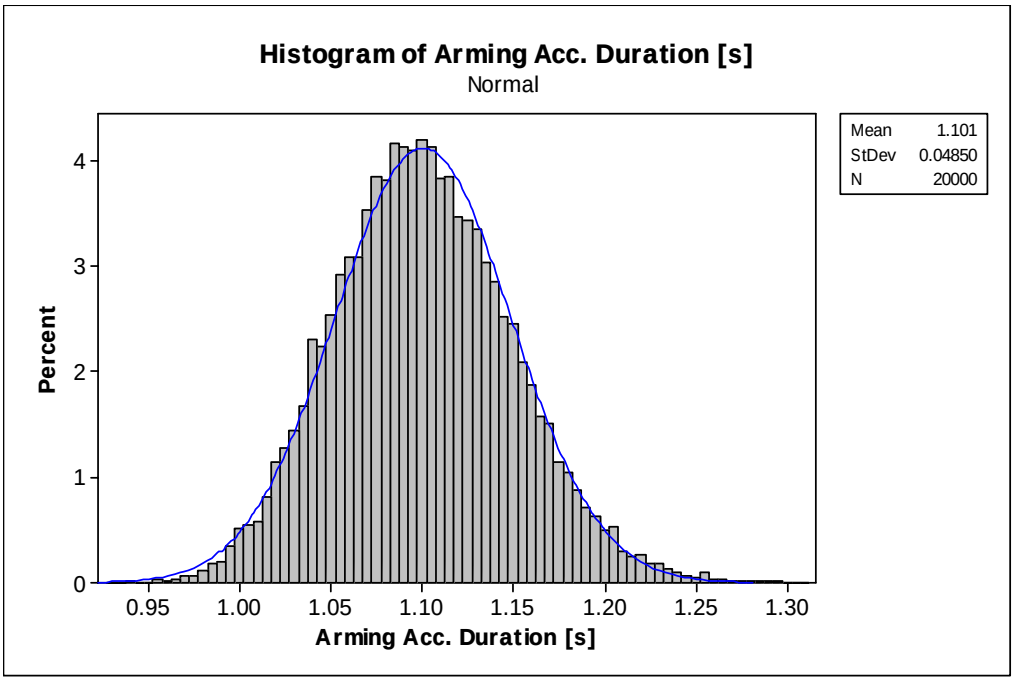

Figure 6.15. Distribution of arming acceleration duration at +60°C

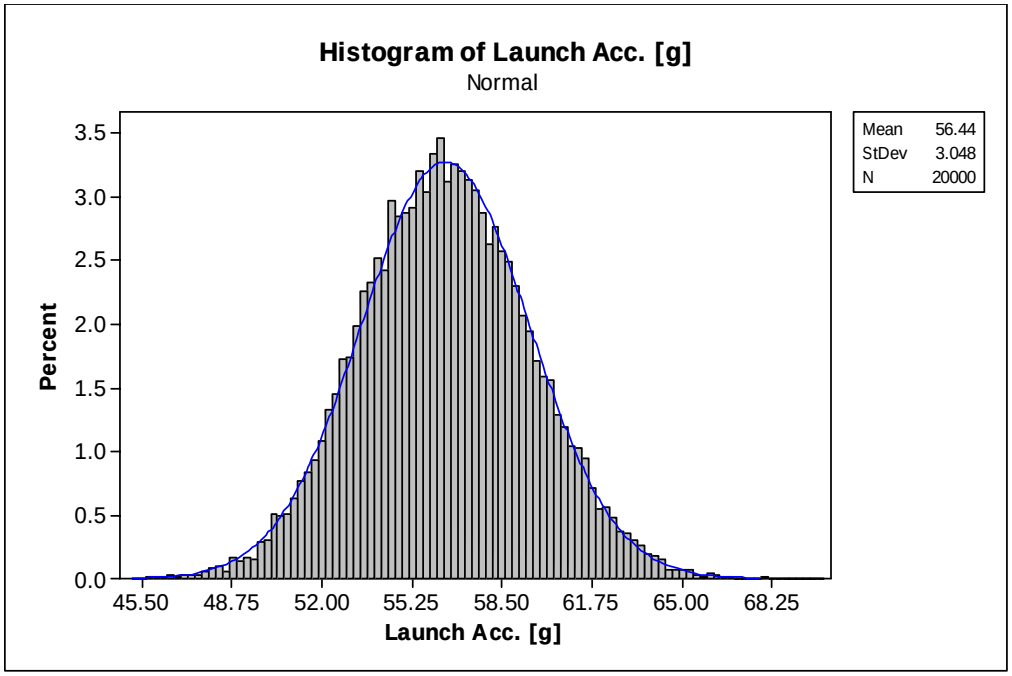

Figure 6.16. Distribution of launch acceleration at +60°C

Table 6.6. Variations in ballistic performance

Performance Parameter	-35°C			+60°C		
	Mean	Standard Deviation	Distance to the Limit (σ)	Mean	Standard Deviation	Distance to the Limit (σ)
Total Impulse [N.s]	7597	49.4	1.96	7683.7	48.2	3.81
Maximum Acceleration [g]	72.827	3.266	8.32	90.741	4.008	2.31
Arming Acceleration Duration [s]	1.3713	0.0602	12.43	1.1007	0.0485	9.85
Launch Acceleration [g]	43.142	2.374	3.43	56.442	3.048	7.03

By considering the distances to the limiting values, it can be said that exceeding maximum acceleration limit at +60°C and obtaining an impulse lower than the limit at -35°C are the most probable failure modes.

6.6 VARIATON OF MAXIMUM STRESS IN THE CASING

The procedure applied to estimate the variation of ballistic performance is also applied to the casing of the rocket motor to estimate the variation of maximum stress. To estimate the maximum stress, first a response surface experiment is designed. Then, the maximum stress is calculated at the response surface experiment points by using ANSYS® Finite Element Software.

In stress variation calculations, the internal pressure of the rocket motor, the thickness of the casing, the casing thickness at the nozzle interface and thickness

of the joint element (Lockwire) are considered as variables. These parameters are shown in Figure 6.17.

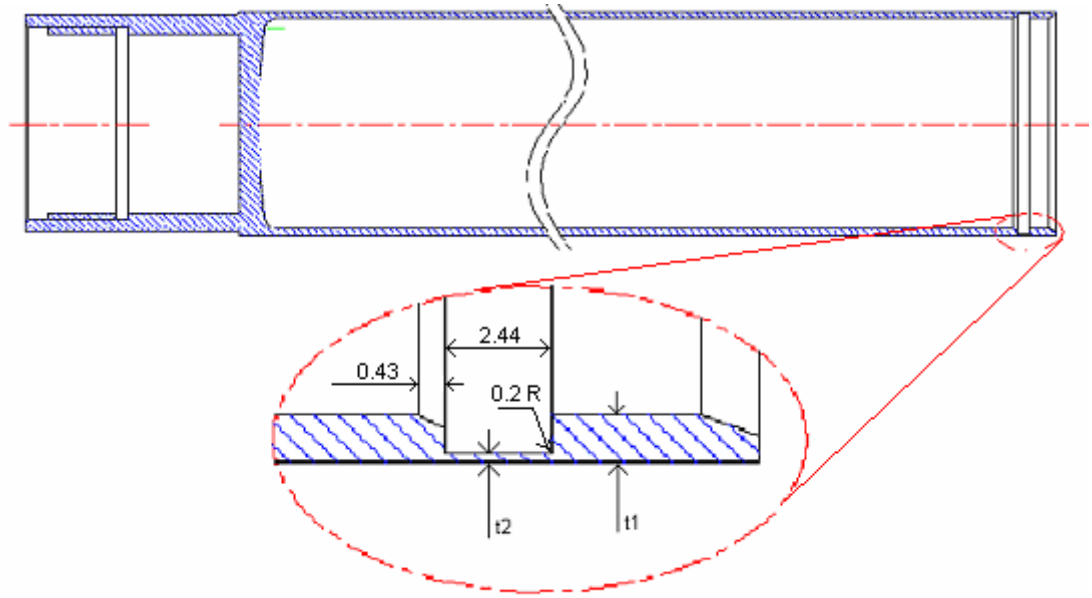

Figure 6.17. Casing of the rocket motor

Similar to the ballistic performance calculations, Circumscribed Central Composite design is used to fit response functions to the stress in the casing. However, different from the previous calculations, effect of the maximum pressure is examined by using ten different pressure levels since maximum pressure can vary in a wide range when the temperature limits are concerned. Hence, response functions are obtained by combining CCC design at -35ºC and at +60ºC. The response surface design used in this analysis is illustrated in 2D in Figure 6.18. According to this RS design, 50 finite element analyses are performed by using ANSYS®. Results of the finite element solutions showed that there are two high stress regions in the casing of the rocket motor. One is at the fore end of the casing and the other is at the aft end where the nozzle is connected by using a lockwire (Figure 6.19, Figure 6.20 and Figure 6.21).

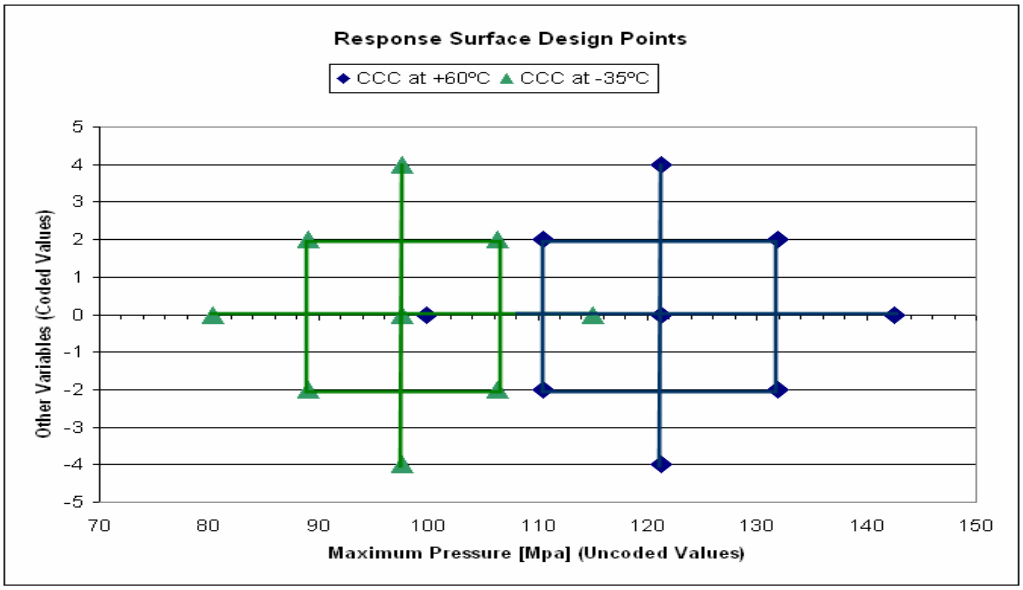

Figure 6.18. Response surface data points for the maximum stress estimation

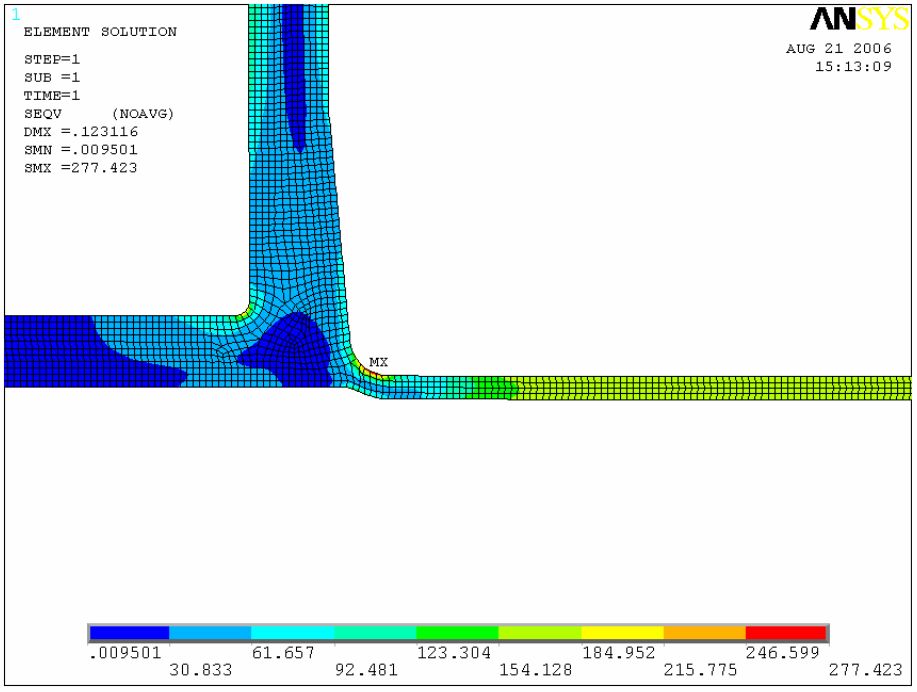

Figure 6.19. von Misses stresses for a sample run (fore end)

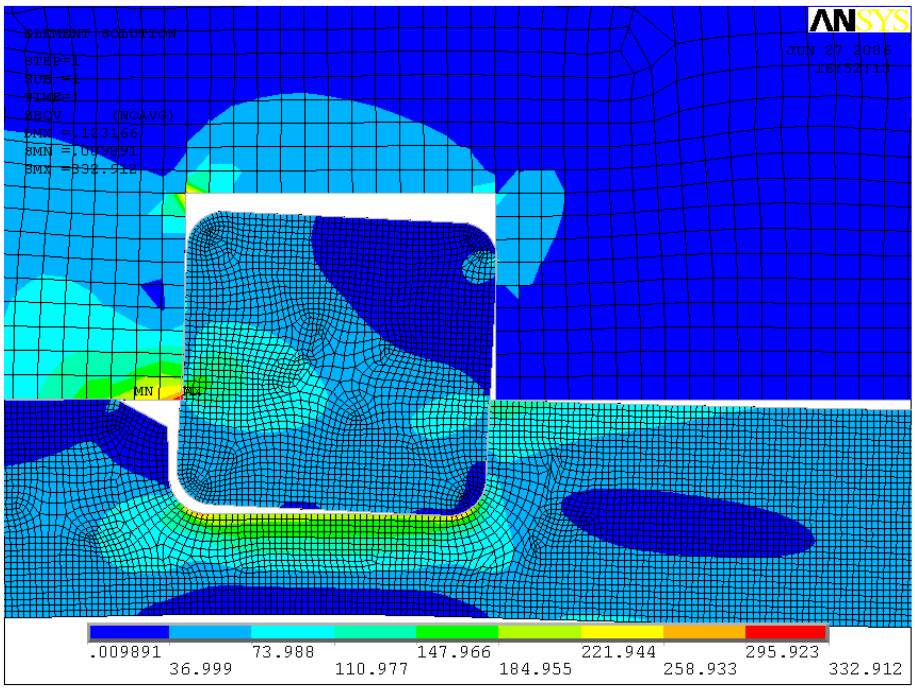

Figure 6.20. von Misses stresses for sample run (motor case-nozzle interface)

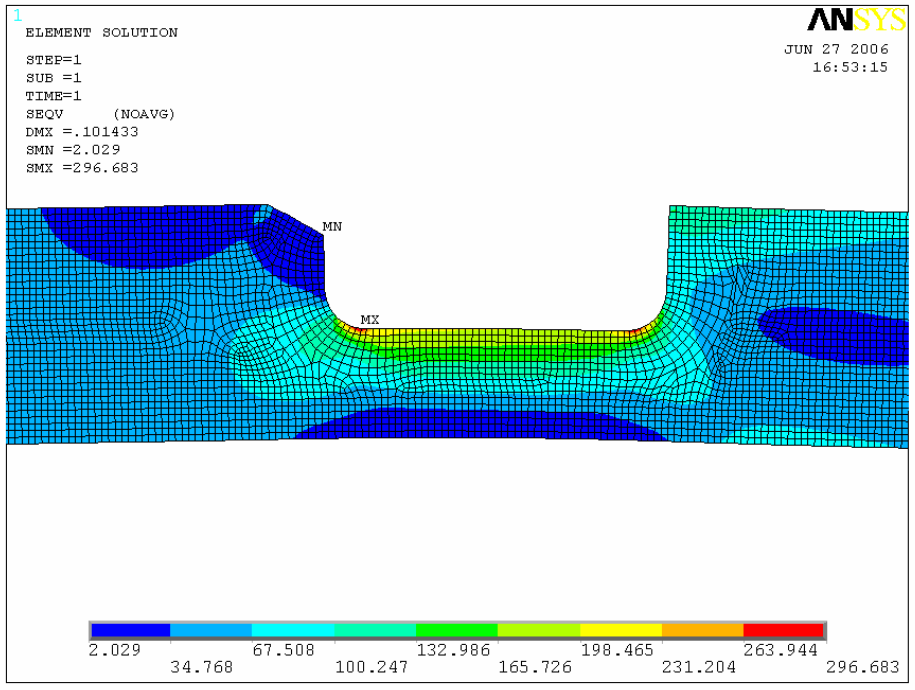

Figure 6.21. von Misses stresses for sample run (aft end)

With the results obtained from the finite element solutions quadratic and cubic response functions are fitted to the maximum stress at the casing fore end and for the maximum stress at the casing aft end. To evaluate the accuracy of the fitted functions 10 additional finite element solution is done at random points by assuming uniform distribution for all variables. Results obtained from the cross validation are given in Table 6.7. Values in Table 6.7 show that, using a cubic function gives result better than the results obtained from a quadratic function. Cross validation results for cubic functions are given in Figure 6.22 and Figure 6.23 .

Table 6.7. Cross validation response surface functions

Response Parameter	**Order of the Response Surface**	**R2 value for Response Surface Fitting**	**Average Error in Cross Validation [MPa]**	**Maximum Error in Cross Validation [MPa]**
Maximum Stress at Fore End	2nd Order	0.99820	1.89 (0.73%)	5.4 (1.69%)
	3rd Order	0.99832	1.86 (0.72%)	5 (1.57%)
Maximum Stress at Aft End	2nd Order	0.98352	4.20 (1.43%)	10.7 (3.63%)
	3rd Order	0.99903	3.27 (1.1%)	5.11 (1.62%)

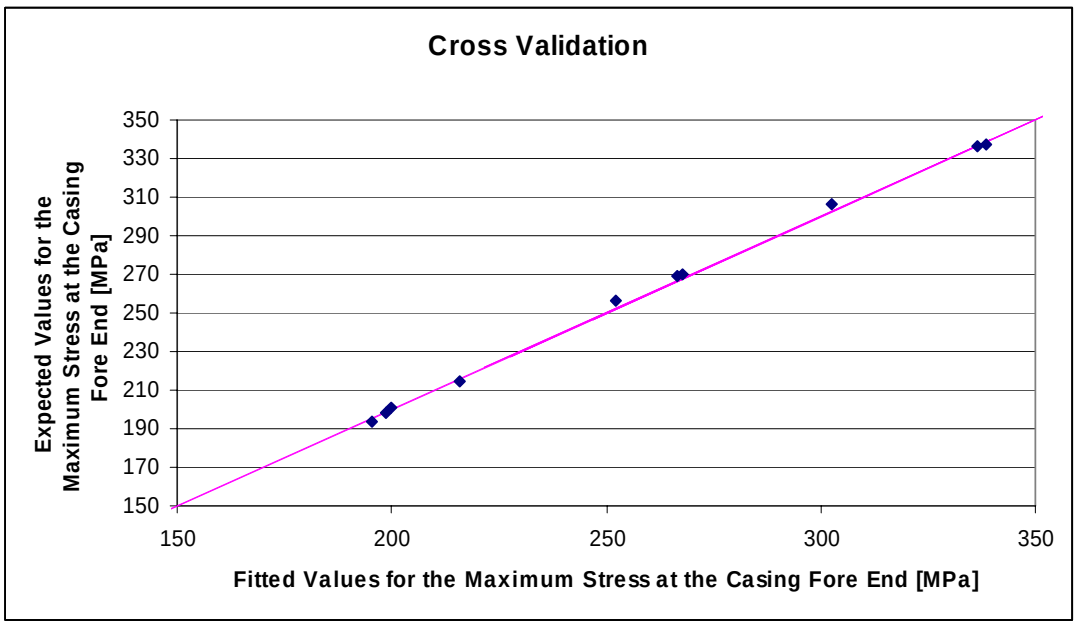

Figure 6.22. Cross validation of the response function for maximum stress at the casing fore end

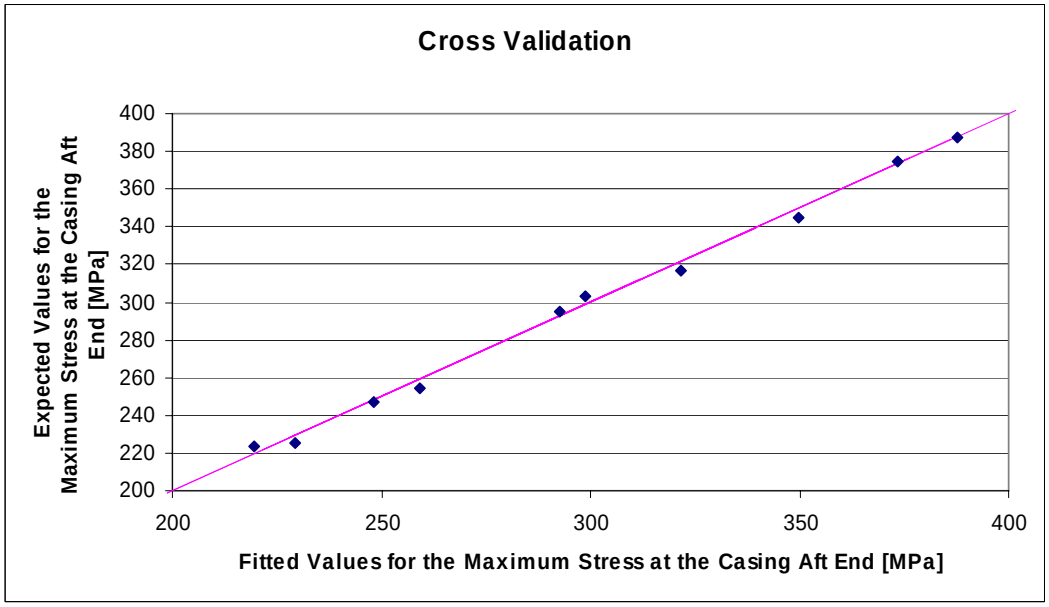

Figure 6.23. Cross validation of the response function for maximum stress at the casing aft end

After setting the estimated equations for the stress, Monte Carlo simulation is performed to investigate the variation in these stress values and to find out

maximum possible stress that the casing may experience. In Monte Carlo simulation, the pressure distributions found in previous sections are used and other parameters such as thickness, lockwire groove depth etc. are assumed to be normally distributed in the range of tolerances.

From the Monte Carlo simulation, the maximum stresses at the aft end and at the fore end are found to be normally distributed and estimated stress distributions are tabulated in Table 6.8 for +60ºC, +20ºC and -35 ºC ambient temperatures.

For all data points in response surface design, the stress values at the fore end is smaller than the stress values at the aft end. Hence, in the reliability calculations, only the stress at casing and nozzle connection is included. Distribution of Maximum Stress at casing and nozzle connection is shown in Figure 6.24 for +60 º C ambient temperatures and given in Appendix D for other ambient temperatures.

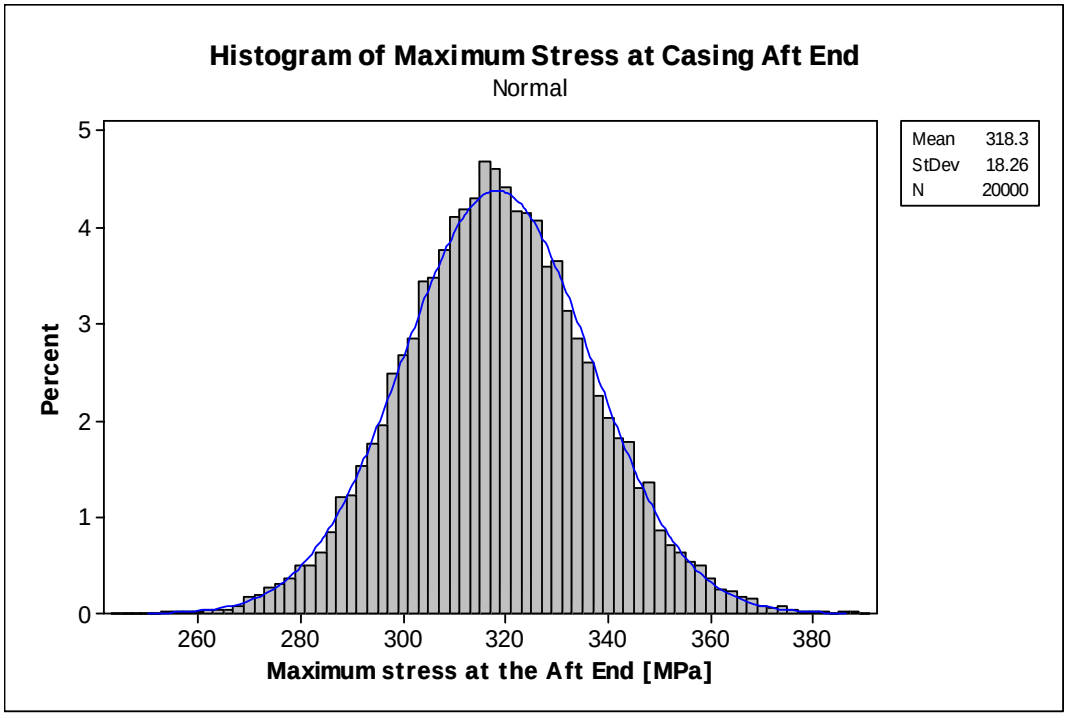

Figure 6.24. Distribution of maximum stress at the aft end (+60°C)

Table 6.8. Variations in maximum stress

Temperature ºC	Variable	Mean [MPa]	StDev [MPa]	C.o.V. [%]	Sample Size in MCS
60	Maximum stress at Aft End	318.34	18.26	5.73	20000
	Maximum Stress at Fore End	274.14	11.83	4.32	20000
20	Maximum stress at Aft End	289.42	16.47	5.69	20000
	Maximum Stress at Fore End	250.59	10.80	4.31	20000
-35	Maximum stress at Aft End	254.7	15.16	5.95	20000
	Maximum Stress at Fore End	221.34	9.68	4.37	20000

6.7 RELIABILITY ESTIMATION

With the distributions estimated so far, the probability of failure associated to each limit state can be calculated separately by using normal distribution probability function.. Then, if there is a constant limit value for the performance, probability of failure Pf^T_i for a limit state function g_i at an ambient temperature T can be written as:

$$Pf_i^T = \phi\left(\frac{\chi_i - \mu^T{}_i}{\sigma^T{}_i}\right) \qquad \text{Eq (6.11)}$$

If there is a lower limit for the performance and

$$Pf_i^T = 1 - \phi\left(\frac{\chi_i - \mu^T{}_i}{\sigma^T{}_i}\right) \qquad \text{Eq (6.12)}$$

If there is an upper limit for the performance, where χ_i is the limit value, ϕ is the standard normal distribution function. μ_i^T is the mean value and σ_i^T is the standard

deviation which are estimated by Monte Carlo simulation of the fitted response surface function for a specific temperature T.

Structural reliability of the casing is calculated by using stress strength interference method. Assuming that deformation of the casing caused by the internal pressure during the ignition does not have important effects on the rocket motor flight performance, probability of bursting of the rocket motor due to high pressure loads was examined. Then, limit value for the stress is the ultimate tensile strength of the casing material which is also defined by a distribution function.

Casing material of the rocket motor examined in this study is Aluminum 2014 T6 which has a yield strength of 412.37 MPa and a tensile strength of 470.78 MPa [53]. In the operating ambient temperature range of the rocket motor, change in strength properties of Al 2014 T6 due to temperature is ±1% [54] and included in the calculations. Coefficient of variation values for the materials similar to the casing material vary between 2.7-5.8% [55]. Since an increase in the coefficient of variation decreases reliability, to be on the safe side casing material's strength properties are assumed to have 5.8% coefficient of variation. Then, the probability of failure estimation problem takes the form of FOSM formula given in Eq(4-2), since the random variables are normally distributed. Application examples of this method to the rocket motor cases can be found in references 13, 14, 15. Calculated probabilities of failure for different temperatures are given in Table 6.9.

As shown in Table 6.9, by assuming all performance functions are uncorrelated, reliability of the rocket motor (only ballistic performance reliability and structural reliability of the casing is included) is calculated as 0.989707, 0.998933 and 0.9751199 for ambient temperature +60°C, +20°C and -35°C respectively. However, correlation among these failure probabilities can be considered in Monte Carlo simulation. Having response surface functions for the rocket motor performance and structural performance, limit state functions can be evaluated in Monte Carlo simulation simultaneously. In this method, random numbers are

generated for each input parameter given in Table 6.1 and all limit state functions are calculated for these inputs. If any of the limit state is exceeded, system is accepted as failed and failure number in the simulation is increased by 1. A sample result window is given in Figure 6.25 and results obtained from MCS are listed in Table 6.10.

Table 6.9. Probability of failure values and Reliability for different temperatures (Calculated with normal distribution function)

Limiting Response	**60°C**	**20°C**	**-35°C**
Total Impulse	6.836×10^{-5}	0.001065	0.024790
Maximum Acceleration	0.010222	1.296×10^{-6}	1.72×10^{-12}
Arming Acceleration Duration	$<10^{-10}$	$<10^{-10}$	$<10^{-10}$
Launch Acceleration	$<10^{-10}$	9.645×10^{-9}	1.08×10^{-5}
Structural Failure	2.967×10^{-6}	7.109×10^{-9}	$<10^{-10}$
Total Probability of Failure	0.010293	0.001067	0.024801
Reliability	0.989707	0.998933	0.975199

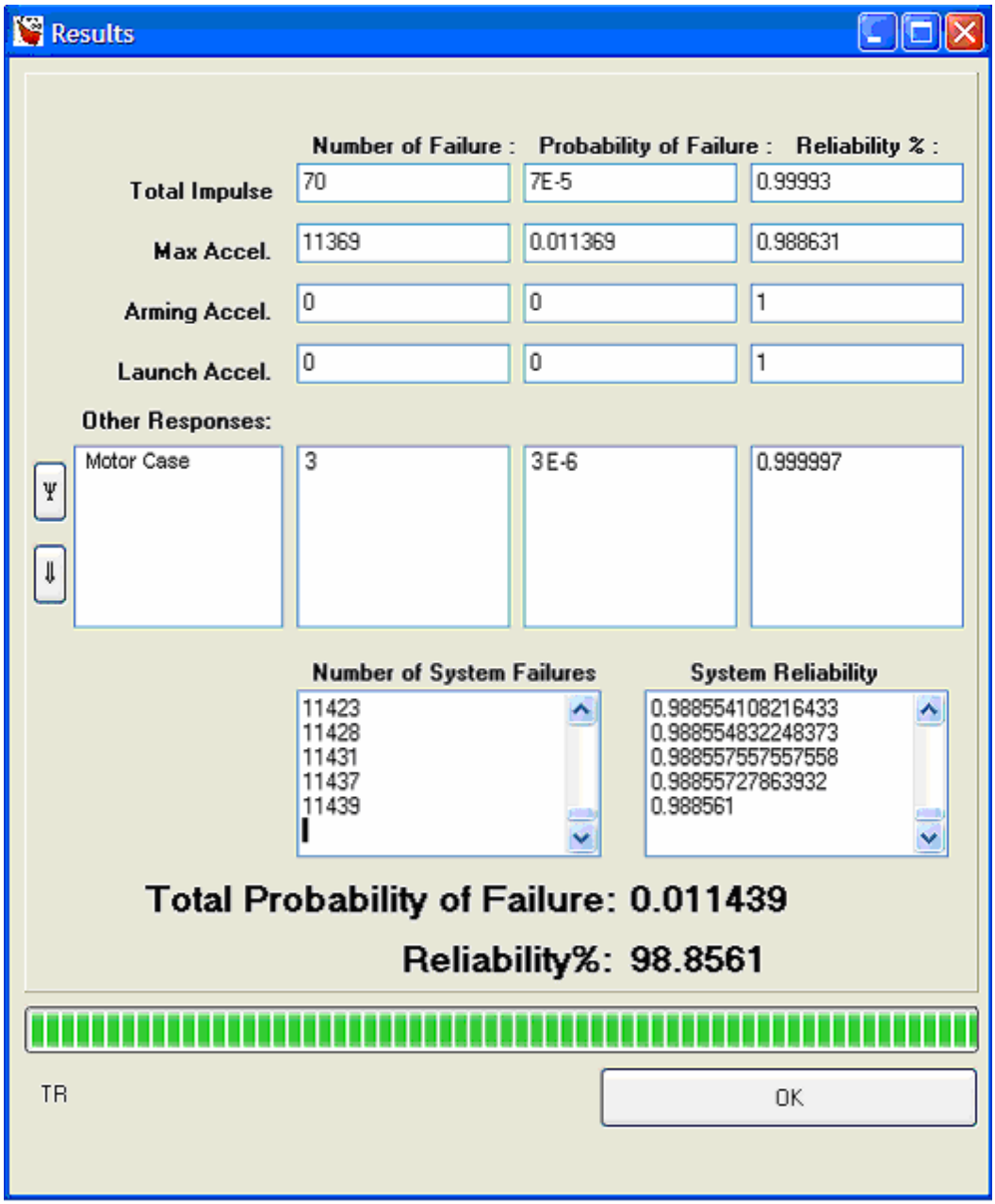

Figure 6.25. Reliability calculation result window for 60ºC

Table 6.10. Probability of failure values and reliability for different temperatures (Calculated with Monte Carlo simulation)

Limiting Response	Estimated Probability of Failure		
	60°C	**20°C**	**-35°C**
Total Impulse	0.000070	0.001109	0.026693
Maximum Acceleration	0.011369	0.000007	$<10^{-6}$
Arming Acceleration Duration	$<10^{-6}$	$<10^{-6}$	$<10^{-6}$
Launch Acceleration	$<10^{-6}$	$<10^{-6}$	0.000211
Casing Failure	0.000003	$<10^{-6}$	$<10^{-6}$
Total Probability of Failure(Without considering correlation)	0.011442	0.001116	0.026904
Reliability (Without considering correlation)	0.988558	0.998884	0.973096
Total Probability of Failure (With considering correlation)	0.011439	0.001116	0.026773
Reliability (With considering correlation)	0.988561	0.998884	0.973227

Since there are small differences between the reliability values estimated by considering correlations and by assuming purely uncorrelated failure probabilities, it can be said that assuming failures purely uncorrelated is a valid assumption.

6.8 MAXİMUM EXPECTED OPERATING PRESSURE and PROOF LOAD ESTIMATION

The maximum expected operating pressure (MEOP) can be simply defined as the limit load that the casing must resist. It is typically defined as the pressure that

will not be exceeded on more than 1 firing in 1000 at the upper firing temperature. At the initial design stage, an allowance for statistical variation will have been included in the limit load. In established designs that load will accurately known from firing records [56]. With the method applied in this study, MEOP can be estimated instead of including an allowance for the variation.

The variation that should be included in MEOP determination at the initial design stages generally get similar values for solid propellant rocket motors. In Reference 18, MEOP is stated to be taken as 15% above the nominal pressure at maximum temperature due to variations of the propellant properties and fabrication of the components. Also in this reference hydrostatic test pressure, which is applied to the rocket motor casing during quality control stages to be sure that casing will resist to MEOP, is determined to be 22% greater than the nominal pressure at maximum ambient temperature. With these ratios, MEOP for the rocket motor into consideration is calculated as 139 bars and hydrostatic test pressure is found to be 147.8 bars.

In section 6.4, in addition to nominal pressure, maximum pressure is found to be normally distributed with a mean of 121.1 bars and a standard deviation of 5.34. With the estimations performed in this study, maximum expected operating pressure can be estimated more accurately and additionally, probability of exceeding MEOP can also be calculated. $\pm 3\sigma$ limits of the pressure profile at maximum operating temperature are given in Figure 6.26 and Cumulative Distribution Function (CDF) of maximum pressure is estimated as shown in Figure 6.27.

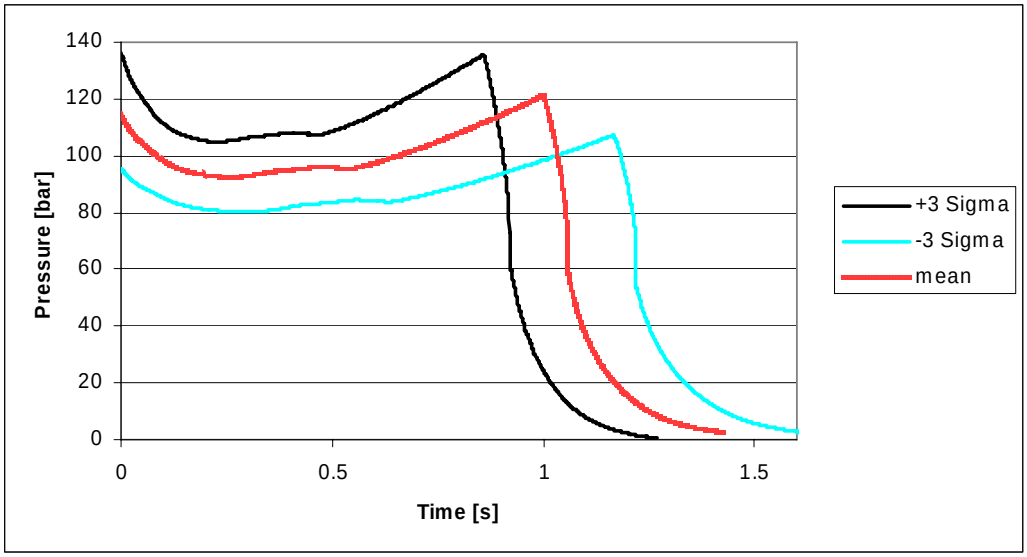

Figure 6.26. ±3σ limits for estimated pressure profile at 60ºC

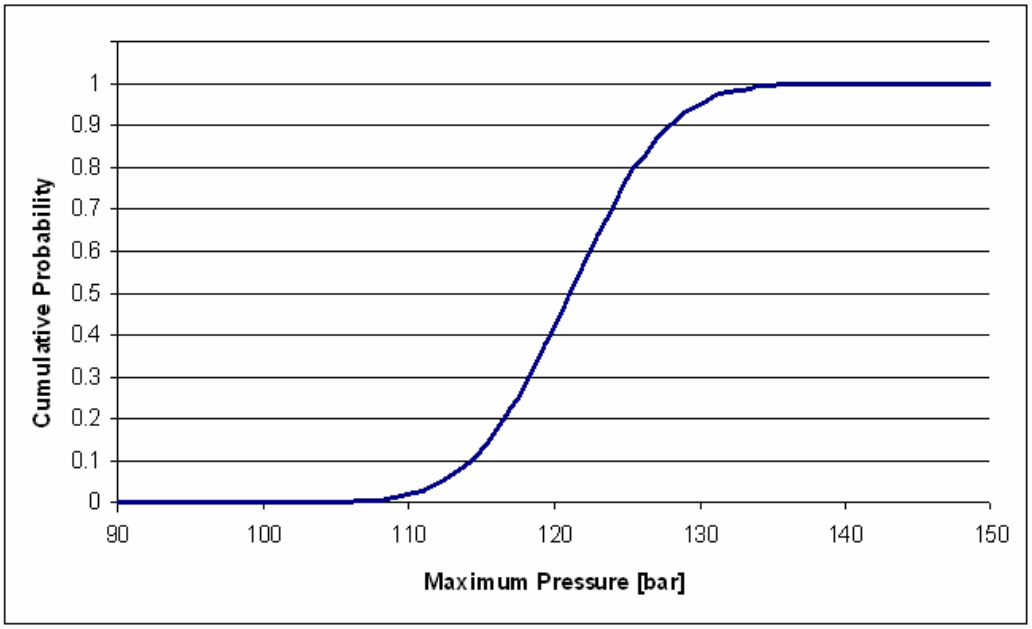

Figure 6.27. CDF of maximum pressure at 60ºC

By utilizing the estimated CDF, probability of exceeding a predefined pressure can be calculated as given in Table 6.11. Then, with the MEOP definition in reference 56, it is found that Maximum Expected Operating Pressure of this

rocket motor is 137.7 bars which is 13.6% above the nominal pressure at maximum operating temperature

Table 6.11. Probability of exceeding a predefined MEOP

Predicted MEOP [Bar]	**Probability of exceeding predicted MEOP**
121.1	0.5
125	0.232592
130	0.047790
135	0.004621
137.7	0.001
140	0.000201
145	0.000004
146.5	0.000001
150	3.1165E-08
155	1.08843E-10

In addition to estimating MEOP, proof load which should be applied to the casing before assembling the rocket motor can also be determined by utilizing the estimated Cumulative Distribution Function of the maximum pressure, response function for the maximum stress and distribution of the maximum stress. With this method, proof load can be set to a value which will increase the casing reliability to an allocated value according to rocket system reliability goal. However, in previous section, probability of failure of the casing was already estimated to be $3x10^{-6}$ and applying a proof load will decrease this value. Although, proof loading increases the reliability, effect of the proof load on the reliability was not included in the calculations since the value estimated without

proof loading is already small. Although the effect of the proof loading is neglected in probability of failure calculations, by using deterministic approach, proof load is determined by multiplying the nominal pressure at maximum operating ambient temperature by a factor of 1.22 which gives 147.8 bars. Finite element analysis shows that applying this pressure to the rocket motor creates a maximum stress of 393.8 MPa which is lower than the yield strength of the casing material.

6.9 SENSITIVITY OF BALLISTIC PERFORMANCE

After defining rocket motor performance by response function, input parameters that have contribution to the variation of the performance can be evaluated by sensitivity analysis. Sensitivities of limit state functions and maximum pressure are calculated by considering the response functions' slopes associated to each variable at the design point. All calculations are performed for 60ºC ambient temperature and the results are given in Figure 6.28 through Figure 6.32 in terms of percent contributions to the change in associated response. In addition, parameters listed in Table 6.12 with the order of the importance for the rocket motor performance.

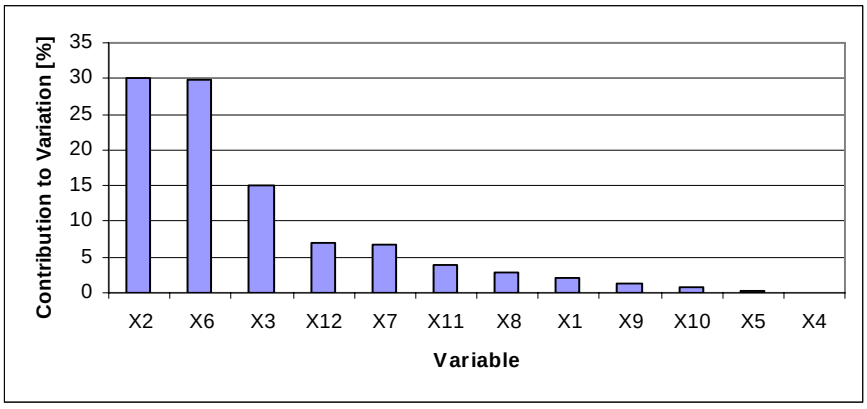

Figure 6.28. Sensitivity of total impulse

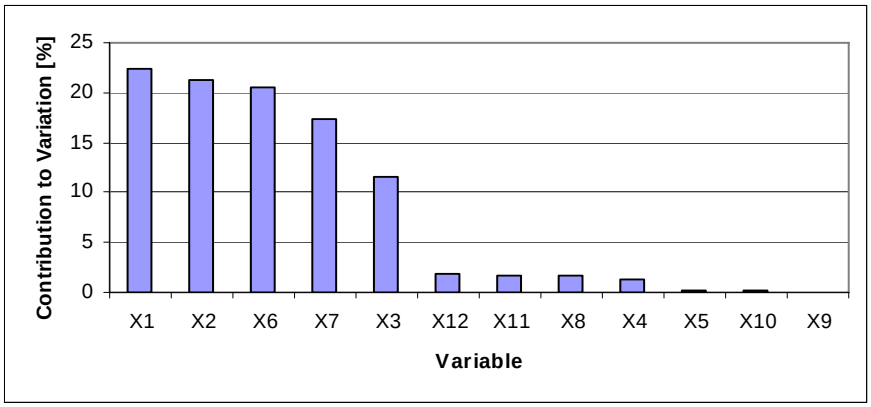

Figure 6.29. Sensitivity of maximum acceleration

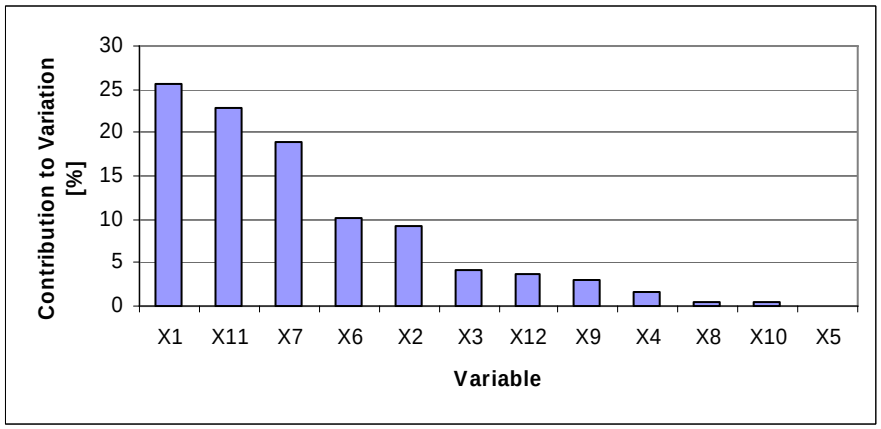

Figure 6.30. Sensitivity of arming acceleration duration

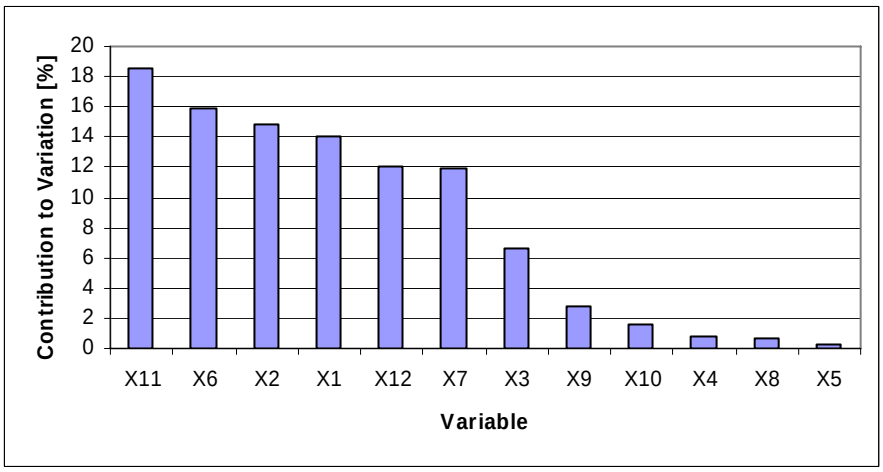

Figure 6.31. Sensitivity of launch acceleration

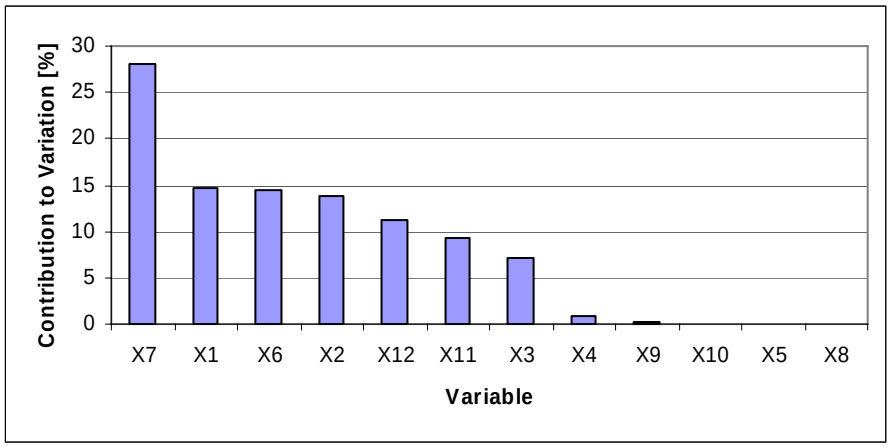

Figure 6.32. Sensitivity of maximum pressure

Table 6.12. Variables effective on the Rocket Motor Performance

Order of Importance	Total Impulse	Max. Acc.	Arming Acc. Duration	Launch Acc.	Max. Pressure
1	X2	X1	X1	X11	X7
2	X6	X2	X11	X6	X1
3	X3	X6	X7	X2	X6
4	X12	X7	X6	X1	X2
5	X7	X3	X2	X12	X12
6	X11	X12	X3	X7	X11
7	X8	X11	X12	X3	X3
8	X1	X8	X9	X9	X4
9	X9	X4	X4	X10	X9
10	X10	X5	X8	X4	X10
11	X5	X10	X10	X8	X5
12	X4	X9	X5	X5	X8

Values shown in Figures 6.28 through 6.32 are sensitivities around the current design point. From the results given in these graphs, it can be concluded that to find an optimum among these performance parameters, one should consider that propellant properties, grain length and throat diameter are more effective parameters.

However, from the view of reliability, sensitivity analysis should be performed by considering the variation range of the input parameters. Besides the effect of input

parameters on the rocket motor performance, their effect on the variation of rocket motor performance should also be calculated. Thus, parameters that are effective on reliability can be determined.

The sensitivities of ballistic performance to these parameters is recalculated by multiplying the response functions' slopes at design point with coefficient of variation associated with each variable. The sensitivity values in the range of variation range of the input parameters are shown in Figure 6.33 to Figure 6.37 and parameters are listed in Table 6.13 according to their effect on the ballistic reliability of the rocket motor.

These results revealed that for the rocket motor examined in this study, there is an obvious effect of Burn Rate Constant, Enthalpy of the Propellant Combustion and Propellant Density on the variation of rocket motor performance, hence on the ballistic performance reliability. Then decreasing variation of these parameters, for example improving production or quality control methods by considering these parameters, will increase the reliability of this rocket motor.

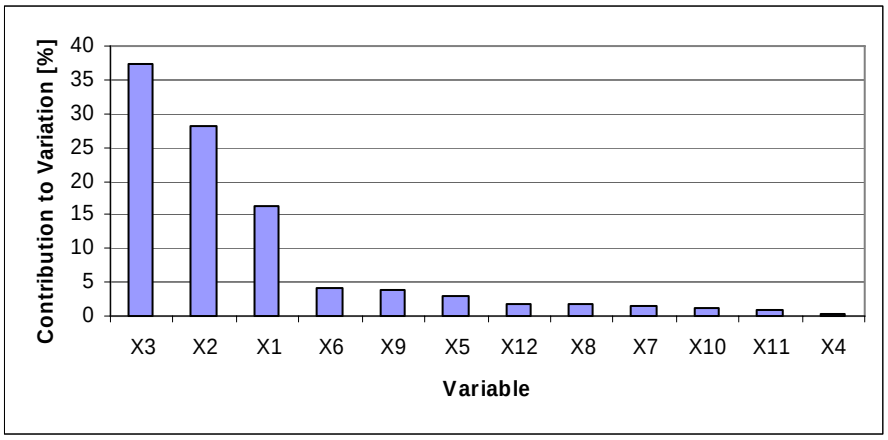

Figure 6.33. Sensitivity of variation in total impulse

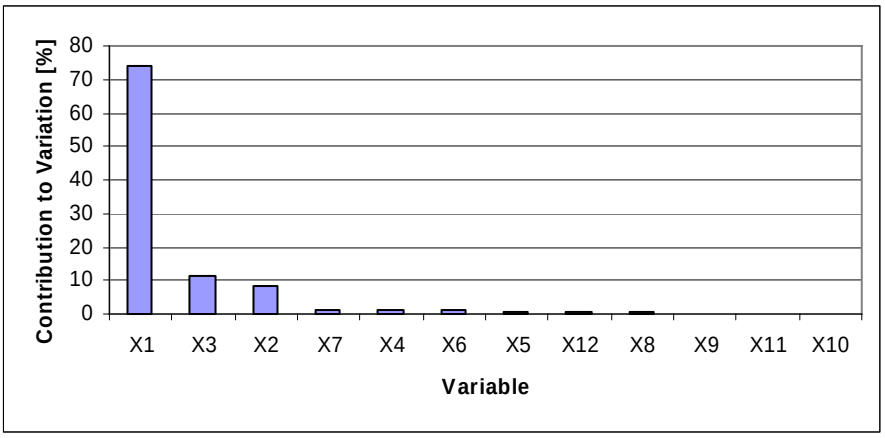

Figure 6.34. Sensitivity of variation in maximum acceleration

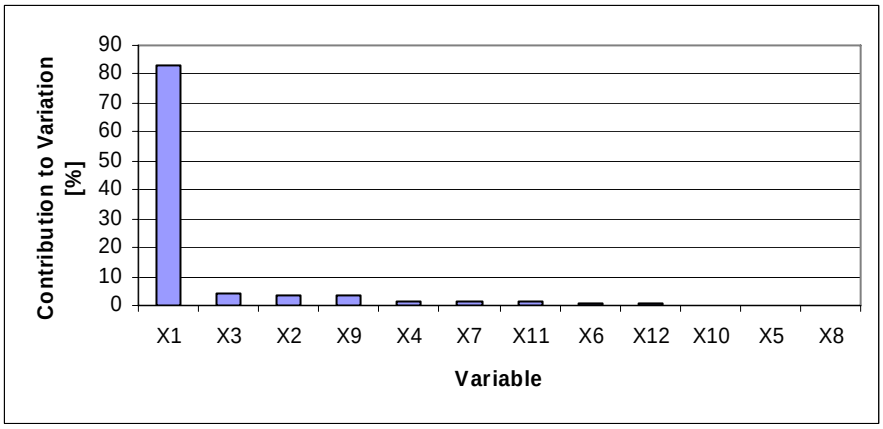

Figure 6.35. Sensitivity of variation in arming acceleration duration

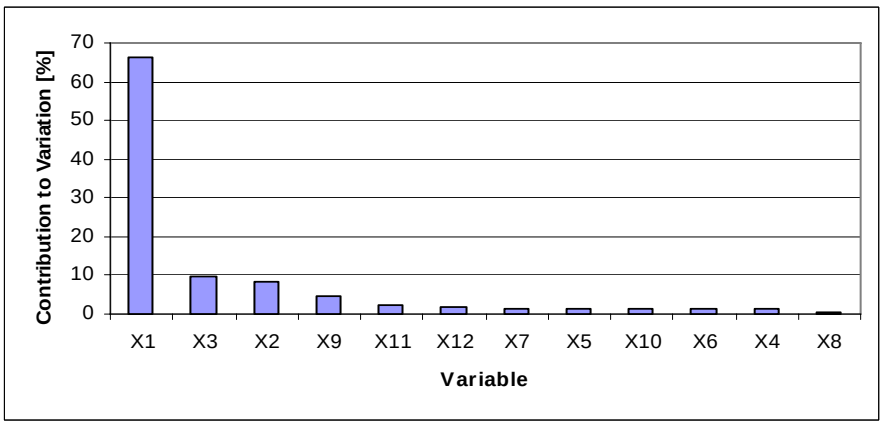

Figure 6.36. Sensitivity of variation in launch acceleration

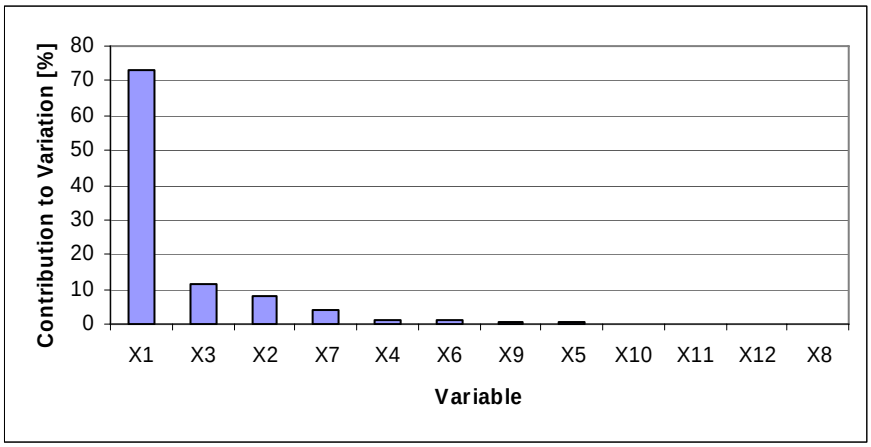

Figure 6.37. Sensitivity of variation in maximum pressure

Table 6.13. Variables effective on the rocket motor ballistic performance variation

Order of Importance	Total Impulse	Max. Acc.	Arming Acc. Duration	Launch Acc.	Max. Pressure
1	X3	X1	X1	X1	X1
2	X2	X3	X3	X3	X3
3	X1	X2	X2	X2	X2
4	X6	X7	X9	X9	X7
5	X9	X4	X4	X11	X4
6	X5	X6	X7	X12	X6
7	X12	X5	X11	X7	X9
8	X8	X12	X6	X5	X5
9	X7	X8	X12	X10	X10
10	X10	X9	X10	X6	X11
11	X11	X11	X5	X4	X12
12	X4	X10	X8	X8	X8

6.10 RELIABILITY BASED DIMENSION ADJUSTMENT

The most practical way of designing a reliable system is considering the reliability requirements in the early design phases. In late design phases, since many parameters are fixed, generally reliability can only be increased by process improvements. However in early design phases, critical parameters that affect the

system performance can be set to optimal points which will increase the system reliability.

In previous sections, reliability of the rocket motor was estimated to be 0.9897098, 0.99893372 and 0.9751098 for three different ambient temperatures. +60ºC, +20ºC, -35ºC respectively. However, these reliability values can be increased by setting a new design point. In this case, an input parameter that is going to be changed should be set to a new value which does not require process improvements and does not affect the manufacturing cost. Also, new values should be selected near to the current design point not to create a negative effect on the other components which are not considered in this thesis study. For example increasing the nozzle throat and exit diameters will decrease the nozzle material thickness which may cause to structural failure of the nozzle. For this purpose, input parameters are changed in ten percent range.

Since they can be easily changed in the design, dimensional parameters are selected to be input parameters for the optimization problem. Then, dimensions which can be used in the optimization process are nozzle throat diameter, nozzle exit diameter and grain geometry parameters L_1, L_2, R_1, and R_2.

Input parameters that are going to be used in the optimization are selected by considering the sensitivity analysis performed in section 6.9. In the sensitivity analysis it was found that grain geometry parameters R_1 and R_2 are not effective on the rocket motor performance. Then, it is tried to find a point where the probability of failure of the rocket motor will be decreased by changing nozzle throat diameter, nozzle exit diameter and grain geometry parameters L_1, L_2.

After setting the input parameters and their ranges, new response surfaces which are valid in ten percent variation range of the input parameters are fitted for two extreme temperatures -35ºC and +60ºC. These response surface functions are used to estimate the mean values of the response parameters: total impulse, maximum acceleration, launch acceleration, arming acceleration duration. Addition to these response parameters, a response function also fitted for the maximum chamber

pressure which is used to estimate the maximum stress at the rocket motor casing. New response surface functions are fitted by using Circumscribed Central Composite design.

Since the objective is to minimize total probability of failure, probability of failure of the rocket motor must be expressed as an analytical function. As the rocket motor performance parameters are found to have normal distribution characteristics, it is assumed that probability of failure associated to each limit state function can be calculated by using Cumulative Distribution Function of Normal Distribution. Also, it is assumed that failure for each limit state function is purely uncorrelated with other failures and standard deviation of performance parameters does not change by changing nozzle throat diameter, nozzle exit diameter and grain geometry parameters L_1, L_2.Then, each probability of failure can be calculated by using equations 6-11, 6-12 and 4-2. The optimization problem to determine new dimensions can be defined as follows:

Minimize

$$\sum_{\substack{i=1..5 \\ T=+60,-35}} Pf_i^T \qquad \text{Eq (6.13)}$$

Subject to

$$-1 \le \phi^c{}_{throat} \le 1$$

$$-1 \le \phi^c{}_{Exit} \le 1$$

$$-1 \le L^c{}_1 \le 1$$

$$-1 \le L^c{}_2 \le 1$$

where the superscript c denotes the coded variable which is the non dimensional value used in response surface design and coded value of a variable x is

$$x^c = \frac{x - \mu_x}{\left(\frac{x_{Max} - x_{Min}}{2}\right)} \qquad \text{Eq (6.14)}$$

By using Microsoft Excel's solver tool with Newton search algorithm [57] new values are estimated as given in Table 6.14 and predicted changes in the responses after setting new design point is given in Table 6.15.

Table 6.14. New design point

Input Parameter	Old Value (Uncoded) (m)	New Value (Uncoded) (m)	Old Value (Coded)	New Value (Coded)
Throat Diameter	0.01175	0.01238	0	0.531915
Exit Diameter	0.06168	0.06478	0	0.501822
Grain Geometry Parameter, L1	0.0156	0.0152	0	-0.24863
Grain Geometry Parameter, L2	0.0111	0.0102	0	-0.78078

Table 6.15. Expected rocket motor performance at new design point

Performance Parameter	Old Values		Expected values after optimization	
	Mean at -35°C	**Mean at +60°C**	**Mean at -35°C**	**Mean at +60°C**
Total Impulse [N]	7597	7683.7	7692.8	7797.8
Maximum Acceleration [g]	72.83	90.74	67.96	85.03
Arming Acceleration Duration [s]	1.371	1.100	1.484	1.187
Launch Acceleration [g]	43.14	56.44	43.02	55.87
Maximum Pressure [bar]	97.8	121.2	89.4	114.2
Objective Function	0.0340826		0.0008358	

Then, estimated reliability of the rocket motor and distribution of the response parameters are recalculated by using the same procedure applied in previous chapters. By this way, new reliability is estimated by considering the correlation between the failures and validity of the optimization results are checked by comparing the expected mean values obtained in the optimization calculations and results obtained from the simulation (Table 6.16). Result window showing the probability of failure for -35°C is given in Figure 6.38 and results are listed in Table 6.17 for +60°C, +20°C, and -35°C.

Table 6.16. Monte Carlo simulation results at new design point

Performance Parameter	**Expected Values after Optimization**		**Simulation result**	
	Mean at -35°C	**Mean at +60°C**	**Mean at -35°C**	**Mean at +60°C**
Total Impulse [N]	7692.8	7797.8	7697.6	7802.701
Maximum Acceleration [g]	67.96	85.03	67.96	84.893
Arming Acceleration Duration [s]	1.484	1.187	1.488	1.19
Launch Acceleration [g]	43.02	55.87	43.23	55.92
Maximum Pressure [bar]	89.4	114.2	86.6	120.5

By comparing the expected values after optimization and the simulation results which are obtained by using new design point, it can be said that the response function used in the optimization procedure gives considerable results. Then, it can be concluded that reliability of a system can be easily increased with small changes in the design parameters during the early design phases without any additional cost.

However if target reliability cannot be reached after changing the dimensions to an optimum point, then improvements in manufacturing processes and material properties should be considered. For the rocket motor studied in this thesis, further development in reliability can be achieved by decreasing the variation in the propellant properties since the sensitivity analysis show that main source of the variation in rocket motor performance is due to the variation in burn rate of the propellant.

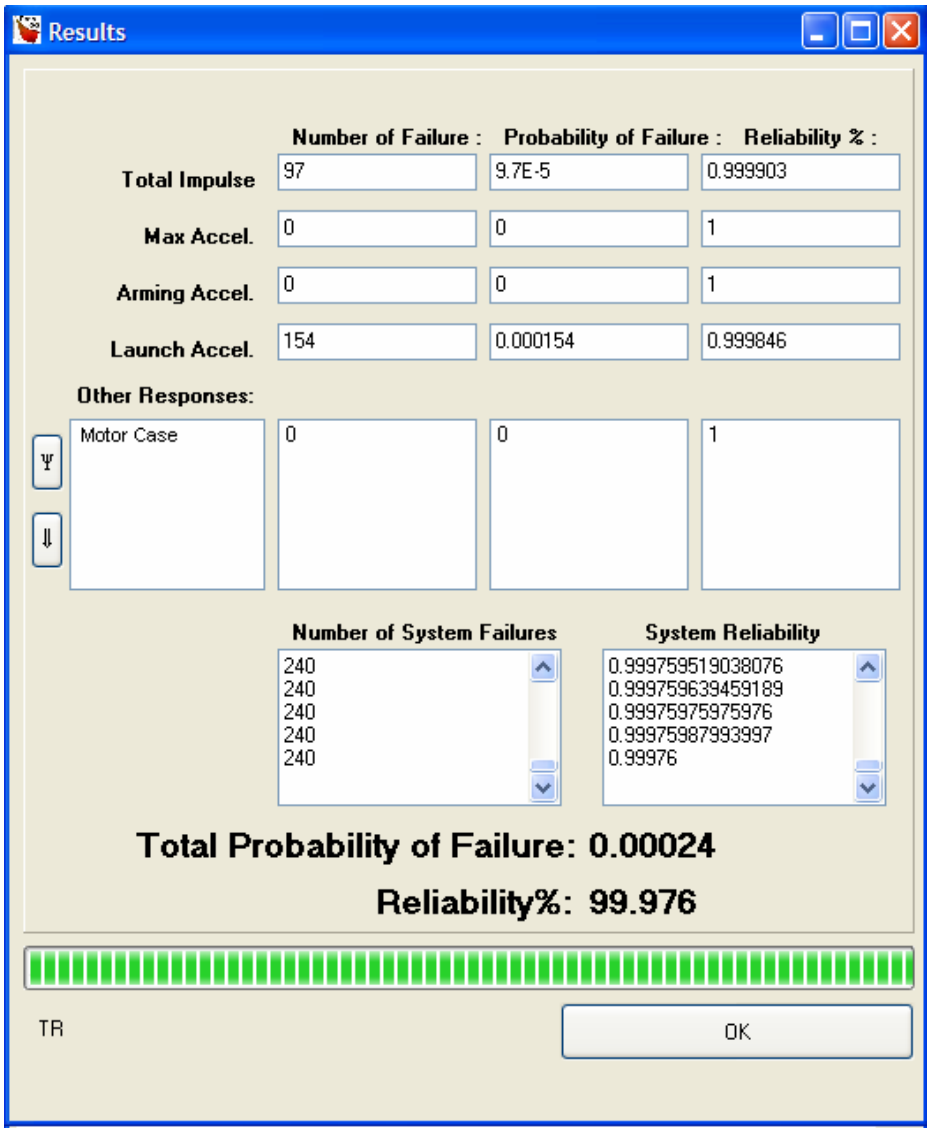

Figure 6.38. Reliability calculation result window for -35ºC at new design point

Table 6.17. Reliability of the rocket motor at new design point

Limiting Response	Estimated Probability of Failure Before Optimization			Estimated Probability of Failure After Optimization		
	60°C	**20°C**	**-35°C**	**60°C**	**20°C**	**-35°C**
Total Impulse	$0.7x10^{-4}$	0.001109	0.026693	$<10^{-6}$	$<10^{-6}$	$0.97x10^{-4}$
Maximum Acceleration	0.011369	$7x10^{-6}$	$<10^{-6}$	$0.48x10^{-5}$	$<10^{-6}$	$<10^{-6}$
Arming Acceleration Duration	$<10^{-6}$	$<10^{-6}$	$<10^{-6}$	$<10^{-6}$	$<10^{-6}$	<10-6
Launch Acceleration	$<10^{-6}$	$<10^{-6}$	0.000211	$<10^{-6}$	$<10^{-6}$	0.000154
Casing Failure	10^{-6}	$<10^{-6}$	$<10^{-6}$	$<10^{-6}$	$<10^{-6}$	$<10^{-6}$
Total Probability of Failure	0.011439	0.001116	0.026773	$0.48x10^{-5}$	$<10^{-6}$	0.00024
Reliability	0.988568	0.998884	0.973227	0.999952	>0.999999	0.99976

CHAPTER 7

DISCUSSION AND CONCLUSION

7.1 SUMMARY OF THE STUDY

In this study reliability of a solid rocket motor was estimated and new design point was proposed to increase the reliability.

Main steps of the procedure are as follows: first the limit state functions, i.e. performance of the system, and input parameters affecting these limit states were determined. Second, response functions valid in the variation range of the input parameters were formed by using response surface method and these functions were validated by the cross validation of the fitted function with the ballistic performance prediction software and finite element analysis software. Then, with the response functions, Monte Carlo simulation was performed to assess current reliability of the system and variation of the responses.

After determining current status of the system, sensitivity analysis was performed and effects of the input parameters on the system performance and system performance variation were determined. Then, input parameters which were going to be used in the optimization were determined by considering their effect on the system and simplicity of changing them. Then, new response surface functions valid in the optimization range were fitted to the limit states. In this step, since the variations in responses could be expressed with a known distribution function – Normal Distribution-, probability of failure due to each limit state was simply

expressed as a normal distribution probability function and calculations are simplified. Then, to find a new design point, summation of these probability functions was minimized. In this step, it was assumed that failure associated to a limit state is purely uncorrelated with other limits and shape of the distribution function of each response remains constant.

Finally, Monte Carlo simulation was repeated for new design point to validate the optimization results and to find a better estimation for reliability at new design point by considering the correlation among the limit state functions. This procedure is also summarized in Figure 7.1.

7.2 CONCLUSIONS AND SUGGESTED FURTHER EXTENSIONS

This thesis study presented the functional reliability of a solid propellant rocket motor and structural reliability of the motor case. The conclusions that can be reached are as follows:

i. By using response surface method, the approximate functions which are valid in the variation rage of the input parameters can be found for the rocket motor performance. However, the experimental points should be selected carefully to decrease the error in the approximation.

ii. In Monte Carlo simulation, instead of calculating responses with a computer code, the functions obtained from the response surface method can be used. In this case, the distribution of the examined response can be estimated with enough accuracy with decreased calculation time.

iii. The location of the points used for the response surface design has effect on the error of the response surface function. In this study, response functions obtained by using the points determined by Central Composite design gave better results than the function obtained by using the points determined by Box-Behnken method.

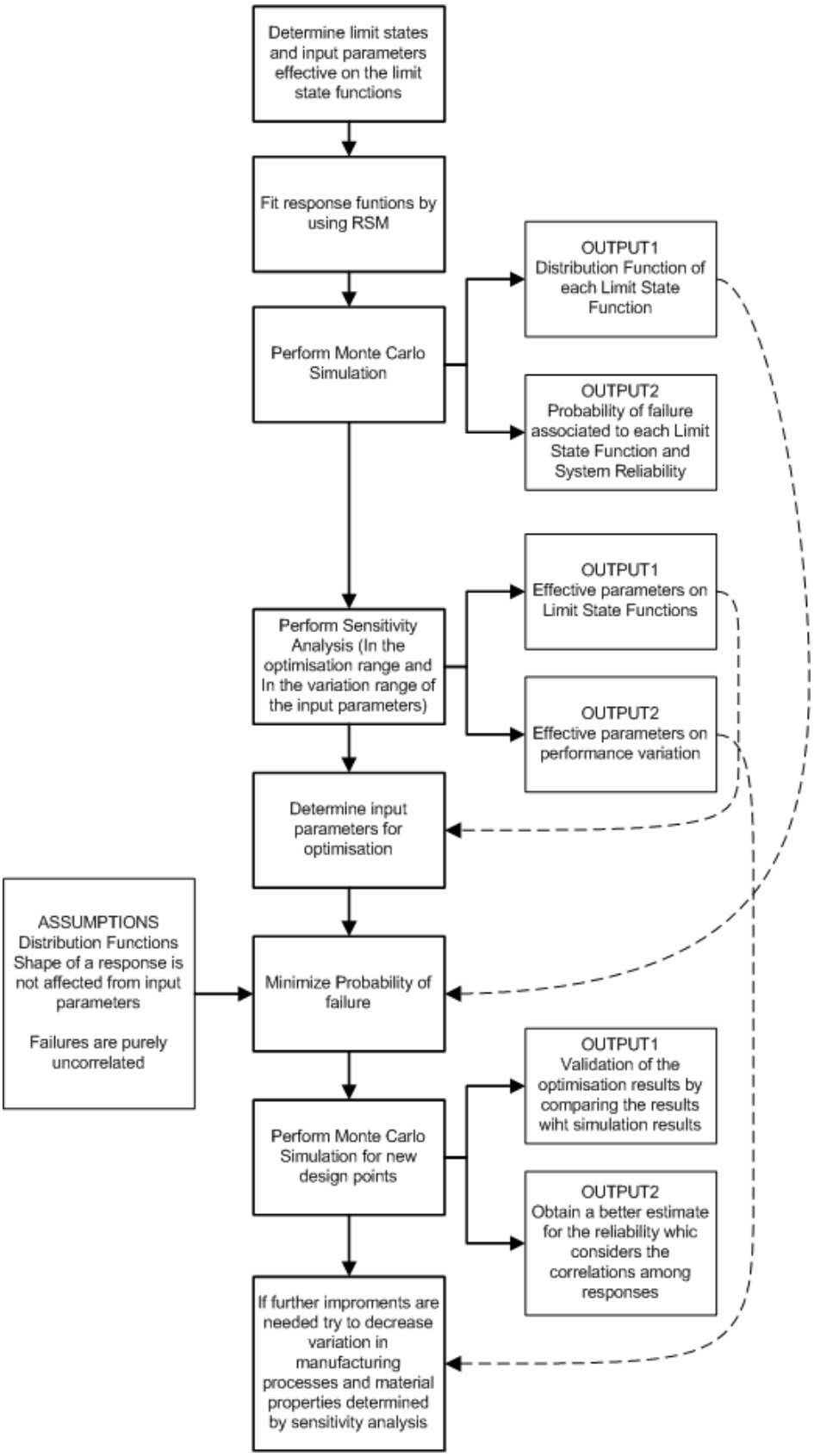

Figure 7.1. Flowchart followed in the study

iv. With the number of input parameters used in this study, response function obtained by using Box-Behnken Design has high errors and cannot be used to estimate the reliability of this rocket motor. It is suggested that; to evaluate the capability of Box-Behnken Design, different case studies with different numbers of variables should be performed. Also, effect of the orbit used in Box-Behnken design should be examined.

v. R^2 is not a valid measure to evaluate the validity of the fitted response function. Instead, cross validation is a better method to be sure that fitted function is valid in range of interest.

vi. The cross validation results show that quadratic response surface model can be used for prediction of the ballistic performance functions

vii. The cross validation results show that accuracy of the response surface function which was fitted to estimate the maximum internal pressure of the rocket motor decreases with increasing pressure values. Although the error is low, this may leads to wrong reliability estimations if the expected reliability is very high. Therefore, as a further extension of this study fitting another response function for the high pressure values should be considered to increase the accuracy of the estimations at the extremes of the pressure.

viii. Compared to the results obtained with ballistic performance, if a quadratic response surface model is used, error of the response surface function of maximum stress is relatively high. This error decreases by increasing the order of the response surface function. For this reason, in this study, a cubic response surface model was used to approximate the stress at the casing. However, as a further extension, higher order models and models which are not limited to polynomials but include logarithmic or trigonometric functions should be evaluated to obtain the minimum error.

ix. Reliability of the rocket motor was assessed at three different temperatures: +60ºC, +20ºC and -35ºC. Estimated current reliability values for these temperatures are: 0.988561, 0.998884 and 0.973227, respectively. These results show that reliability of the rocket motor decreases at temperature extremes.

x. The simulation results show that; most possible failure of the rocket motor at high temperatures is due to the maximum acceleration limits. The probability of exceeding maximum acceleration limit at +60ºC is fount to be 1.14%

xi. At low temperatures, inability of the rocket motor to provide needed total impulse to reach desired range is the most possible failure mode. The probability of failure due to the total impulse limit is found to be 2.66% at -35 ºC.

xii. The most probable failure location of this rocket motor casing is at the casing-nozzle connection.

xiii. The burn rate constant is the most effective variable on the variations in ballistic performance of the rocket motor. Hence, special attention should be given to reduce variations and tightly control it.

xiv. The maximum expected operating pressure of this rocket motor is found to be 137.7 bars. In the literature, it is generally suggested to multiply the nominal pressure at maximum operating temperature with a safety factor of 1.15 to estimate the MEOP of a rocket motor. If this safety factor is applied MEOP of this rocket motor is found to be 139.4 bars which is 1.2% higher than the MEOP determined in this study. Then, using a safety factor of 1.15 is a reasonable assumption at initial design.

xv. It is a known fact that increasing reliability at later stages of the design is difficult and costly. However, it is shown that reliability of a rocket motor can be easily increased in early design phases.

xvi. By considering the failure modes included in this study, a new design point was proposed to increase the reliability. New design point was found by changing grain geometry dimensions and nozzle dimensions. New reliability values are estimated as 0.999952 at +60 ºC, 0.999760 at -35 ºC and larger than 0.999999 at 20 ºC.

xvii. In this study, Direct Monte Carlo simulation method was used to estimate the performance distribution and the probability of failure values. However, using other Monte Carlo simulation techniques such as Importance Sampling and Latin Hypercube Sampling, accuracy of the estimation can be increased.

xviii. As a suggested further extension of the study, other failure modes of the rocket motor in the overall life cycle conditions should be included to predict the reliability of the motor. The mean and the standard deviations for input parameters used in this study do not include the aging and degradation of materials. Same procedure should be applied with aged material properties to estimate the reliability after 10 years of storage period.

xix. Although the error of the ballistic performance prediction software was neglected in this study, it is suggested that after collecting enough test data, this error can be included in the calculations to increase the accuracy of the results.

REFERENCES

[1]. Kececioglu D.," Reliability Engineering Handbook" Volume I, PTR Prentice-Hall Inc, New Jersey,1991

[2]. Lewis E. E., "Introduction to Reliability Engineering", John Willey and Sons Inc, New York, 1996

[3]. Defense Standard 00-40 (Part 6), "Reliability And Maintainability", Ministry Of Defense, 9 December 1988

[4]. Hasofer, A.M.; Lind, N.C., "Exact and Invariant Second-Moment Code Format," Journal of the Engineering Mechanics, Division 100, 1974, pp. 111-121.

[5]. Rackwitz, R., B. Fiessler, "Structural Reliability under Combined Random Load Sequences", Computers and Structures, Vol. 9, 1978, pp489-494.

[6]. Liu, P.-L., Der Kiureghian A., "Optimization algorithms for structural reliability analysis, Report UCB/SESM-86/09, Berkeley, California, 1986

[7]. Bucher, C.G. and Bourgund, U., "A Fast and Efficient Response Surface Approach for Structural Reliability Problems.", Structural Safety, 7, 1990, pp. 57-66

[8]. Box, G. E. P., and K. B. Wilson, "On the experimental attainment of optimum conditions", J. Roy. Stat. Soc., Ser. B, 13,1, 1951

[9]. Faravelli, L., "Response-Surface Approach for Reliability Analysis.", Journal of Engineering Mechanics, ASCE, 1989,115(12), pp 2763-2781

[10]. Rajashekhar, M.R. and Ellingwood, B.R. (1993). "A New Look at the Response Surface Approach for Reliability Analysis", Structural Safety, Vol 12, pp 205-220.

[11]. Liu, Ying Wei, Moses, Fred, "A Sequential Response Surface Method and its Application in The Reliability Analysis of Aircraft Structural", Structural Safety , v16, 1994, Elsevier Science Publishers B.V., Amsterdam, Neth, p 39-46

[12]. Grandhi, R. V., and Wang, L., “Higher-order Failure Probability Calculation Using Nonlinear Approximations,” Computer Methods in Applied Mechanics and Engineering, Vol. 168, 1999, pp. 185-206.

[13]. Rajagopalant, S., Sundaresan M., "Structural Reliability of Rocket Motor Hardware-A Probabilistic Approach, Reliability Engineering", Elsevier Applied Science Publishers Ltd., England, 1985. Vol 12, pp 193-203

[14]. Ekstrom J.L., Allred A.G.,Verifying Reliability of Solid Rocket Motors (SRMs) at Minimum Cost, Reliability and Maintainability Symposium, IEEE, 1991 PP 502-508

[15]. Wang Zheng, Structural Reliability Design on Solid Rocket Motor Case, AIAA/SAE/ASME/ASEE 29th Joint Propulsion Conference and Exhibit,28-30 June 1993, Montery, CA, USA

[16]. Smith S. L., Spear G. B., Cornwell M. D.,” Statistical Monte Carlo Prediction For Thermal Reliability”, AIAA 94-3183, 30th AIAA Joint Propulsion Conference June 27-29, 1994 / Indianapolis, USA

[17]. Arkin, C. M., "The rocket handbook for amateurs; an illustrated guide to the safe construction, testing, and launching of model rockets" J. Day Co., New York,1959

[18]. Platzek H., “Preliminary Solid Rocket Motor Design Techniques”, Naval Weapons Center, California, 1979

[19]. National Aeronautics and Space Administration, “Solid Rocket Motor Metal Cases”, Marshall Library, NASA SP 8025,1970

[20]. Sutton G. P., “Rocket Propulsion Elements”, John Willey and Sons Inc., NY, 2001

[21]. Rocket Basics, Thiokol Corporation, Retrieved on 23 August 2006, from the World Wide Web: http://www.fas.org/man/dod-101/sys/missile/docs/RocketBasics.htm

[22]. National Aeronautics and Space Administration, “Solid Rocket Motor Internal Insulation”, Marshall Library, NASA SP 8093,1976

[23]. National Aeronautics and Space Administration, “Solid Rocket Motor Igniters”, Marshall Library, NASA SP 8051, 1971

[24]. The ordnance shop, Retrieved on 23 August 2006, from the World Wide Web: http://www.ordnance.org/rockets.htm

[25]. National Aeronautics and Space Administration, “Solid Propellant Grain Design and Internal Ballistic”, Marshall Library, NASA SP 8076,1972

[26]. National Aeronautics and Space Administration, “Solid Rocket Motor Performance Analysis and Prediction”, Marshall Library, NASA SP 8339,1971

[27]. Jensen G. E., Netzer D. W., “Tactical Missile Propulsion” Volume 170 Progress in Astronautics and Aeronautics AIAA., Virginia, pp58-84

[28]. National Aeronautics and Space Administration, “Solid Rocket Thrust Vector Control”, , NASA SP 8114, Lewis Research Center, Ohio,1974

[29]. International Experimental Aerospace Society, Retrieved on 21 August 2006, from the World Wide Web: http://www.users.qwest.net/~jhove1/IEAS/tech/failures.html

[30]. IEEE, “Communications-Based Train Control (CBTC) Functional and Performance Requirements”, IEEE P1474.1.

[31]. Von Alven W. H., “Reliability Engineering”, ARINC Research Corporation-Printice Hall Inc, New Jersey, 1964

[32]. NIST/SEMATECH e-Handbook of Statistical Methods, June 11, 2006, from the World Wide Web: http://www.itl.nist.gov/div898/handbook/

[33]. Rene L. Bierbaum R. L., Wright D. L.,” Reliability Assessment Methodology For 1 -Shot Systems” IEEE 2002 Proceedings Reliability And Maintainability Symposium, 2002

[34]. Isaac E. I., Stames, J. H, “Safety Factor And The Non-Deterministic Approaches” American Institute of Aeronautics and Astronoutics,AIAA-99-1614, 1999

[35]. Carter A. D. S., “Mechanical Reliability and Design”, Macmillian Press Ltd.,London,1997

[36]. Kececioglu D., “Robust Engineering Design by Reliability With Emphasis on Mechanical Components & Structural Reliability” , DEStech Publications, Volume I,2003, pp 25-131

[37]. Military Handbook, Reliability Prediction of Electronic Equipment, MIL-HDBK-217F, 1991.

[38]. NSWC-98, Handbook of Reliability Prediction Procedures for Mechanical Equipments, 1998.

[39]. Bozkaya K. Kuran B. “Reliability of Guided Munitions” Ankara International Aerospace Conference, Ankara, 2005

[40]. Nelson N., “Accelerated Testing, Statistical Models, Test Plans and Data Analyses” John Willey and Sons Inc, New York, 1990

[41]. Vasilliou P., Mettas A., “Understanding Accelerated Life-Testing Analysis”, Reliability and Maintainability Symposium Tutorial, 2001

[42]. Kececioglu D. Jacks A. J, “The Arrhenius, Eyring, Inverse Power Law and Combination Models in Accelerated Life Testing” Journal of Reliability Engineering, Vol 8, 1984

[43]. Craney T. A., “Probabilistic Engineering Design” R & M Engineering Journal, Vol. 23-2, June 2003

[44]. Long, M. W and Narciso J. D.,” Probabilistic Design Methodology For Composite Aircraft Structures,” DOT/FAA/AR-99/2 Northrop Grumman Commercial Aircraft Division, June 1999

[45]. Rackwirtz R. “Reliability analysis-Past, Present and Future”, 8th ASCE Specialty Conference on Probabilistic Mechanics and Structural Reliability

[46]. Verderaime, V., ”Illustrated Structural Application of Universal First-Order Reliability Method”, NASA Technical Paper 3501, 1994

[47]. Rubinstein R. Y., "Simulation and the Monte Carlo Method", John Wiley and Sons Inc, 1981

[48]. Robert C. P., Casella G., "Monte Carlo Statistical Methods", Springer Science and Business Media Inc, 2004

[49]. Czitrom V., ”One Factor at a Time versus Designed Experiments”, American Statistical Association, 1999, Vol 53, No: 2, pp 126-131

[50]. Myers, R. H. and Montgomery, D. C. Response surface methodology: Process and Product Optimization Using Designed Experiments, Wiley & Sons, NY, 2002.

[51]. Montgomery D. C., “Design and Analysis of Experiments”, John Willey and Sons Inc, 5th Edition, NY,1997

[52]. Kim, S., and Na, S., “response surface method Using Vector Projected Sampling Points”, Structural Safety,Vol.19 (1), 1997, pp.3-19.

[53]. Zor Ö. , “A Study on Production Line Qualification (PQL) Solution Heat Treatment Process”, M.S.Thesis Report, Middle East Technical University, 2003

[54]. Military Handbook MIL-HDBK-5J “Metallic Materials And Elements For Aerospace Vehicle Structures”, USA Department Of Defense, 2003

[55]. Haugen E. B., ”Probabilistic Mechanical Design”, John Willey and Sons Inc.,NY,1980

[56]. Jensen G. E., Netzer D. W.(Edited), “Tactical Missile Propulsion” American Institute of Aeronautics and Astronautics Inc., Virginia,

[57]. Onwubiko C., “Introduction to Engineering Design Optimization” Prentice Hall Inc,2000

APPENDIX A

RELIABILITY INDEX FOR A LINEAR LIMIT STATE

Let L and C are two random variables and failure occurs when L exceeds C (Figure A.1) then the performance function g(L,C) is:

$$g(L,C)=c-l \qquad \text{Eq (A.1)}$$

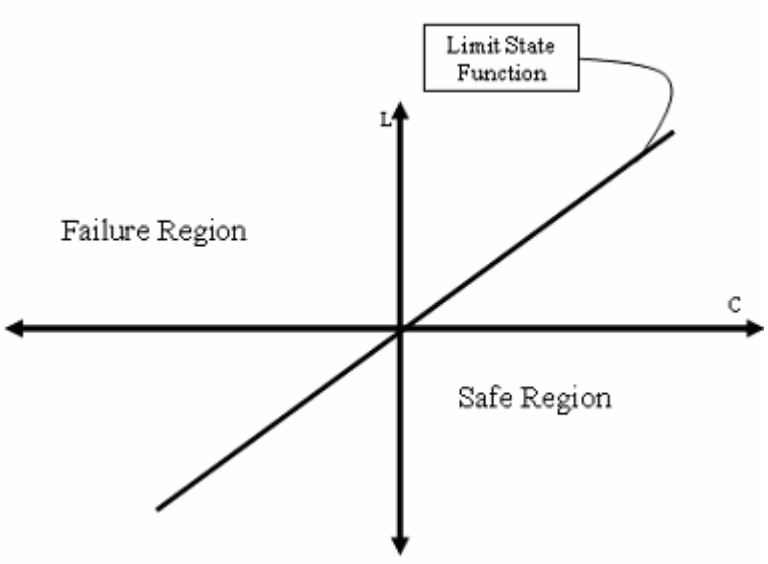

Figure A.1. Failure region and safe region for g(C,L)

and l>c is the failure state, if L and C are normally distributed

$$f_L(l) = \frac{1}{\sqrt{2.\pi}.\sigma_l}.e^{\left[-\frac{1}{2}.\frac{l-\mu_c}{\sigma_l^2}\right]} \qquad \text{Eq (A.2)}$$

and

$$f_C(c) = \frac{1}{\sqrt{2.\pi}.\sigma_c}.e^{\left[-\frac{1}{2}.\frac{c-\mu_c}{\sigma_c^2}\right]} \qquad \text{Eq (A.3)}$$

where μ and σ are mean value and standard deviation respectively. Then the expected value of the reliability is calculated by Equation (A.4).

$$R = \int_{-\infty}^{\infty}\left[\int_{-\infty}^{c} f_L(l).dl\right] f_C(c).dc \qquad \text{Eq (A.4)}$$

$$R = \int_{-\infty}^{\infty}\left[\int_{-\infty}^{c} \frac{1}{\sqrt{2.\pi}.\sigma_l}.e^{\left[-\frac{1}{2}.\frac{l-\mu_s}{\sigma_l^2}\right]}.\frac{1}{\sqrt{2.\pi}.\sigma_c}.e^{\left[-\frac{1}{2}.\frac{c-\mu_c}{\sigma_c^2}\right]} dl.dc\right] \qquad \text{Eq (A.5)}$$

Equation (A.5) can be written in x and y domain (Figure A.2) where x and y are defined as:

$$x = \frac{c-\mu_c}{\sigma_c} \qquad \text{Eq (A.6),}$$

$$y = \frac{l-\mu_s}{\sigma_l} \qquad \text{Eq (A.7)}$$

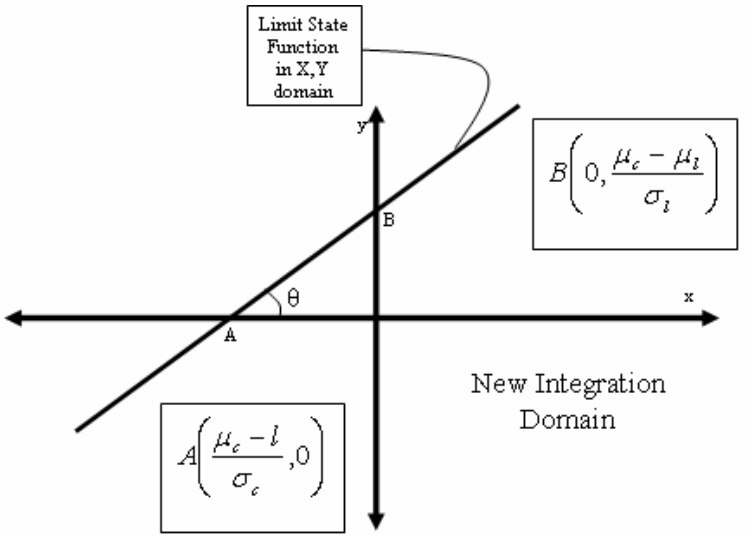

Figure A.2. New failure and safe region after converting C and L to standard normal distribution

$$R = \frac{1}{2\pi} \int_{-\infty}^{\infty} \left[\int_{-\infty}^{\frac{\sigma_c x + \mu_c - \mu_l}{\sigma_s}} e^{\left[-\frac{1}{2}.(x^2+y^2) \right]} dy \right] .dx \qquad \text{Eq (A.8)}$$

By rotating the axes by θ R can be written as a single standardized normal distribution and failure line will be parallel to x axis (Figure A.3).

$$x_\theta = x.\cos\theta + y.\sin\theta$$
$$y_\theta = -x.\sin\theta + y.\cos\theta$$
$$x_\theta^2 + y_\theta^2 = x^2 + y^2$$

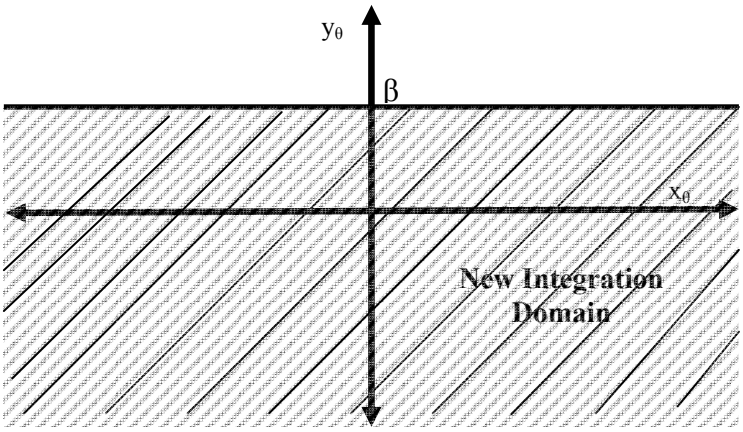

Figure A.3. New Integration domain after rotation

it is known that

$$\frac{1}{2\pi}\int_{-\infty}^{\infty} e^{-\frac{1}{2}x_\theta^2}\,dx_\theta = \phi(\infty) = 1 \qquad \text{Eq (A.9)}$$

then we have just the second integration term and reliability is become:

$$R = \frac{1}{2\pi}\int_{-\infty}^{\beta} e^{\left[-\frac{1}{2}.y_\theta^2\right]}dy_\theta \qquad \text{Eq (A.10)}$$

and ß is defined as:

$$\beta = \frac{\mu_c - \mu_l}{\sqrt{\sigma_c^2 + \sigma_l^2}} = \frac{\mu_M}{\sigma_M} \qquad \text{Eq (A.11)}$$

which is the reliability index defined by Cornell for a first order limit state function and in general form with n variables

$$\mu_M = g(X_1, X_2, ...X_n)$$

$$\sigma_M^2 = \sum_{i=1}^{n} \left(\frac{\partial g}{\partial x_i} \right)^2 \sigma_i^2 + \sum_{i \neq j} \sum \left(\frac{\partial g}{\partial x_i} \right) . \left(\frac{\partial g}{\partial y_i} \right) . \rho_{ij} . \sigma_i . \sigma_j$$

and probability of failure is

$$P_f = 1 - \phi(\beta) \qquad \text{Eq (A.12)}$$

where Φ is the Standard normal distribution.

APPENDIX B

CROSS VALIDATION OF RESPONSE FUNCTIONS FOR-35°C AND 20°C

B.1. CROSS VALIDATION RESULTS FOR 20 ºC

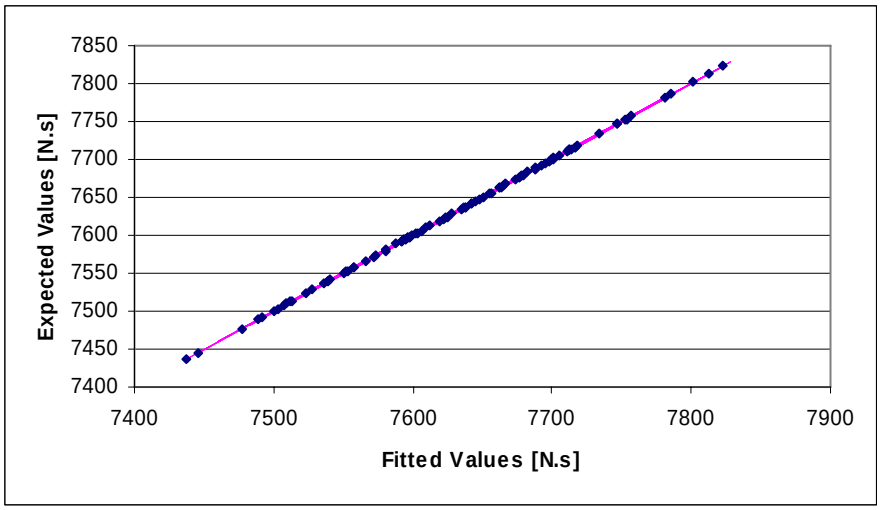

Figure B.1. Expected vs. Fitted values for the response function of total impulse [N.s] at 20°C (Maximum Absolute Error = 1.014)

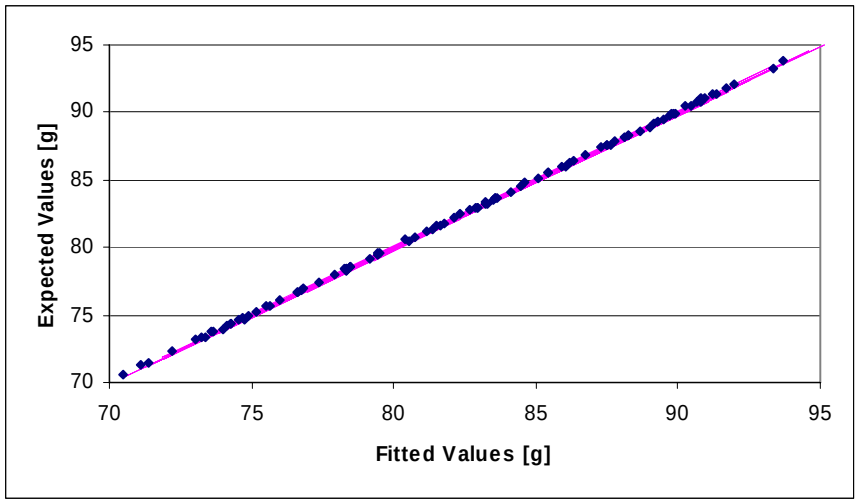

Figure B.2. Expected vs. Fitted values for the response function of maximum acceleration [g] at 20°C (Maximum Absolute Error = 0.268)

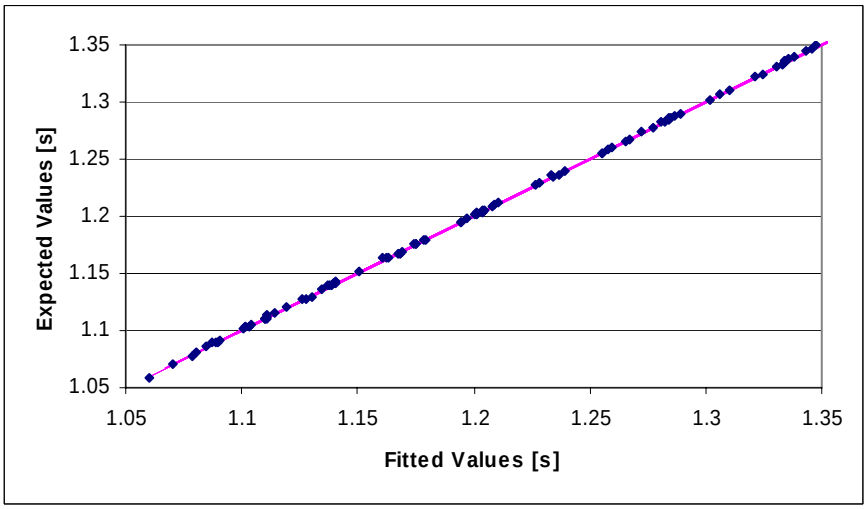

Figure B.3. Expected vs. Fitted values for the response function of arming acceleration duration [s] at 20°C (Maximum Absolute Error = 0.0038)

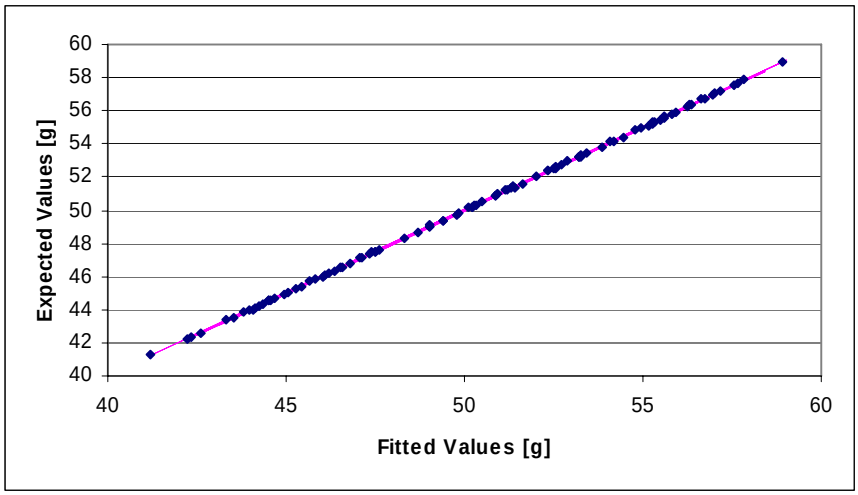

Figure B.4. Expected vs. Fitted values for the response function of launch acceleration [s] at -20°C (Maximum Absolute Error = 0.117)

B.2. CROSS VALIDATION RESULTS FOR -35 ºC

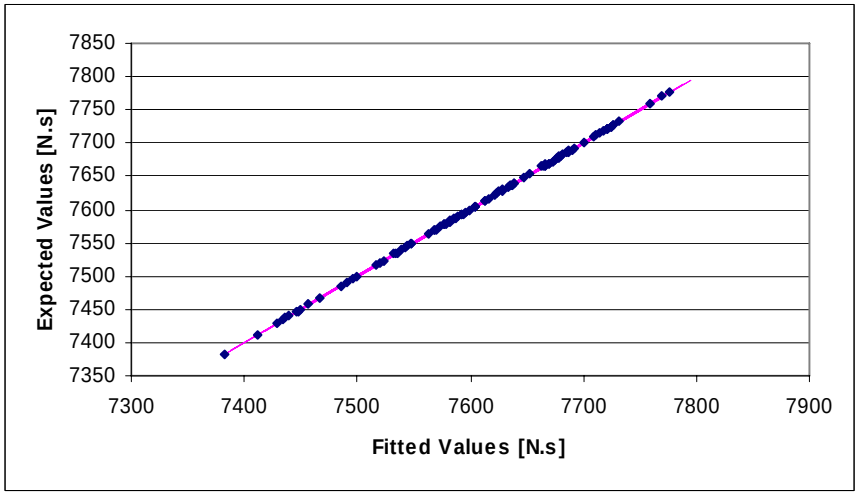

Figure B.5. Expected vs. Fitted values for the response function of the total impulse [N.s] at -35 °C (Maximum Absolute Error = 1.771)

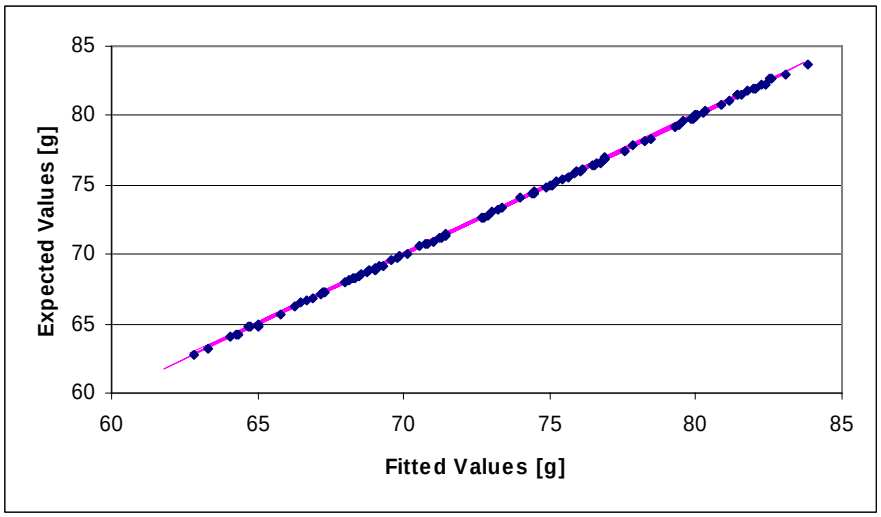

Figure B.6. Expected vs. Fitted values for the response function of maximum acceleration [g] at -35 °C (Maximum Absolute Error = 0.187)

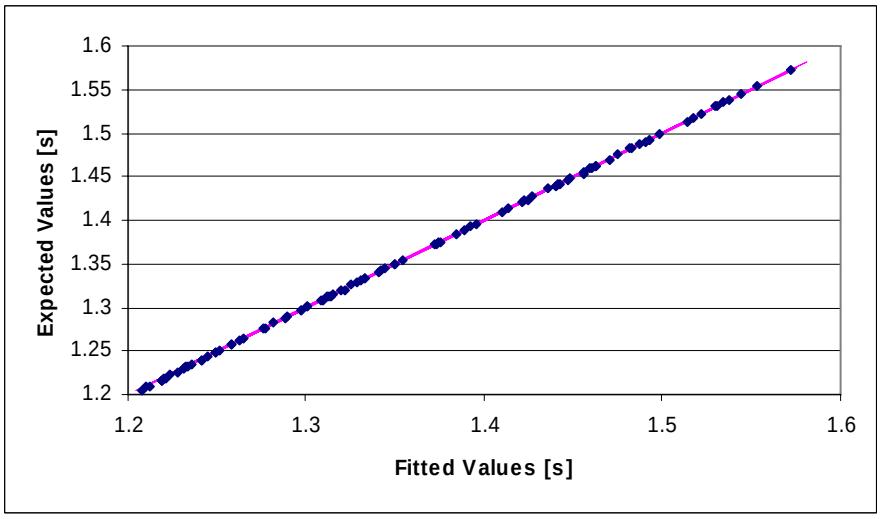

Figure B.7. Expected vs. Fitted values for response function of arming acceleration duration [s] at -35 °C (Maximum Absolute Error = 0.0025)

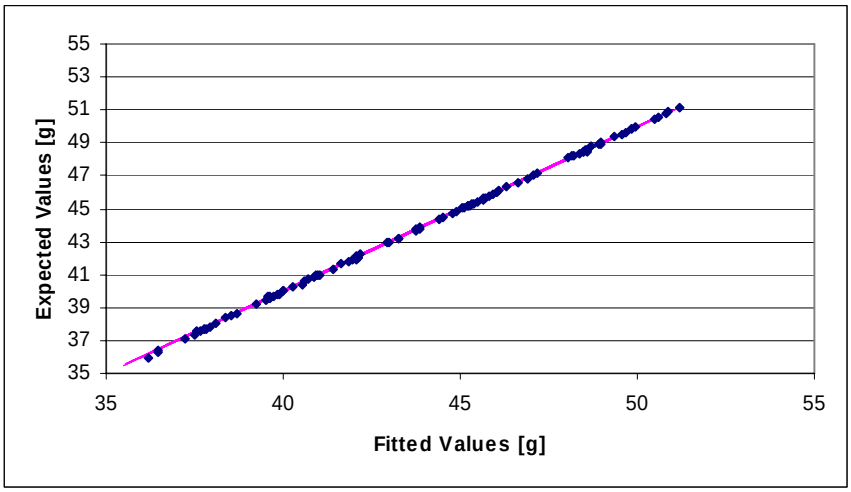

Figure B.8. Expected vs. Fitted values for response function of launch acceleration at -35 °C (Maximum Absolute Error = 0.222)

APPENDIX C

ESTIMATED RESPONSE FUNCTIONS

Table C.1. Estimated response functions for +60ºC

Coefficients of response functions (With coded units, k=1)					
TERM	**Total Impulse [N.s]**	**Max. Acceleration [g]**	**Arming Acceleration Duration [s]**	**Launch Acceleration [g]**	**Max. Pressure [bar]**
Constant	7683.8	90.66	1.099	56.393	121.18
L_{Grain}^2	-0.05898	0.00226	0.00000	0.00030	-0.00304
$L_{Grain}xH$	-0.03288	0.02395	0.00010	0.02146	0.03454
$L_{Grain}xa_r$	0.00027	0.01116	0.00004	0.00043	-0.00496
$L_{Grain}xS_{Temp}$	0.11609	0.00454	-0.00004	0.00230	0.00268
$L_{Grain}x\rho$	-0.01480	-0.00154	0.00002	-0.00051	0.00210
$L_{Grain}x\zeta$	-0.01253	0.00080	-0.00002	-0.00057	-0.00310
$L_{Grain}x\Phi_{Throat}$	0.01263	-0.00029	-0.00002	-0.00021	-0.00034
$L_{Grain}x\Phi_{Exit}$	-0.02492	-0.00185	0.00004	0.00152	0.00054
$L_{Grain}xR_1$	0.01827	0.00096	-0.00002	0.00052	-0.00055
$L_{Grain}xR_2$	-0.01398	-0.00059	-0.00002	0.00052	0.00037
$L_{Grain}xL_1$	-0.02275	0.00326	0.00005	-0.00105	-0.00285
L_{Grain}	36.09600	0.62713	-0.00241	0.44112	0.80341
H^2	-0.51007	0.02815	0.00173	0.03000	0.07709
Hxa_r	-0.02028	0.00299	0.00002	0.00262	0.00407
HxS_{Temp}	-0.02052	0.01574	0.00007	0.01818	0.02193
$Hx\rho$	0.00972	0.00191	0.00001	-0.00195	0.00079
$Hx\zeta$	0.02330	-0.00393	-0.00007	-0.00320	-0.01351
$Hx\Phi_{Throat}$	0.08261	0.00145	-0.00007	0.00226	0.00066
$Hx\Phi_{Exit}$	-0.00866	0.00091	0.00012	0.00752	0.00070
HxR_1	-0.00166	-0.01015	0.00002	0.00171	0.00166
HxR_2	-0.00944	0.00034	0.00005	0.00452	0.00074
HxL_1	-0.00917	0.00071	-0.00005	-0.00296	-0.00048
H	15.50000	3.92850	-0.04816	2.97370	5.23950
a_r^2	0.01805	0.00592	0.00000	0.00075	-0.00397
a_rxS_{Temp}	0.00922	-0.00216	0.00001	0.00062	0.00193
$a_rx\rho$	0.00105	-0.00443	-0.00002	-0.00020	0.00198
$a_rx\zeta$	-0.00541	-0.00109	-0.00001	-0.00023	-0.00173
$a_rx\Phi_{Throat}$	0.00931	0.00195	0.00002	-0.00009	-0.00071
$a_rx\Phi_{Exit}$	0.00633	0.00404	-0.00001	0.00080	-0.00174
a_rxR_1	-0.00380	-0.00024	0.00002	-0.00023	0.00148
a_rxR_2	-0.02845	-0.00107	-0.00001	-0.00120	-0.00163
a_rxL_1	-0.01344	0.00412	0.00001	-0.00049	-0.00091

Table C.1. Estimated response functions for +60ºC (Continued)

Coefficients of response functions (With coded units, k=1)					
TERM	**Total Impulse [N.s]**	**Max. Acceleration [g]**	**Arming Acceleration Duration [s]**	**Launch Acceleration [g]**	**Max. Pressure [bar]**
a_r	0.28748	0.07491	-0.00090	0.05754	0.10359
S_{Temp}^2	0.02300	0.00517	0.00000	0.00141	-0.00410
$S_{Temp}x\rho$	-0.01241	0.00110	-0.00001	-0.00070	0.00180
$S_{Temp}x\zeta$	-0.00802	-0.00052	0.00001	-0.00066	-0.00084
$S_{Temp}x\Phi_{Throat}$	0.01845	0.00007	0.00001	0.00054	-0.00045
$S_{Temp}x\Phi_{Exit}$	-0.00866	0.00066	0.00001	0.00130	0.00040
$S_{Temp}xR_1$	-0.00784	-0.00027	0.00001	0.00015	-0.00279
$S_{Temp}xR_2$	-0.01028	-0.00329	0.00001	0.00030	0.00060
$S_{Temp}xL_1$	-0.01123	0.00215	0.00002	-0.00037	-0.00065
S_{Temp}	27.11900	0.43559	-0.00202	0.36940	0.57721
ρ^2	0.02791	0.00429	0.00000	0.00070	-0.00083
$\rho x\zeta$	-0.00947	-0.00066	0.00001	-0.00032	-0.00185
$\rho x\Phi_{Throat}$	-0.00947	0.00102	0.00001	-0.00065	0.00141
$\rho x\Phi_{Exit}$	0.00698	-0.00310	-0.00002	0.00002	0.00060
ρxR_1	-0.01152	-0.00457	0.00001	-0.00048	0.00363
ρxR_2	-0.00867	0.00223	-0.00002	-0.00051	-0.00182
ρxL_1	-0.00050	-0.00255	-0.00004	0.00010	-0.00273
ρ	-2.95100	0.03803	-0.00006	-0.06450	0.02477
ζ^2	0.02508	0.00429	0.00000	0.00075	-0.00052
$\zeta x\Phi_{Throat}$	0.00539	-0.00029	-0.00001	0.00016	0.00052
$\zeta x\Phi_{Exit}$	-0.00106	-0.00123	-0.00001	-0.00010	-0.00045
ζxR_1	0.00038	-0.00316	-0.00001	-0.00060	0.00268
ζxR_2	-0.00888	0.00010	-0.00001	-0.00051	-0.00068
ζxL_1	0.00511	-0.00212	-0.00002	0.00004	0.00070
ζ	-1.45300	-0.08949	0.00099	-0.07121	-0.28166
Φ_{Throat}^2	-0.00533	0.00005	0.00000	-0.00005	-0.00092
$\Phi_{Throat}x\Phi_{Exit}$	-0.00728	0.00262	-0.00001	0.00029	-0.00168
$\Phi_{Throat}xR_1$	-0.00925	-0.00148	0.00002	-0.00021	-0.00052
$\Phi_{Throat}xR_2$	-0.00497	-0.00405	-0.00001	0.00029	0.00296
$\Phi_{Throat}xL_1$	0.00127	-0.00140	0.00001	-0.00007	-0.00051
Φ_{Throat}	1.68360	0.02438	0.00003	0.01082	-0.00040
Φ_{Exit}^2	0.02331	-0.00044	0.00000	0.00141	-0.00087
$\Phi_{Exit}xR_1$	-0.00233	0.00490	0.00002	0.00037	-0.00390
$\Phi_{Exit}xR_2$	0.01173	0.00116	-0.00004	0.00084	0.00149
$\Phi_{Exit}xL_1$	0.00097	0.00395	0.00001	-0.00009	-0.00141
Φ_{Exit}	-3.56050	-0.00006	-0.00201	0.21144	0.02452
R_1^2	0.01080	0.00013	0.00005	0.00030	-0.00092
R_1xR_2	-0.00964	-0.00265	-0.00001	-0.00041	0.00265
R_1xL_1	0.01138	-0.00343	-0.00002	-0.00015	-0.00070
R_1	1.15480	-0.00265	-0.00015	0.06010	-0.00758
R_2^2	0.00784	0.00482	0.00005	0.00048	-0.00087
R_2xL_1	-0.00988	-0.00313	-0.00002	-0.00046	0.00273
R_2	-0.72672	-0.00606	-0.00108	0.09608	0.01384
L_1^2	0.01704	0.00597	0.00000	0.00061	-0.00401
L_1	-1.74040	0.01020	0.00025	-0.08176	0.00715

Table C.2. Estimated response functions for +20ºC

Coefficients of response functions(With coded units, k=1)					
TERM	**Total Impulse [N.s]**	**Max. Acceleration [g]**	**Arming Acceleration Duration [s]**	**Launch Acceleration [g]**	**Max. Pressure [bar]**
Constant	7649.9	82.749	1.206	50.408	110.58
L_{Grain}^2	-0.09277	-0.00702	0.00000	-0.00045	0.00067
$L_{Grain}xH$	-0.02803	0.02308	0.00011	0.01980	0.03156
$L_{Grain}xa_r$	0.00980	0.00375	-0.00002	0.00050	-0.00331
$L_{Grain}xS_{Temp}$	0.12586	0.00234	0.00000	0.00342	0.00172
$L_{Grain}x\rho$	-0.01698	0.00217	0.00000	-0.00067	0.00063
$L_{Grain}x\zeta$	-0.02022	-0.00186	0.00002	-0.00069	-0.00184
$L_{Grain}x\Phi_{Throat}$	0.01409	-0.00548	0.00000	-0.00003	0.00230
$L_{Grain}x\Phi_{Exit}$	-0.02353	0.00170	-0.00002	0.00134	0.00036
$L_{Grain}xR_1$	0.00464	0.00095	0.00005	0.00050	-0.00048
$L_{Grain}xR_2$	-0.00477	0.00038	0.00000	0.00081	-0.00050
$L_{Grain}xL_1$	-0.02123	0.00159	0.00003	-0.00067	0.00052
L_{Grain}	36.16900	0.57574	-0.00266	0.39743	0.73026
H^2	-0.61567	0.01839	0.00190	0.02611	0.03704
Hxa_r	-0.00748	0.00270	-0.00005	-0.00036	-0.00136
HxS_{Temp}	-0.03252	0.01389	0.00009	0.01666	0.02167
$Hx\rho$	0.00473	0.00244	-0.00003	-0.00216	0.00086
$Hx\zeta$	0.01581	-0.00541	-0.00002	-0.00311	-0.01189
$Hx\Phi_{Throat}$	0.06103	-0.00072	0.00003	0.00136	0.00047
$Hx\Phi_{Exit}$	-0.02772	0.00088	0.00008	0.00727	0.00088
HxR_1	-0.00158	0.00916	-0.00011	0.00164	-0.00313
HxR_2	-0.03039	0.00120	0.00003	0.00408	0.00039
HxL_1	-0.00648	0.00345	0.00000	-0.00288	-0.00206
H	16.87700	3.60250	-0.05276	2.68530	4.75150
a_r^2	-0.00014	-0.00026	0.00000	-0.00001	0.00014
a_rxS_{Temp}	-0.00119	-0.00144	0.00000	-0.00027	0.00120
$a_rx\rho$	-0.00600	0.00230	0.00000	-0.00011	-0.00042
$a_rx\zeta$	-0.00577	-0.00230	0.00002	-0.00016	0.00045
$a_rx\Phi_{Throat}$	0.00517	0.00183	0.00000	0.00050	-0.00053
$a_rx\Phi_{Exit}$	0.00714	-0.00323	-0.00002	0.00072	-0.00159
a_rxR_1	-0.00600	0.00023	-0.00002	-0.00075	0.00034
a_rxR_2	-0.02828	0.00019	0.00003	-0.00153	0.00033
a_rxL_1	-0.01184	0.00081	0.00000	-0.00042	-0.00047
a_r	-0.00260	-0.00097	-0.00003	-0.00032	0.00101
S_{Temp}^2	-0.01768	-0.00450	-0.00005	0.00016	0.00010
$S_{Temp}x\rho$	-0.02878	0.00067	0.00002	-0.00084	-0.00220
$S_{Temp}x\zeta$	-0.01411	-0.00270	-0.00003	-0.00083	-0.00077
$S_{Temp}x\Phi_{Throat}$	0.02277	0.00102	-0.00002	0.00052	-0.00031
$S_{Temp}x\Phi_{Exit}$	-0.00317	-0.00236	0.00000	0.00130	0.00109
$S_{Temp}xR_1$	0.00456	0.00152	0.00003	0.00017	-0.00147
$S_{Temp}xR_2$	-0.00688	0.00225	-0.00002	0.00095	0.00420
$S_{Temp}xL_1$	-0.00194	-0.00191	0.00002	-0.00047	-0.00053
S_{Temp}	27.16800	0.40668	-0.00218	0.33292	0.52924
ρ^2	-0.00588	-0.00419	0.00000	-0.00028	0.00019
$\rho x\zeta$	-0.01258	0.00147	0.00000	-0.00030	-0.00152
$\rho x\Phi_{Throat}$	-0.00405	-0.00178	0.00002	-0.00023	-0.00050
$\rho x\Phi_{Exit}$	0.00792	-0.00063	0.00000	-0.00011	-0.00038
ρxR_1	-0.00625	-0.00709	0.00000	-0.00017	0.00425
ρxR_2	0.00109	-0.00139	-0.00002	-0.00008	-0.00148

Table C.2. Estimated response functions for +20ºC (Continued)

Coefficients of response functions(With coded units, k=1)					
TERM	**Total Impulse [N.s]**	**Max. Acceleration [g]**	**Arming Acceleration Duration [s]**	**Launch Acceleration [g]**	**Max. Pressure [bar]**
$\rho x L_1$	-0.00238	-0.00164	-0.00002	0.00019	-0.00228
ρ	-2.95510	0.03153	-0.00004	-0.05952	0.02338
ζ^2	-0.01154	-0.00026	-0.00005	-0.00050	0.00050
$\zeta x \Phi_{Throat}$	0.01347	0.00244	0.00000	0.00019	-0.00128
$\zeta x \Phi_{Exit}$	-0.00200	0.00113	-0.00002	-0.00013	0.00050
$\zeta x R_1$	-0.00452	-0.00431	0.00002	-0.00009	0.00175
$\zeta x R_2$	-0.00430	-0.00039	0.00000	-0.00006	-0.00052
$\zeta x L_1$	-0.00030	-0.00098	0.00000	0.00023	0.00022
ζ	-1.48180	-0.07791	0.00101	-0.06385	-0.25745
Φ_{Throat}^2	-0.00650	-0.00030	-0.00005	-0.00006	0.00014
$\Phi_{Throat} x \Phi_{Exit}$	0.00241	0.00103	0.00000	0.00003	-0.00058
$\Phi_{Throat} x R_1$	-0.00077	-0.00088	0.00000	-0.00016	0.00039
$\Phi_{Throat} x R_2$	0.00073	-0.00080	0.00002	0.00013	0.00041
$\Phi_{Throat} x L_1$	0.00655	-0.00073	0.00002	0.00011	-0.00039
Φ_{Throat}	1.55130	0.01935	0.00006	0.00903	-0.00031
Φ_{Exit}^2	-0.03426	-0.00043	-0.00005	-0.00063	0.00005
$\Phi_{Exit} x R_1$	0.00164	0.00069	0.00002	0.00022	0.00039
$\Phi_{Exit} x R_2$	-0.01077	-0.00283	0.00000	-0.00009	0.00034
$\Phi_{Exit} x L_1$	0.00786	0.00095	0.00000	-0.00005	-0.00039
Φ_{Exit}	-3.50740	-0.00184	-0.00219	0.19614	0.01826
R_1^2	-0.01242	-0.00026	-0.00005	-0.00032	0.00014
$R_1 x R_2$	0.00366	-0.00502	0.00000	0.00003	0.00334
$R_1 x L_1$	-0.00631	-0.00961	0.00000	-0.00017	0.00764
R_1	1.14740	-0.00525	-0.00013	0.05629	-0.00512
R_2^2	-0.01101	-0.00423	0.00000	-0.00023	0.00014
$R_2 x L_1$	0.01531	-0.00059	-0.00002	0.00039	-0.00138
R_2	-0.69012	-0.00461	-0.00120	0.08875	0.01056
L_1^2	-0.01265	-0.00428	0.00000	-0.00037	0.00014
L_1	-1.73980	0.00638	0.00024	-0.07637	0.00485

Table C.3. Estimated response functions for -35ºC

Coefficients of response functions(With coded units, k=1)					
TERM	**Total Impulse [N.s]**	**Max. Acceleration [g]**	**Arming Acceleration Duration [s]**	**Launch Acceleration [g]**	**Max. Pressure [bar]**
Constant	7597.7	72.78	1.369	43.111	97.604
L_{Grain}^2	-0.09380	0.00035	0.00004	0.00004	-0.00414
$L_{Grain} x H$	-0.08832	0.02253	0.00017	0.01919	0.01933
$L_{Grain} x a_r$	-0.00513	-0.00250	0.00000	-0.00023	0.00102
$L_{Grain} x S_{Temp}$	0.10505	-0.00177	0.00003	0.00136	0.00403
$L_{Grain} x \rho$	-0.00805	-0.00389	0.00000	-0.00016	0.00289
$L_{Grain} x \zeta$	-0.00426	0.00108	0.00006	-0.00020	-0.00406
$L_{Grain} x \Phi_{Throat}$	0.02029	-0.00227	0.00003	0.00059	0.00145
$L_{Grain} x \Phi_{Exit}$	-0.01301	0.00616	-0.00003	0.00095	-0.00345

Table C.3. Estimated response functions for -35ºC (Continued)

Coefficients of response functions(With coded units, k=1)					
TERM	**Total Impulse [N.s]**	**Max. Acceleration [g]**	**Arming Acceleration Duration [s]**	**Launch Acceleration [g]**	**Max. Pressure [bar]**
$L_{Grain}xL_1$	-0.00227	-0.00131	0.00000	-0.00027	0.00166
$L_{Grain}xR_1$	0.00204	-0.00123	-0.00003	0.00113	0.00152
$L_{Grain}xR_2$	-0.00276	-0.00095	0.00000	0.00000	-0.00009
L_{Grain}	36.31700	0.51239	-0.00314	0.34205	0.64861
H^2	-0.78765	0.01750	0.00225	0.01887	0.01222
Hxa_r	0.03095	-0.00177	-0.00006	-0.00408	-0.00402
HxS_{Temp}	-0.05649	0.01219	0.00016	0.01677	0.01431
$Hx\rho$	0.00146	0.00559	-0.00003	-0.00291	0.00117
$Hx\zeta$	0.03232	-0.00209	-0.00009	-0.00348	-0.00791
$Hx\Phi_{Throat}$	0.06987	0.00406	0.00000	0.00041	-0.00286
$Hx\Phi_{Exit}$	-0.04965	0.00123	0.00016	0.00764	-0.00152
HxR_1	-0.00385	-0.00034	0.00003	-0.00222	-0.00155
HxR_2	-0.03474	0.00050	0.00006	0.00391	-0.00016
HxL_1	0.00874	0.00017	0.00000	-0.00264	0.00213
H	19.28200	3.21340	-0.06008	2.32740	4.21330
a_r^2	-0.01182	-0.00013	0.00004	0.00000	-0.00060
a_rxS_{Temp}	0.00023	-0.00097	-0.00002	0.00006	0.00041
$a_rx\rho$	0.00518	-0.00150	-0.00002	0.00039	0.00208
$a_rx\zeta$	0.00279	-0.00106	0.00002	0.00025	0.00084
$a_rx\Phi_{Throat}$	-0.02145	-0.00184	-0.00002	-0.00023	0.00077
$a_rx\Phi_{Exit}$	-0.00102	0.00061	-0.00005	-0.00041	0.00080
a_rxR_1	0.00499	0.00188	0.00002	0.00008	-0.00061
a_rxR_2	0.00913	-0.00016	0.00002	0.00202	-0.00050
a_rxL_1	-0.00682	-0.00058	-0.00002	-0.00019	0.00063
a_r	-0.51486	-0.08530	0.00163	-0.06184	-0.11367
S_{Temp}^2	-0.01093	0.00252	0.00004	0.00084	-0.00184
$S_{Temp}x\rho$	-0.00160	-0.00323	0.00002	-0.00042	0.00359
$S_{Temp}x\zeta$	-0.00237	-0.00214	-0.00002	-0.00022	-0.00030
$S_{Temp}x\Phi_{Throat}$	0.00396	-0.00064	-0.00002	-0.00002	0.00063
$S_{Temp}x\Phi_{Exit}$	-0.02515	0.00128	0.00002	0.00081	0.00047
$S_{Temp}xR_1$	0.00087	0.00023	0.00002	0.00108	0.00075
$S_{Temp}xR_2$	-0.00093	-0.00017	0.00002	-0.00080	0.00070
$S_{Temp}xL_1$	0.00243	0.00041	0.00002	-0.00019	-0.00070
S_{Temp}	27.28600	0.36243	-0.00250	0.28576	0.47118
ρ^2	-0.00638	0.00406	0.00000	0.00035	-0.00254
$\rho x\zeta$	0.00305	-0.00127	-0.00002	-0.00020	-0.00091
$\rho x\Phi_{Throat}$	0.00254	-0.00092	-0.00002	-0.00206	0.00064
$\rho x\Phi_{Exit}$	-0.00401	-0.00150	0.00002	-0.00008	0.00208
ρxR_1	-0.00430	0.00311	-0.00005	-0.00047	-0.00058
ρxR_2	-0.00479	-0.00477	0.00002	-0.00063	0.00069
ρxL_1	0.00035	-0.00103	0.00005	0.00005	-0.00209
ρ	-2.96010	0.02463	-0.00003	-0.05276	0.01968
ζ^2	-0.01115	0.00305	0.00000	0.00017	-0.00060
$\zeta x\Phi_{Throat}$	-0.00801	0.00283	-0.00005	-0.00023	-0.00081
$\zeta x\Phi_{Exit}$	0.00276	-0.00306	-0.00002	-0.00009	0.00075
ζxR_1	-0.01026	0.00089	-0.00002	-0.00042	-0.00066
ζxR_2	-0.00362	0.00108	-0.00002	-0.00070	-0.00092
ζxL_1	-0.00754	0.00316	-0.00002	0.00000	-0.00045
ζ	-1.54810	-0.07376	0.00124	-0.05507	-0.22820

Table C.3. Estimated response functions for -35ºC (Continued)

Coefficients of response functions(With coded units, k=1)					
TERM	**Total Impulse [N.s]**	**Max. Acceleration [g]**	**Arming Acceleration Duration [s]**	**Launch Acceleration [g]**	**Max. Pressure [bar]**
Φ_{Throat}^2	-0.00952	-0.00009	0.00000	0.00035	-0.00056
$\Phi_{Throat}x\Phi_{Exit}$	0.00521	0.00075	0.00002	0.00005	-0.00080
$\Phi_{Throat}xR_1$	-0.00568	0.00211	0.00002	-0.00016	-0.00073
$\Phi_{Throat}xR_2$	-0.00379	0.00445	-0.00002	-0.00009	-0.00053
$\Phi_{Throat}xL_1$	-0.00037	0.00150	0.00002	-0.00080	-0.00084
Φ_{Throat}	1.34680	0.01470	0.00008	0.00614	-0.00021
Φ_{Exit}^2	-0.02896	0.00278	0.00004	0.00004	-0.00117
$\Phi_{Exit}xR_1$	0.00627	0.00219	-0.00002	0.00102	-0.00064
$\Phi_{Exit}xR_2$	-0.00546	-0.00156	-0.00002	0.00077	0.00194
$\Phi_{Exit}xL_1$	-0.00782	0.00155	0.00002	0.00041	0.00072
Φ_{Exit}	-3.42500	-0.00218	-0.00253	0.17502	0.01691
R_1^2	-0.01244	-0.00009	0.00004	-0.00009	-0.00060
R_1xR_2	-0.00523	-0.00202	-0.00002	-0.00038	0.00056
R_1xL_1	-0.00302	0.00100	0.00002	-0.00052	-0.00075
R_1	1.16240	-0.00418	-0.00016	0.05417	-0.00357
R_2^2	-0.00541	0.00402	0.00000	0.00031	-0.00268
R_2xL_1	0.00665	0.00422	-0.00002	-0.00011	-0.00220
R_2	-0.63935	-0.00311	-0.00142	0.07721	0.00960
L_1^2	-0.00377	0.00402	0.00000	0.00035	-0.00263
L_1	-1.75260	0.00943	0.00031	-0.06862	0.00252

APPENDIX D

ESTIMATED DISTRIBUTIONS OF RESPONSES FOR-35°C AND 20°C

D.1. ESTIMATED DISTRIBUTIONS FOR 20°C

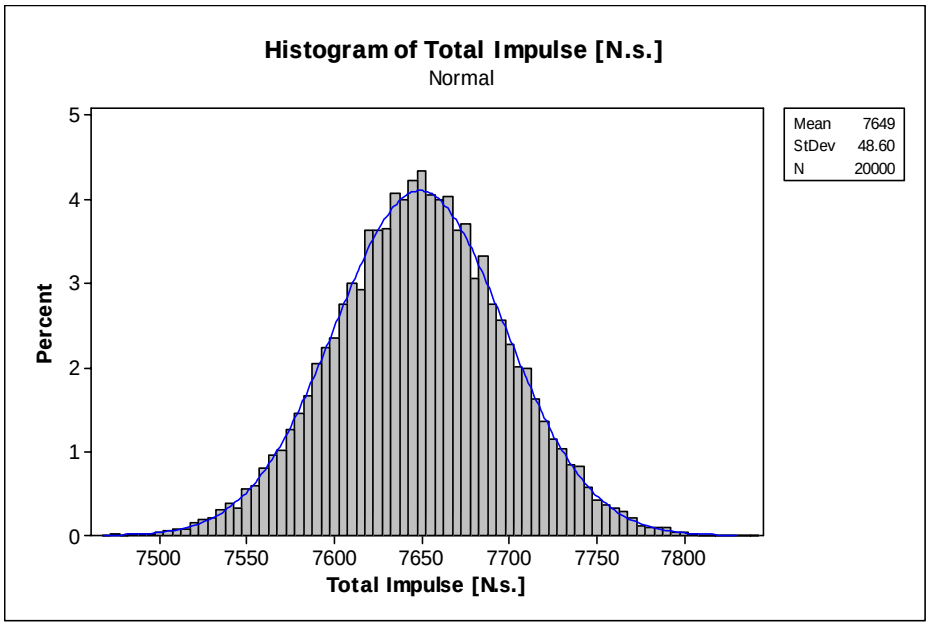

Figure D.1. Distribution of the total impulse at 20ºC

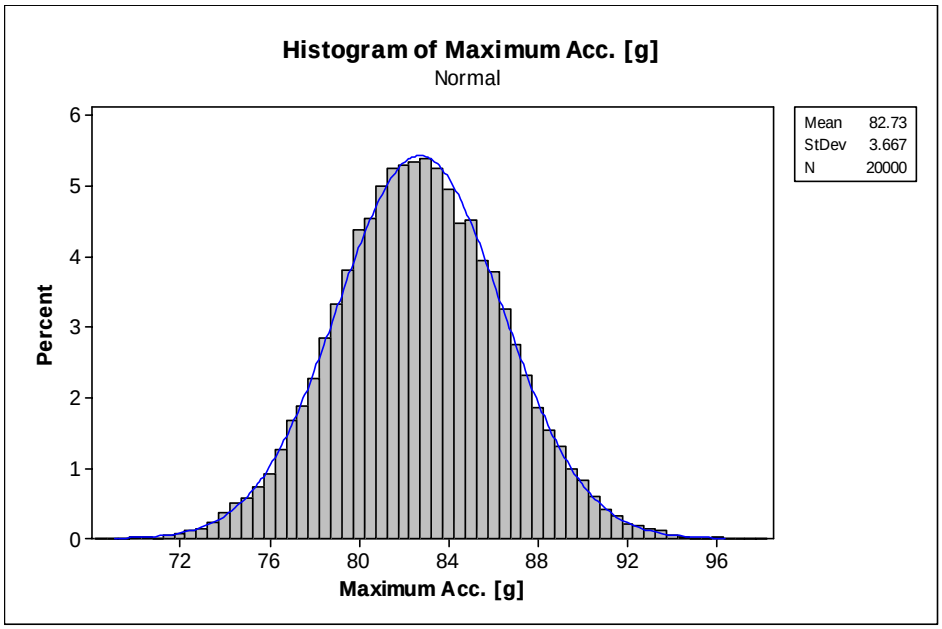

Figure C.2. Distribution of maximum acceleration at 20ºC

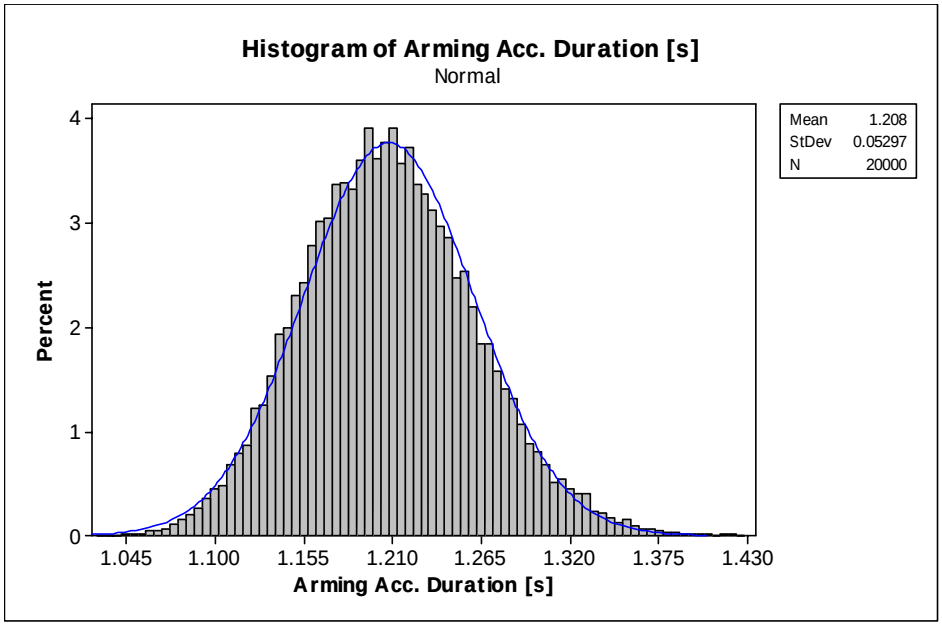

Figure D.3. Distribution of arming acceleration duration at 20ºC

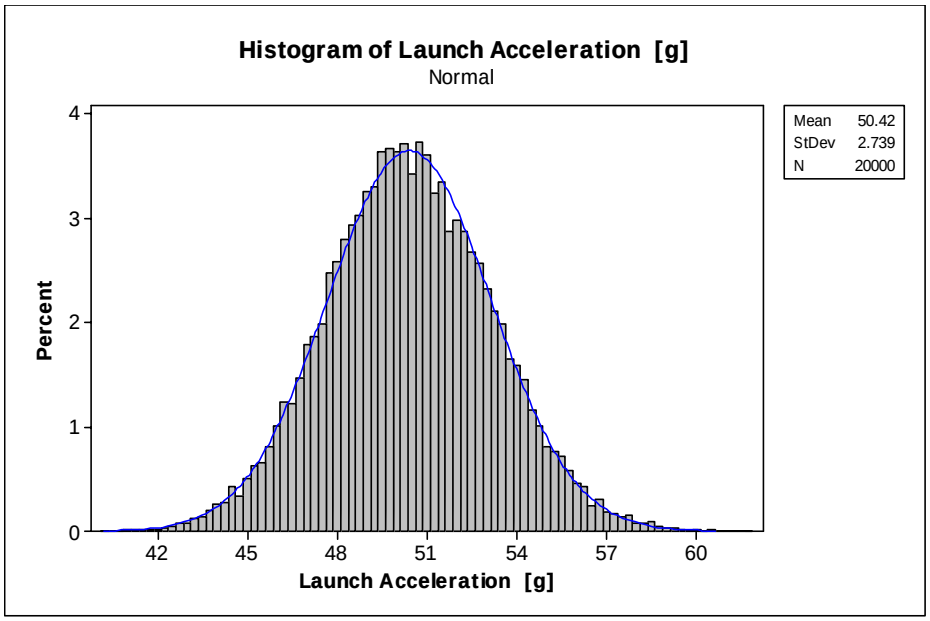

Figure D.4. Distribution of launch acceleration at 20ºC

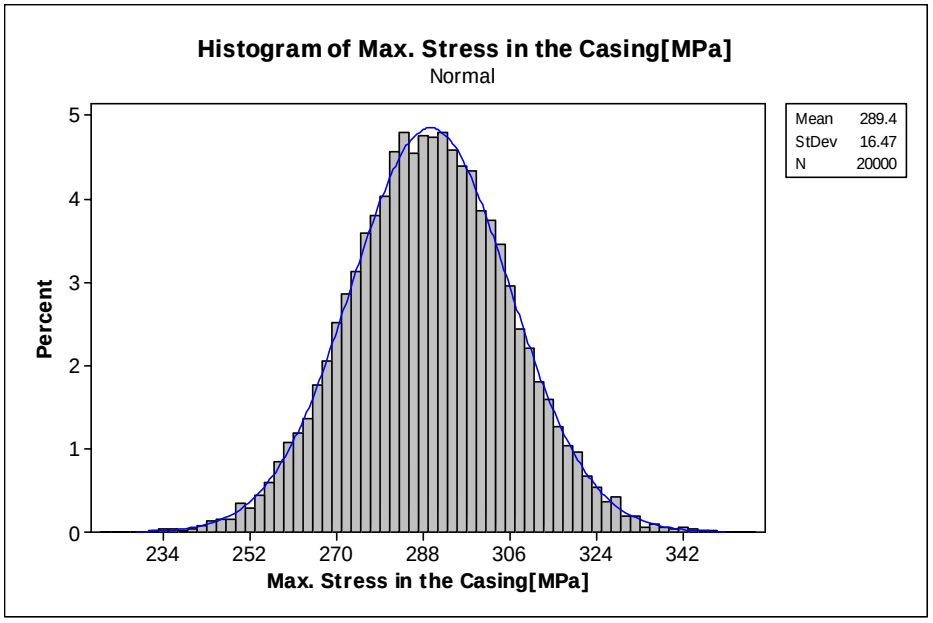

Figure D.5. Distribution of maximum stress at 20ºC

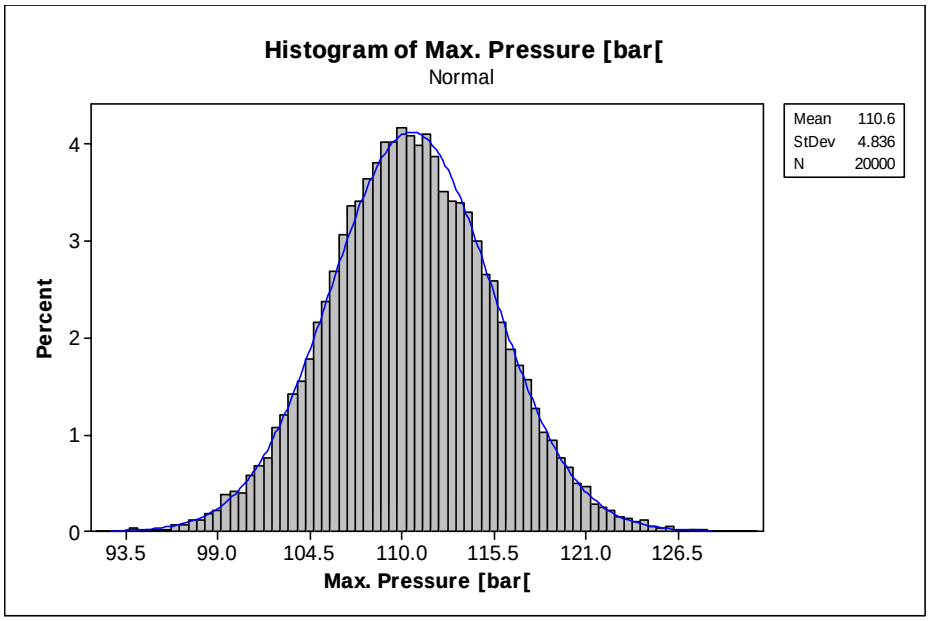

Figure D.6. Distribution of maximum pressure at 20ºC

D.2. ESTIMATED DISTRIBUTIONS FOR -35°C

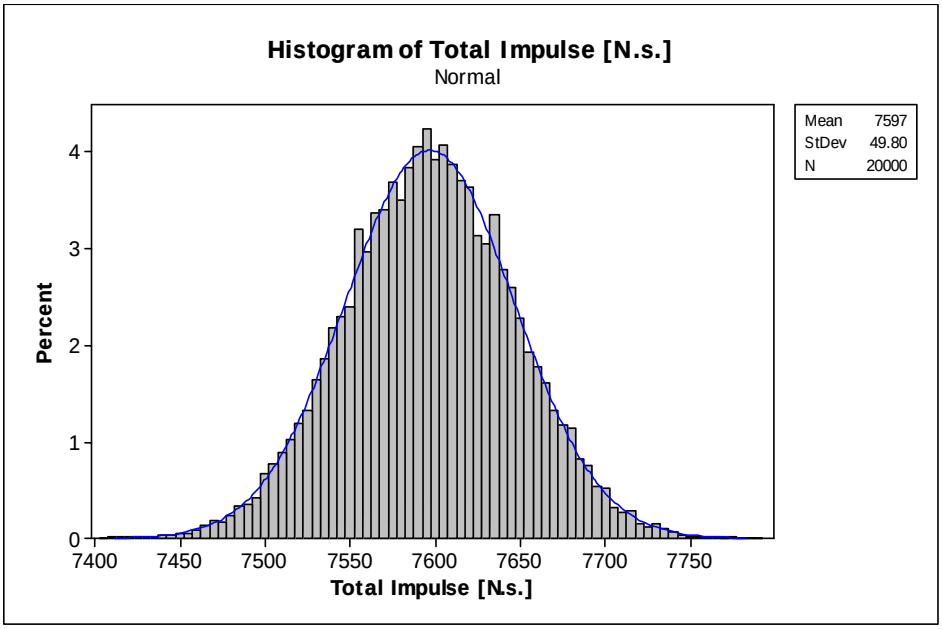

Figure D.7. Distribution of the total impulse at -35ºC

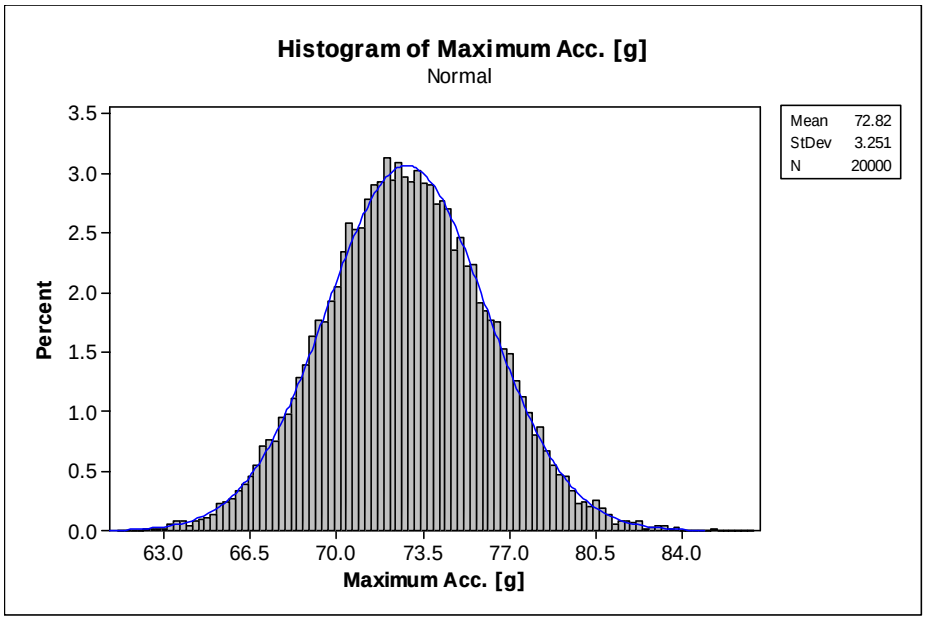

Figure D.8. Distribution of maximum acceleration at -35ºC

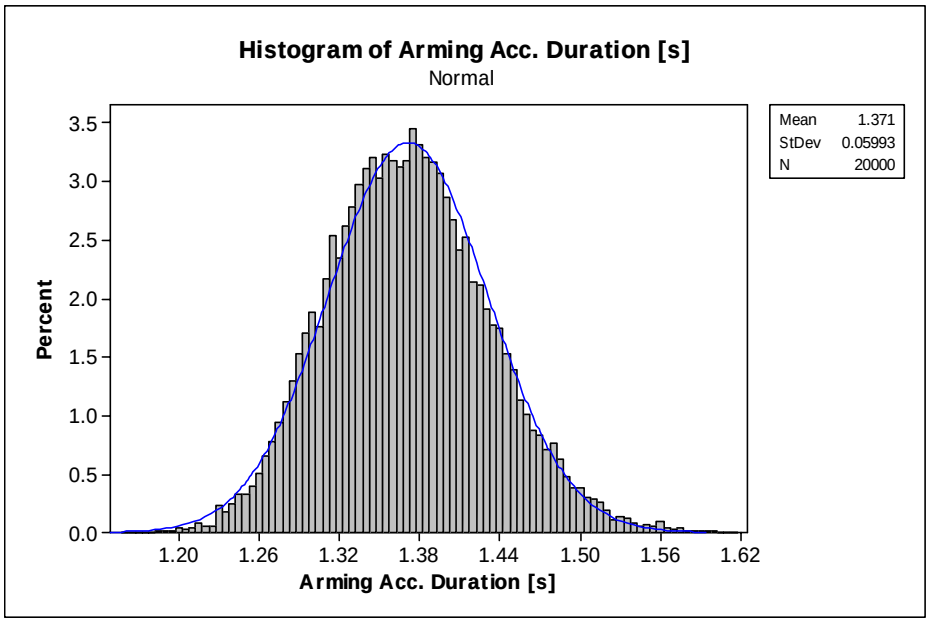

Figure D.9. Distribution of arming acceleration duration at -35ºC

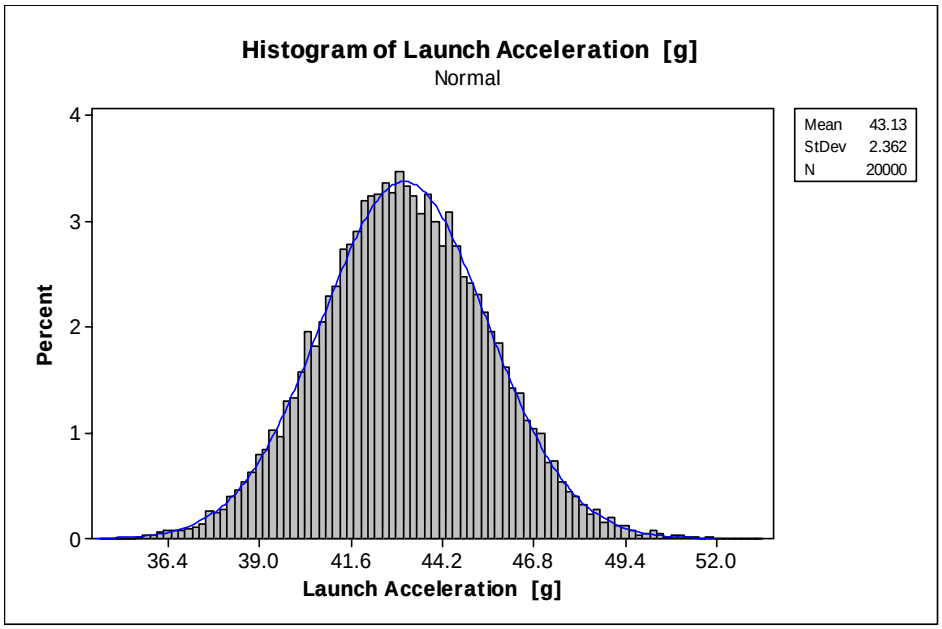

Figure D.10. Distribution of launch acceleration at -35ºC

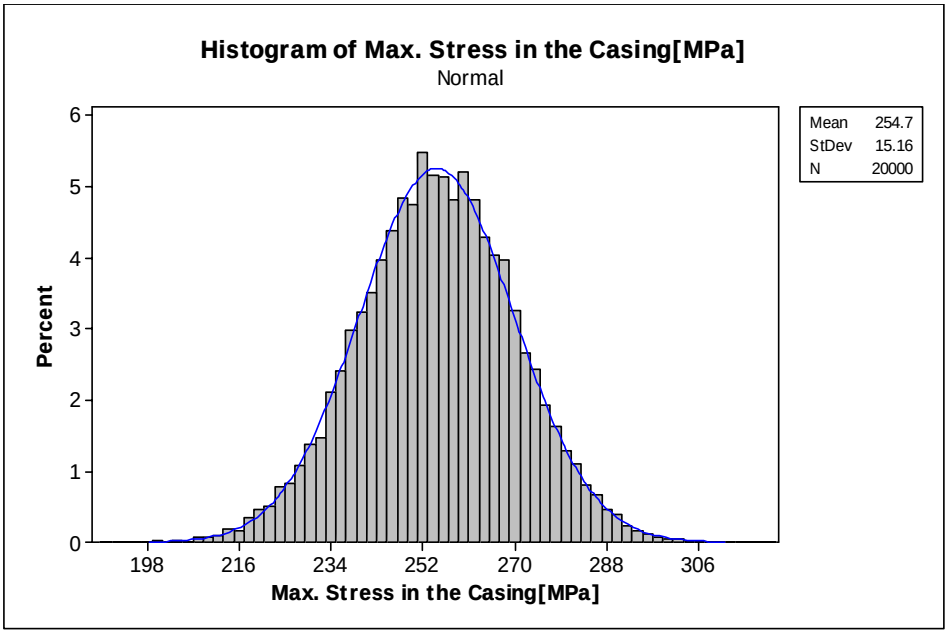

Figure D.11. Distribution of maximum stress at -35ºC

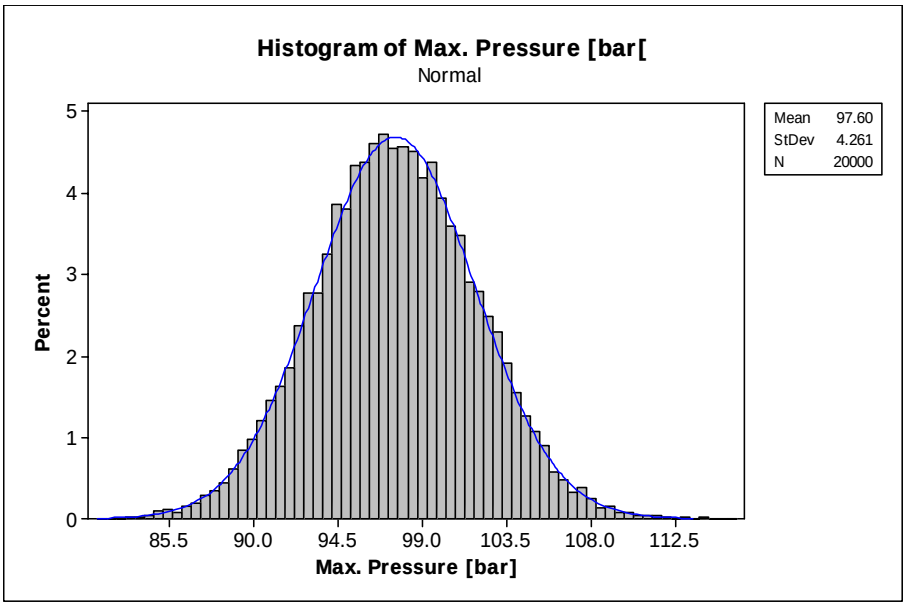

Figure D.12. Distribution of maximum pressure at -35ºC